New Materials and Techniques for Miniaturised Chromatography

by

Oscar Gustav Potter

A thesis submitted in fulfillment of the requirements for

the degree of

Doctor of Philosophy

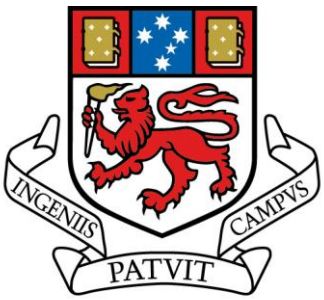

UNIVERSITY
OF TASMANIA

Submitted February 2011

Declaration

To the best of my knowledge, this thesis contains no copy or paraphrase of material previously published or written by another person, except where due reference is made in the text of the thesis.

Oscar Gustav Potter

15 Febuary 2011

Oscar Gustav Potter

15 February 2011

ACKNOWLEDGEMENTS

Throughout my PhD candidature I have been assisted, supervised and guided by my two supervisors Dr Emily Hilder and Dr Michael Breadmore. I am very grateful to them for their support throughout the project and for providing me with the means to conduct experiments, publish my work and try out my own ideas. Their support was also crucial for providing me with the opportunities to gain experience by conducting research in an overseas lab, attending conferences and meeting interesting scientists and other contacts.

I am also grateful for the discussions and suggestions I have received from the numerous people with whom I have shared a lab or office during my candidature. These people include Ryan Nai, Lea Mauko, Tim Causon, Esme Candish, David Schaller, Dr Joe Hutchinson, Tom Kazarian, Jessica Gathercole, Kara Johns, Dr Eadaoin Tyrell, Dr Phil Zakaria, Wei Boon Hon (Jason), Dr Anna Nordberg, Jeremy Deverell, Dr Ivo Nischang, Dr Pavel Levkin, William Percey, Professor Paul Haddad, Professor Pavel Nesterenko, Dr Joselito Quirino, Dr Robert Shellie, Dr Rosanne Guijt, Professor Brian Yates, and Dr Greg Dicinoski.

Some people provided me with very practical assistance. Dr Jana Krenkova assisted me with the mass spectrometry work for the boronate affinity monoliths. Dr Marian Snauko assisted in setting up the Agilent capillary chromatography equipment. Mark Thomas helped me set up and test early versions of the photochemical eluent control apparatus. Dr Cameron Johns gave me a cation exchange capillary column that he had previously packed (packed with SCS-1 material). Peter Dove of the Central Science Laboratory assisted me with the fabrication for development of the prototype photochemical eluent control system.

John Davis, also of the Central Science Laboratory, prepared cables and controllers for the LEDs.

I am especially grateful to Dr Frantisek Svec for his support and advice throughout my work on boronate affinity monoliths and also for the opportunity to work at Lawrence Berkeley National Laboratory (LBNL) in California which helped to provide me with the confidence and inspiration to pursue my ideas on photochemical eluent control. I am in debt to the Australian-American Fulbright Commission for supporting my stay at LBNL and also to the Institute of International Education (West Coast Centre) for providing me with many valuable and enjoyable experiences through the activities that they organised whilst I was in California.

I also wish to thank my family, friends and housemates for their constant support throughout this experience.

List of abbreviations

μTAS	micro total analysis systems
AMPBA	4-aminomethylphenylboronic acid
BAC	boronate affinity chromatography
BuMA	butyl methacrylate
CDMEP	2-chloro-1-(2,5-dimethylphenyl)ethanone
DeCl	desyl chloride
EDMA	ethylene glycol dimethacrylate
ESI	electrospray ionisation
GMA	glycidyl methacrylate
HEPES	4-(2-hydroxyethyl)-1-piperazineethanesulfonic acid
HPBA	4-hydroxyphenylboronic acid
HPLC	high performance liquid chromatography
ID	internal diameter
LC	liquid chromatography
LED	light emitting diode
MALDI	matrix-assisted laser desorption ionisation
MeCN	acetonitrile
MS	mass spectrometry
PEEK	polyether ether ketone
PEG	poly(ethyleneglycol)
PTFE	poly(tetrafluoroethylene)
psi	pounds per square inch
SEM	scanning electron micrograph/microscopy
TRIM	trimethylolpropane trimethacrylate
UV	ultraviolet

List of Publications

O. G. Potter, M. C. Breadmore, E. F. Hilder, Boronate functionalised polymer monoliths for microscale affinity chromatography, *Analyst (Cambridge, UK)* **2006**, *131*, 1094-1096.

O. G. Potter, E. F. Hilder, Porous polymer monoliths for extraction: diverse applications and platforms, *Journal of Separation Science* **2008**, *31*, 1881-1906.

O. G. Potter, M. E. Thomas, E. F. Hilder, M. C. Breadmore, LED controlled flow photolysis for concentration gradients in microfluidic systems, *Chemical Communications*, **2010,** *46,* 3342-3344.

Australian Provisional Patent Application: "Photochemical Control of Chemical Compositions", application number 2009905802, filed 30th November **2009**.

O.G Potter, M. C. Breadmore and E. F. Hilder, Photochemical control of chromatography eluent*s*, *Analytical Chemistry*, (in preparation)

O.G. Potter, J. Krenkova, F. Svec, E. F. Hilder and M. C. Breadmore, Monolithic capillary columns with boronate functionalities for on-line microscale affinity chromatography of nucleosides and glycated peptides, *Journal of Separation Science* (Submitted in **2010**)

International Presentations

O.G. Potter, E.F. Hilder and M.C. Breadmore. Porous polymer monoliths for boronate affinity applications (oral presentation), *31st International Symposium on Capillary Chromatography & Electrophoresis*, Albuquerque, New Mexico, USA, 28-30th November **2007**

O.G. Potter, F. Svec, E.F. Hilder, M.C. Breadmore, Improved polymer monoliths for boronate affinity chromatography (oral presentation). *22nd International Symposium on Microscale Bioseparations & Methods for Systems Biology*, Berlin, Germany, 9-13th March **2008**

O.G. Potter, F. Svec, E.F. Hilder and M.C. Breadmore. Polymer monolith capillary columns for boronate affinity chromatography (poster presentation), *ACROSS Symposium on Advances in Separation Science*, University of Tasmania, Hobart, 8-10th December **2008**.

E. F. Hilder, O. G. Potter, M. E. Thomas and M. C. Breadmore, Photochemical eluent generation for chromatography (oral presentation), *34th International Symposium on Capillary Chromatography*, Riva del Garda, Italy, 1-4th June **2010**

Oscar G. Potter, Mark E. Thomas, Emily F. Hilder, Michael C. Breadmore, Photochemical Control of Chromatography Eluents (poster presentation), *35th International Symposium on High Performance Liquid Phase Separations and Related Techniques*, Boston, MA, USA, June 19-24th **2010**

Abstract

This thesis describes two bodies of work in which new methods were developed to aid the miniaturisation and integration of chromatography.

The first body of work deals with the development of new stationary phases for boronate affinity chromatography. Porous polymer monoliths were developed for use as microscale boronate affinity extraction materials. The monoliths were prepared *in situ* from poly(butyl methacrylate-*co*-ethylene dimethacrylate) confined inside 100 μm ID fused silica capillaries. A 2-step sequential photoinitiated grafting procedure was then used to create a layer of poly(glycidyl methacrylate) on the pore surface of the monoliths. Finally, the pendant glycidyl groups on this grafted layer were functionalised by ring-opening reactions with either *p*-hydroxyphenylboronic acid or *p*-(aminomethyl)phenylboronic acid, yielding boronate extraction columns with capacities of 2.3 μmol/mL or 0.03 μmol/mL respectively. The *p*-hydroxyphenylboronic acid functionalised column was stable at up to 250 bar pressure. It was interfaced to an electrospray ionization mass spectrometer where its selectivity was demonstrated by separation of glycated and non-glycated peptides. The broad diol selectivity of the material was further demonstrated by extraction of 11 nucleosides and by extraction of guanosine from a spiked urine sample.

The second body of work deals with the conception and development of a new approach to controlling eluent composition gradients in chromatography. Gradient liquid chromatography typically relies on systems with multiple pumps that mix stock solutions at varied ratios or systems with electrolytic eluent generation. This thesis introduces an entirely new method in which a photosensitive chemical is dissolved in the eluent and irradiated at variable

intensities as it is pumped through a photoreaction tube to create isocratic or gradient eluent profiles. Six different acid-generating photochemical reagents were tested and it was found that 2-chloro-1-(2,5-dimethyphenyl)ethanone was the most suitable chemical for generating acid concentration gradients. The system was demonstrated for capillary scale inorganic cation exchange chromatography with suppressed conductivity detection and pH gradient reversed phase chromatography with on-line mass spectrometry detection. The advantages of this photochemical approach to eluent generation, including greater solvent compatibility than electrochemical methods and greater design simplicity for simpler miniaturised chromatography systems, are discussed.

TABLE OF CONTENTS

Preface

Miniaturisation and integration

Miniaturisation and integration have been amongst the most significant themes in liquid chromatography over the past two decades [1, 2], in association with a wider trend towards chemical and (bio)analytical systems that use smaller dimensions to their advantage [3]. Miniaturisation of chromatography refers to a reduction in the size of the column and, correspondingly, a reduction in the volume of the stationary phase and the flow rate of the liquid phase compared to traditional methods. It can also refer to the reduction in the size of all or any of the other parts of chromatography instrumentation. Meanwhile, integration refers to bringing the different processes of chromatography (sample preparation, injection, separation, detection) together into one system. Integration often goes hand-in-hand with miniaturisation because it can serve similar purposes.

Rather than one single driving force, the miniaturisation and integration of chromatographic systems has been encouraged by several perceived advantages that have relevance for different types of application. Some benefits are obvious, such as the potentially reduced production costs of building equipment with smaller parts. Likewise, reduced consumption of reagents, especially eluent reagents, can lead to lower running costs and environmental benefits [4]. The palpable benefits of miniaturised and integrated chromatographic systems also include the fact that they are potentially portable or field-deployable, which may be of tremendous benefits in areas such clinical diagnostics, environmental monitoring and forensic science. Meanwhile, integration and automation of sample preparation, separation and detection can lead to greater ease-of-use,

which can further reduce the costs of chromatographic analysis and increase its availability. The ease-of-use advantage becomes especially important when working with small sample volumes. For example, it is difficult to draw a 1 μL eluted fraction from a microscale affinity chromatography separation up into a handheld syringe for direct infusion analysis by ESI-MS or spotting onto a MALDI plate. Yet a 1 μL fraction can easily be delivered to such detection systems if the column is hyphenated online to an ESI source or connected to a MALDI spotting device. Ease of use is becoming more and more important with the growing interest in multidimensional analysis and more complex sample preparation as well as interest in examining biological samples of limited quantity.

Several of the forces driving miniaturisation and integration are of a more technical nature. Miniaturised and integrated chromatography systems have shorter and lower diameter fluid conduits, which translates to smaller extra-column volumes. This can reduce both hydrodynamic band broadening and sample diffusion, potentially giving greater separation efficiency. Faster analysis speeds are also possible, especially if cheap and compact devices can be used for parallel processing. These goals have been furthered by the development of monolithic stationary phases which are able to be operated at relatively high flow rates without corresponding loss in separation efficiency [5]. Meanwhile, advances in the design and manufacture of microfluidic chips have made it easier to tightly integrate small components and analysis steps into a single, robust system [3].

Given that the reduction in production and running costs are often important goals of miniaturisation and integration, there is interest in substituting expensive materials with cheaper alternatives. Sometimes the goal is to have a device which

is so cheap that it could be used once and then disposed, and this can require radical new technologies. For example, Hendersen *et al*. produced a microfluidic device in which platinum electrodes were substituted with easily processed conducting polymer electrodes [6], whilst Pais *et al*. designed disposable microfluidic chips that perform fluorescence detection using integrated thin film organic LEDs for excitation [7]. One of the most exciting recent developments in materials substitution is the development of patterned paper microfluidic chromatography [8], which has been championed by George Whitesides as an affordable analytical technology for the third world.

One of the greatest challenges in miniaturisation has been the development of detectors that can operate in systems with very low flow rates and fluid conduits in the micrometer range. Fortunately, miniaturised chromatography can benefit from some of the same technology that has been used for capillary and microfluidic chip electrophoresis systems, which have always operated in this scale. For example, miniaturised conductivity detectors, including capacitively coupled contactless conductivity detectors, are now widely available [9] and have been successfully applied to microscale chromatography [10]. Meanwhile, absorbance detection suffers from reduced sensitivity in miniaturised systems because the path length of absorbance flow cells normally needs to be reduced along with the column. Miniaturised detectors with steady and intense LED light sources were developed and were even found to give improved performance versus mercury lamps with diode array detectors [11].

Despite all this, the most conspicuous microscale chromatographic systems are not in fact any cheaper than traditional chromatographic systems. Microscale gradient-capable pumping instruments, such as those sold by Dionex Corporation

and Agilent Technologies, take up a similar amount of bench-space and have similar costs to the systems that use traditional 4 mm ID chromatography columns. Furthermore, many of these systems use up as much reagent as traditional scale HPLC because they rely on flow splitting to achieve microscale flow rates, with the bulk of the eluent shunted off to waste. Nevertheless, these systems have been popular because there is another very important reason why miniaturised chromatography is advantageous which has nothing to do with size, cost or portability. The use of smaller column volumes and lower flow rates have the advantage that the sample will be less "diluted" by the liquids in the chromatography system. In cases where the sensitivity of the detector is more affected by *concentration* rather than the absolute quantity of the analytes, this advantage can be tremendous.

This is effectively the case for ESI-MS, which has become the "killer app" of low flow rate chromatography because the electrospray ionisation process works best at flow rates in the order of microlitres per minute and lower [12]. For ESI-LC-MS, there are essentially two approaches to delivering this low flow rate. The first is to use a high flow rate chromatographic system and then to split the flow down to a lower flow rate between the outlet of the column and the ESI source. Whilst this approach can work very well [13], it involves wasting most of the sample, which will be shunted off to waste with the bulk of the effluent. This may be untenable in cases where sample quantity is severely limited, especially if the concentration of the analytes in that sample are also very limited. Such cases include the analysis of small tissue and fluid samples for biological research. The other approach is to use a chromatographic system with flow rates in the range of microlitres per minute or hundreds of nanolitres per minute [12]. Such systems

deliver all of the sample into the ESI source, effectively allowing highly sensitive analysis of very small sample quantities by the incredibly powerful analytical tools of MS and MS/MS [13].

Goal

The goal of this PhD project was to help address two of the technical challenges associated with the miniaturisation and integration of chromatography. The first part of the thesis deals with the development of new stationary phase materials for boronate affinity chromatography (BAC), a type of chromatographic extraction which has been difficult to miniaturise. The new materials are based on porous polymer monoliths and the research serves to assess the broader potential of porous polymer monoliths for miniaturised chromatographic extraction and affinity chromatography.

The second part of the thesis deals with the conception and development of a new approach to controlling the composition of chromatography eluents based on photochemical reactions. The approach is demonstrated for two distinct classes of chromatography and the wider implications of the concept are discussed with regards to emerging microfluidic technologies.

References

1. Novotny, M., *J. High Resolut. Chromatogr.* 1987, *10*, 248-56.

2. Manz, A., Graber, N., Widmer, H. M., *Sens. Actuators, B* 1990, *B1*, 244-8.

3. Ohno, K.-I., Tachikawa, K., Manz, A., *Electrophoresis* 2008, *29*, 4443-4453.

4. Sheldon, R. A., *Green Chem.* 2007, *9*, 1273-1283.

5. Guiochon, G., *J*. *Chromatogr*. *A* 2007, *1168*, 101-168.

6. Henderson, R. D., Guijt, R. M., Haddad, P. R., Hilder, E. F., Lewis, T. W., Breadmore, M. C., *Lab Chip* 2010, *10*, 1869-1872.

7. Pais, A., Banerjee, A., Klotzkin, D., Papautsky, I., *Lab Chip* 2008, *8*, 794-800.

8. Martinez, A. W., Phillips, S. T., Butte, M. J., Whitesides, G. M., *Angew*. *Chem*., *Int*. *Ed*. 2007, *46*, 1318-1320.

9. Kubán, P., Hauser, P. C., *Anal*. *Chim*. *Acta* 2008, *607*, 15-29.

10. Kubán, P., Hauser, P. C., *J*. *Chromatogr*. *A* 2007, *1176*, 185-191.

11. King, M., Paull, B., Haddad, P. R., Macka, M., *Analyst* 2002, *127*, 1564-1567.

12. Ishihama, Y., *J*. *Chromatogr*. *A* 2005, *1067*, 73-83.

13. Noga, M., Sucharski, F., Suder, P., Silberring, J., *J*. *Sep*. *Sci*. 2007, *30*, 2179-2189.

1 Polymer Monoliths for Miniaturised and Integrated Affinity Chromatography

1.1 Background

The author of this thesis co-wrote a critical and comprehensive review on polymer monoliths for chromatographic extraction which was published in *Journal of Separation Science* in 2008 [1]. The review dealt with monoliths for all types of chromatographic extraction, including those based on ion exchange and reversed phase interactions, as well as extractions that involve more specific affinity interactions and molecular imprinting. This chapter is an update of that review which has been refined to focus on polymer monoliths for miniaturised affinity chromatography. Readers who are interested in this topic might also like to read some recent reviews that cover the broader topic of affinity chromatography using monolithic supports [2-4].

1.2 Introduction

1.2.1 Principles of Affinity Chromatography and Affinity Extraction

The term 'affinity chromatography' refers to liquid chromatography methods based on highly selective interactions between complex ligands such as proteins, peptides or metal chelate moieties. Other than its emphasis on so-called 'biological' or 'molecular recognition' binding interactions, affinity chromatography also differs from most other forms of chromatography in the sense that it typically emphasises different chromatographic properties. Whilst HPLC typically relies on numerous cycles of sorption and desorption, with an

emphasis on maximising theoretical plates to improve separation resolution, it is rare to talk about theoretical plates in the context of affinity chromatography. Rather, there is instead a focus on achieving sorption that is as strong and as selective as possible. This is typically followed by a desorption step in the form of a step gradient to facilitate rapid and complete desorption of the target species. In this sense, most affinity chromatography procedures more closely resemble solid phase extraction [5] than they do HPLC. Like solid phase extraction, affinity chromatography is usually (but not always) just one part of a multi-step analytical procedure, and depending on the context it may often be considered to be a sample cleanup or preconcentration process.

In the context of chromatographic procedures, preconcentration generally refers to the act of binding low abundance target molecules from a large volume sample onto a stationary phase and then eluting them off in a small volume of eluent so as to increase their concentration. This procedure can also be called 'sample enrichment'. Meanwhile, sample cleanup describes one of two scenarios. It may describe an extraction where the target compounds are not analytes but rather are species in the sample matrix that can interfere with detection of the analyte. If the targets that are removed are proteins, this process is sometimes termed 'depletion' [6-8]. On the other hand, sample cleanup can also describe a direct extraction of the target compound out of a matrix that could have interfered with its analysis.

Despite the varied goals and eclectic nomenclature, different affinity chromatography methods share many similar requirements and give rise to common challenges. The first and most obvious is the need for an effective stationary phase. Varilova *et al*. [9] provide an excellent introduction to the numerous supports for affinity chromatography. They include porous and non-

porous packed particle stationary phases of silica or polymer beads, as well as agarose gels, dextrans, and monolithic stationary phases made of continuous polymer or silica. The morphology of the stationary phase material can have powerful implications for mass transport, permeability and hydrodynamic band-broadening [9]. It also determines the surface area, which can be a limiting factor for binding capacity.

The surface chemistry of the solid support determines the binding strength and selectivity of the stationary phase. The surface of an affinity chromatography sorbent normally needs to be modified by attaching the complex functionalities or ligands that are required for highly selective binding of target analytes [2].

Affinity chromatography requires appropriate mobile (liquid) phases. The sorbent may need to be exposed to a preconditioning solution before the binding step. The binding step may require adjustment to the sample matrix, and the sample should be carried in a mobile phase which encourages sorption of the target molecules whilst preventing adsorption of unwanted compounds. A prolonged washing step is sometimes used to remove unbound or weakly bound compounds from the stationary phase. Finally, the eluting buffer needs to be chosen to ensure rapid and complete desorption of the target compound. This can occur either by inducing a change in the structure or behaviour of the binding ligand or target through by altering such properties as pH or temperature [10]. Alternatively, elution can be achieved by introducing a molecule which competes with the target molecules for the binding sites [3].

Whilst affinity chromatography is a mature and well established approach for numerous applications in bioanalytical chemistry, it is still largely carried out as an offline method in formats such as spin columns, packed pipette tips and wide-

bore columns. The development of miniaturised affinity chromatography methods is expected to offer potential advantages in terms of costs, analysis times, ease-of-use, portability, integration and the ability to analyse samples of severely limited quantity.

1.2.2 Polymer Monoliths

In the context of functional solid materials for separation purposes, the term monolith describes a flow-porous (macroporous), highly crosslinked and therefore rigid, monolithic material that acts as a support for the stationary phase in a separation process. Such materials generally fall into one of two categories, nominally polymer and silica monoliths. Silica monoliths are rigid inorganic materials which are typically prepared by thermally controlled condensation of a sol-gel of alkoxysilanes and are outside the scope of this review. Several recent reviews have focused on their synthesis and application to analytical separations [11-13]. Whilst silica monoliths are sometimes used for affinity chromatography [14-16], they are generally not as popular as polymer monoliths for separating large molecules such as proteins because most of their surface area is in the form of mesopores which are accessable only by diffusion. This reduces separation efficiency for large, slow-diffusing molecules such as proteins[2].

Porous polymer monoliths are produced by polymerisation of organic monomers, including crosslinkers. The porosity of these materials is determined by porogenic solvents or pore-forming reagents such as polyethylene glycol (PEG). A wide range of monomers have been used for the synthesis of polymer monoliths and nearly thirty distinct monomers were encountered whilst the author conducted a literature review in 2008 [1]. However, most of these polymer monoliths can be grouped into one of several broad categories. Methacrylate and acrylate

monoliths are the most widely reported type. Vlakh and Tennikova have recently published an excellent review on the preparation of methacrylate monoliths [17]. These types of monolith are usually formed by radical polymerisation and are made rigid by crosslinkers such as ethylene dimethacrylate (EDMA). Styrenic monoliths are also prepared by radical polymerisation and employ styrene and substituted derivatives, using divinylbenzene (DVB) as a crosslinker. The pore size of styrenic and methacrylate type monoliths can be controlled across two orders of magnitude by varying the composition of the porogenic solvent mixture [18]. Epoxy resin monoliths are prepared by condensation of epoxy resins and amines. The porous structure of epoxy resin monoliths can be controlled by pore-forming reagents such as PEG [19].

The advantages of monolithic stationary phases for high performance chromatography and electrochromatography have been well described [20, 21]. Many of these advantages are also applicable to the use of polymer monoliths for affinity chromatography techniques. One potential advantage is that mass transport on polymer monolithic stationary phases is dominated by convection. This means that sorption of targets onto the stationary phase is less limited by diffusion than it is in the case of macroporous/mesoporous beads. In general, this allows the use of higher linear flow velocities, which can be a great advantage for high throughput analyses or extractions from very large sample volumes. Monoliths are also more hydrodynamically porous than packed particle beds. With the exception of perfusion chromatography, flow in an ideally packed column of spherical sorbent particles is forced in the relatively restricted interstitial spaces. Polymer monoliths are usually at least 60% porous and it is widely assumed that most of this porosity is accessible to fluid flow.

Chemical stability is another feature of polymer monoliths that is often cited as an advantage, especially when compared to silica based stationary phases which degrade in very low and moderately high pH solutions [22].

One argument against polymer monoliths is that they do not have a high surface area compared to many modern sorbent materials. This is a disadvantage because binding capacity increases with surface area. However, the high surface area of materials such as porous silica beads is only accessible by diffusion, which means that separations on these materials may become poorer as flow velocity is increased. This also applies to the higher surface area silica monoliths. Most of their surface area is found within networks of mesopores which are restricted enough to limit the sorption of slow diffusing macromolecules such as proteins [2]. In some cases, it may be completely impossible for the macromolecules to reach the binding sites in the mesopores, and the surface area of the mesopores is then irrelevant. However, in those cases where the macromolecules can reach the restricted surface of mesopores by diffusion, these binding sites can actually cause a problem by slowing the rate of mass transport on and off the stationary phase. In high performance chromatography this is observed as a decrease in plate height that worsens with increased linear flow velocity. For affinity chromatography, this effect could be observed as a drop in binding capacity at higher flow rates, or as inefficient desorption of the target compounds leading to less concentrated eluted fractions.

The popularity of polymer monoliths in the literature is only partly explained by their performance advantages. An equally significant advantage, perhaps an even more important one, is their ease of synthesis. Polymer monoliths can be formed *in situ* – within a capillary, column, pipette tip or even in a microfluidic channel

on a chip [23]. They can be moulded into any shape and have been demonstrated in structures as large as 8 L to as small as a few nL in the channel of a microfluidic chip [24]. Polymer monoliths are often prepared in capillaries with internal diameters as low as 100 μm. Recent work by Nischang *et al*. has demonstrated that it is possible to physically downscale methacrylate monoliths to form within 10 μm or even 5 μm ID capillaries provided that steps are taken to ameliorate the effects of confinement on the polymerisation process [25, 26]. This probably represents a redundant capability because such dimensions are probably too small for most affinity chromatography applications. In any case, it is uncertain whether there would be any advantage to filling columns with such small diameters with an affinity chromatography stationary phase material. If such small internal diameters were needed, it might be more appropriate to work with porous layer open tubular (PLOT) columns which are showing strong potential as media for high resolution chromatography [27, 28].

The potential for polymer monoliths to be formed *in situ* is particularly important for micro and nanoscale devices where the incorporation of particulate sorbent materials is difficult and plagued by poor reproducibility [29]. Methacrylate polymers have an additional advantage in that they can be photoinitiated using UV light and masking. This approach allows for precise and convenient spatial control over the formation of a monolithic column within a capillary of microfluidic channel [30].

With all of these advantages, it should not be surprising that polymer monoliths are becoming indispensable materials for bioanalytical chemistry technology. Reviews in 2009 by Saunders *et al*. [31] and Roberts *et al*. [22] predicted that

importance of polymer monoliths in bioanalytical chemistry will continue to grow.

1.3 Polymer monoliths for various types of affinity chromatograph

This section covers the various types of affinity chromatography that have been demonstrated using polymer monoliths and the synthetic methods that have been used to prepare them, with an emphasis on miniaturised and microscale systems.

1.3.1 Immobilised proteins and peptides

Affinity chromatography that uses immobilised ligands of biological origin can be termed "bioaffinity chromatography". Furthermore, specific terms such as "immunoaffinity chromatography" and "lectin chromatography" are sometimes used to describe affinity chromatography that uses proteins of immunological or plant origin, respectively [2].

Whilst a variety of polymer materials have been used to create monoliths with bioaffinity functionality, this field has been heavily dominated by the use of glycidyl methacrylate (GMA), and in particular poly(GMA-*co*-EDMA) monoliths. This trend may be partly explained by the ease of *in situ* synthesis of this type of monolith and the availability of well characterised procedures in the literature. The relatively low surface area of methacrylate type monoliths is not of such a great concern in the case of bioaffinity chromatography because the target analytes are often slow-diffusing macromolecules which cannot efficiently access the higher surface area of materials with hierarchical porous structures.

The use of poly(GMA-*co*-EDMA) monoliths for affinity chromatography has already undergone significant commercialisation. BIA separations (Lubljana, Slovenia) markets GMA-based polymer monoliths as part of their Convective Interactive Media (CIM) product line. CIM are short, wide diameter columns and they may be purchased with a variety of immobilised affinity ligands. CIM disks may also be acquired in the native epoxy state so that researchers can use them to immobilise their own ligands [32, 33]. However, the smallest CIM disks have a relatively large volume of 0.1 mL and they operate at high flow rates, usually above 100 μL/min. Therefore, they can not be considered to be truly miniaturised chromatography devices. Nevertheless, their commercial success has helped to reinforce the idea of porous poly(GMA-*co*-EDMA) monoliths as a standard starting material for creating monolithic affinity chromatography stationary phases.

The key advantage of GMA-based monoliths is the reactivity of the surface epoxide groups, particularly towards amine nucleophiles. Epoxide groups provide a convenient point of covalent attachment for a virtually endless variety of affinity ligands. The simplest approach to covalent attachment is to allow a nucleophile on the ligand, typically an amine from an amino acid residue, to attack the epoxide group. However, it is common to first modify the epoxide group itself in order to better control the reaction [34] or to introduce a spacer arm [35].

An objective comparison of several immobilisation methods was performed by Mallik *et al*. [36] by attaching human serum albumin (HSA) to a poly(GMA-*co*-EDMA) monolith. In the simplest approach, they allowed the amine residues on the protein to react directly with the epoxide groups. For three other methods they began by hydrolysing the epoxy groups to diols using dilute sulfuric acid.

Following this, three alternative reactions were used to convert the diols to either aldehydes, succinimidyl carbonate groups or imidazolyl carbamate groups. These intermediate functional groups were then used to attach the HSA. They observed that the direct reaction of protein with the epoxy group provided the lowest conversion of functional groups, whilst the reaction using the aldehyde as an intermediate, known as the Schiff base method, gave the highest loading of HSA. The Schiff base method also yielded the monolith with the greatest performance for bioaffinity chromatography, which compared favourably against a silica based HSA monolith.

El Rassi *et al*. [37, 38] introduced an ionizable monomer, [2-(methacryloyloxy)ethyl] trimethylammonium chloride (META) to produce poly(GMA-*co*-EDMA-*co*-META) monoliths that could generate a stable electroosmotic flow (EOF) and thus be operated in electrochromatography mode without a pump. These monoliths were used to bind mannan and lectins to perform affinity chromatography separations, achieving significant enrichment of protein samples. This approach was taken further by coupling poly(GMA-*co*-EDMA) monolithic capillary columns with different immobilised lectins in tandem [34]. This scheme was successfully used to resolve α_1-acid glycoprotein into two glycoform fractions. This approach was extended in subsequent work in which they coupled eight different monoliths in tandem for microscale depletion of the top eight most abundant proteins in human serum in a single run [8]. The tandem affinity columns were coupled to an immobilised trypsin monolithic column to integrate depletion and digestion of proteins.

GMA monoliths are typically prepared by thermally initiated copolymerisation of GMA with EDMA. However, trimethylolpropane trimethacrylate (TRIM) is an

interesting alternative to EDMA. As a trifunctional crosslinker, it has the potential to create highly rigid structures. Pan *et al*. [39] prepared and compared monoliths made of poly(GMA-*co*-TRIM) and poly(GMA-*co*-EDMA) and found that the TRIM monolith had better mechanical stability than its EDMA counterpart. The surface epoxide groups of these two types of monolith were converted to aldehydes groups and used for covalent attachment of Protein A. The resulting bioaffinity monoliths were then used for extraction of IgG from human serum without observing any non-specific adsorption of BSA. The TRIM monolith had a good combination of surface area and permeability and compared favourably against the poly(GMA-*co*-EDMA) monolith in terms of mechanical stability and having a narrow pore size distribution. This clearly showed that poly(GMA-*co*-TRIM) is a good base material for affinity monolith chromatography despite EDMA remaining the preferred crosslinker for most researchers.

Hahn *et al*. showed that it was feasible to create an affinity monolith using pre-conjugated GMA [40]. In this approach GMA was reacted with a peptide directed against lysozyme prior to the monolith polymerisation process. The peptide-GMA conjugate had a strong interfering effect on the morphology of the monolith, however they were able to re-optimise the polymerisation conditions and create an effective affinity monolith with 30% conjugated GMA. Despite their success, this approach has not been popular because it is more complicated and does not offer a clear advantage over the more widely accepted method of reacting onto the surface epoxide groups of a poly(GMA-*co*-EDMA) monolith.

The almost exclusive use of GMA as an attachment monomer may not be entirely justified on chemical grounds. There is at least one other monomer, namely

4,4-dimethyl-2-vinylazlactone, that may provide a more convenient and reactive functional group for attaching proteins and peptides to the monolith surface [41, 42]. The paucity of reports that use alternative reactive monomers such as 4,4-dimethyl-2-vinylazlactone may be partly explained by the fact that alternative monomers are not as widely available as GMA.

Stationary phases with immobilised metals, normally used for 'immobilised metal affinity chromatography' (IMAC), can also be used as a starting points for constructing bioaffinity chromatography stationary phases. This was demonstrated by Feng *et al*., who prepared a poly(GMA-*co*-EDMA) monolith inside 200 µm ID capillaries and modified them to be used for "chelating concanavlin A chromatography" [43]. The first steps were to react the surface epoxide groups with iminodiacetic acid (IDA) and then to load the resulting functional groups with Cu(II). Next, a solution of concanavlin A (Con A) was pumped through the monolith, which attached to the Cu(II), forming "sandwich" structures which served as semi-immobilised binding groups. The monolith could then be used to capture glycoproteins from various samples using this ligand.

In the case of traditional Con A affinity chromatography where the Con A is covalently bound to the stationary phase, bound proteins would be eluted by washing the column with a high concentration of α-D-mannopyranoside. This creates problems downstream because of the incompatibility of this reagent with mass spectrometry and the difficulties associated with removing this sugar from C18 stationary phases [43]. These problems are particularly pronounced in microscale systems where handling and processing the tiny eluted fraction is impractical. The monolith designed by Feng *et al*. allowed them to avoid this problem by instead using a solution of ammonium hydroxide as the eluent for the

desorption step, inducing the release of the entire sandwich complex and the bound protein, which can be regenerated later by applying more $CuSO_4$ and Con A.

1.3.2 Alternative types of affinity chromatography

In addition to proteins, peptides and small metabolites, affinity chromatography can be used to extract the polynucleotides which are the most important analytes for molecular biologists. Satterfield *et al*. used photopolymerised poly(GMA-*co*-EDMA) capillary monoliths for microscale extraction of eukaryotic messenger RNA (mRNA) from a matrix that included a large amount of ribosomal RNA (rRNA) [44]. This separation took advantage of the fact that mRNA has a so-called "polyA tail", meaning that it has a block of adenosine nucleotides at one end. A 30-mer of dT with an amine spacer group was reacted with the epoxide groups to create ligands with strong selective affinity for the mRNA. The monolith was able to extract at least 16 µg of mRNA from 315µg of total RNA and was resistant to buffers at least up to pH 9. In addition, the monolith showed excellent stability without loss of performance after drying or storage for several months.

Xu *et al*. demonstrated the use of polymer monoliths for gold-thiol affinity chromatography [10]. This type of separation relies on the interaction between thiol groups and gold, and has therefore gained attention because of its potential use in selectively extracting peptides or proteins with cysteine residues. Xu *et al*. began by preparing a poly(GMA-*co*-EDMA) monoliths inside 100 µm ID capillaries. They then proceeded to react the columns with either sodium hydrogren sulphide or cysteamine to form monoliths with –SH functional groups

on the pore surface. It was found that the latter reaction gave a better functional group loading.

The next step of attaching gold nanoparticles to the thiol groups was more difficult and several methods were trialed [10]. Xu *et al*. found that the best way to attach gold particles was to pump a solution of chloroauric acid trisodium citrate through the monolith at a temperature of 100°C, whereby the gold nanoparticles precipitated out of solution *in situ* and attached to the thiol-modified pore surface of the monolith. The monoliths prepared by this method were hyphenated on-line to a reversed phase column and were then used to selectively retain cysteine-containing peptides. The cysteine containing peptides could be washed off using an aqueous solution of β-mercaptoethanol. This allowed the cysteine peptides to be analysed separately from the non-cysteine containing peptides, effectively reducing sample complexity. Unfortunately, the β-mercaptoethanol was difficult to remove and the regeneration procedure was consequentially somewhat inconvenient. It was necessary to heat the monolith and pump water through it for at least one hour at a temperature of 80°C or more before it could be used again.

1.4 Integrated platforms and formats

1.4.1 Microfluidic Chips

Microfluidic chips are a promising platform for analysis because they offer a robust and compact way to integrate analysis procedures with minimum dead volume [45]. Chip based separation is now maturing as a technology, with commercial products on the market including chip based chromatography [46] and electrophoresis [47] systems from Agilent which are designed to reduce

sample handling and analysis times. However, the number of reports of polymer monoliths for affinity chromatography in microfluidic chips has been surprisingly low [2], and it is interesting to note that Agilent have chosen to work with a packed particle bed rather than a monolithic stationary phase in their commercial MS chip [46].

The first demonstration of a polymer monolith for affinity chromatography in a microfluidic chip was by Mao *et al*. [48]. This group demonstrated separation of glycoforms for lectin affinity chromatography. They employed glass chips and used chemical etching to form channels with cross-sectional dimensions of 70 μm x 20 μm. Poly(GMA-*co*-EDMA) monoliths were synthesized *in situ* within the channels according to a published method [49]. Pisum sativum agglutinin (a lectin) was immobilised by reaction with the epoxy groups on the monolith surface. Mao *et al*. were then able to selectively bind the different glycoforms of chicken and turkey ovalbumin. The different glycoforms of the fluorescently labelled glycoproteins could be eluted with partial resolution by introducing a step gradient of displacing sugar into the monolith. Another impressive aspect of this work was that the entire separation process operated using EOF. This is a prized achievement in the field of miniaturised separations because it eliminates the need for a bulky or expensive external or internal pump device. The goal of increased analysis speed was well satisfied – the entire analysis process could be completed within 400 seconds.

Li and Lee [6] prepared short sections of poly(GMA-*co*-TRIM) monoliths in etched glass chips. Photomasking served as a relatively simple method for spatially controlling the formation of the monolith in the channel. Cibacron-blue-3G-A was immobilised onto the monolith using ethylene diamine as a reactive

bridge. This dye was intended to act as an affinity ligand for lysozyme and human albumin. MALDI-TOF and a stereo fluorescence microscope were used to detect the labelled proteins and they found that they could selectively retain lysozyme over non-specifically bound protein cytochrome c. Li and Lee then attempted to selectively extract human albumin from cerebrospinal fluid as a sample cleanup procedure. Whilst they were able to demonstrate selective removal of albumin over another ubiquitous protein, transferrin G, there was a significant level of non-specific adsorption. In related work, Li and Lee in collaboration with Craighead and Yang [50] prepared a methacrylate-based monolith on a chip that functioned both as an on-chip electrospray interface as well as a solid phase extraction material.

1.4.2 Other integrated formats

Polymer monolith affinity chromatography stationary phases have been coupled on-line to a variety of complementary analytical processes. Key to this success has been the versatility that results from their *in situ* polymerisation.

Bedair *et al*. coupled a monolith for lectin affinity chromatography with ESI-MS/MS [51] . They formed a poly(GMA-*co*-EDMA) monolith by photoinitiated polymerisation directly within an electrospray emitter . The monolith was then functionalised with Concanavalin A using a Schiff base method. In addition to serving as a stationary phase for preconcentration, the monolith also served as a nanospray interface for sheathless coupling to MS/MS detection. Whilst convenience alone might have justified this integration, it also provided a potential performance benefit because there was zero dead-volume between the column and the spray. Bedair *et al*. applied this system to the preconcentration of glycopeptides from a tryptic digest of bovine pancreatic ribonuclease B for

structural elucidation by MS/MS. However, the adsorption step was not performed online. Rather, the capillary column was removed from the MS for the sample loading step and had to be reconnected to the MS/MS before elution by acetic acid in 50% acetonitrile solution. No glycopeptides were able to be detected in the non-enriched sample. However, after preconcentration of 20 μL of sample on the column they were able to detect five different glycoforms of the glycosylated peptide that were known to be in the tryptic digest of the protein.

Some of the most exciting uses for affinity chromatography polymer monoliths have for hyphenated affinity chromatography-capillary electrophoresis (CE). Lee's group [52] developed a polymer monolith for immunoaffinity chromatography which was coupled online to a capillary electrophoresis (CE) step. Protein G was immobilised on a poly(GMA-*co*-TRIM) monolith and its capability to extract IgG in a formate/formic acid buffer was demonstrated [52]. The adsorbed IgG was released by injecting a plug of 50 mmol/L formic acidic. Using this method, Lee's group were able to detect IgG in samples with estimated concentrations as low as ~1 nmol/L. This procedure relied on the use external pressure for moving the mobile phase during the adsorption and desorption step, and electrical potential was not applied until after the analyte was eluted beyond the extraction/preconcentration column. However, there was only one analyte in the system, so there was no true electrophoretic separation. Nevertheless, the authors stress that their technique is applicable to any protein for which an antibody is available, and later [53] demonstrated that the binding of IgG was a very specific.

Lee's group expanded on their work by directly coupling the Protein G monolith [52] to a poly(BuMA-*co*-EDMA) monolith for sample enrichment [53]. From an

injection of a sample of 100 µg/L IgG, 5 µg/L lysozyme and 5 µg/L of cytochrome c, the IgG was captured on the Protein G column whilst the other proteins passed through and were extracted/concentrated by the hydrophobic monolith. Their technique then required that the hydrophobic preconcentration capillary be disconnected from the immunoextraction column and then installed in a CE instrument. Following washing, preconditioning and elution [53], the two low-concentration proteins were successfully separated by CE, free from interference by the high abundance protein. In this sense, the affinity chromatography monolith served as a sample cleanup step. The long term goal would be selective removal of all high abundance proteins (depletion) from a complex sample such as serum in order to allow preconcentration of very low abundance proteins downstream. This would be coupled directly to fast, high-resolution CE. Whilst this is a very exciting concept, Lee *et al*. conceed that there is a long way to go. Such a system would require affinity for a wide range of high abundance proteins. Furthermore, the capacity of the affinity extraction would need to be thousands of times that of the preconcentration phase so that it could remove all of the high abundance proteins from the sample stream whilst processing enough sample to allow a significant amount of low abundance proteins to reach the preconcentration monolith. Nevertheless, this is an excellent example of a potential integrated analysis system based on affinity chromatography polymer monoliths. The application of monoliths to the removal of signal-obscuring high abundance proteins is further elaborated in a recent review by Josic and Clifton [4].

Several researchers have used affinity chromatography polymer monoliths for more seamlessly integrated affinity chromatography-CE. Vizioli *et al*.

demonstrated this in 2005 with an IMAC porous polymer monolith [54]. This monolith was prepared by irradiation (γ-rays) of a mixture of GMA and diethylene dimethacrylate. This preparation technique has a disadvantage in the sense that the monolith was not truly prepared *in situ*. Rather, a section of the capillary in which this monolith was prepared was cut out and fixed between pieces of open capillary using PTFE sleeves and epoxy resin. IDA, attached by reaction with the epoxy groups on the monolith surface in a solution of DMSO, was used as a metal-chelating ligand. By treating the IDA-reacted monolith with $CuSO_4$ solution, a Cu(II) loading of 1.55 μg/g of monolith was achieved. The IMAC columns were characterised and were shown to be very effective at selectively retaining peptides with histidine residues. The peptides were eluted by infusing the capillary with a solution containing 5 mmol/L imidazole. Once they were eluted from the monolith, the peptides were separated by electrophoresis in the open capillary downstream of the monolith.

Zhang *et al*. also prepared an Cu(II)-type IMAC column for direct coupling with CE separation [55]. A 1 cm section of poly(GMA-*co*-EDMA) monolith that was prepared *in situ* by thermally initiated free-radical polymerisation was reacted with IDA and loaded with Cu(II) ions. This reaction was achieved in aqueous solution, whereas Vizioli *et al*. had shown that the reaction in DMSO was more efficient [54]. Zhang *et al*. worked with a sample solution of four synthetic peptides and were able to demonstrate sample enrichment to factors of at least several hundred. Their procedure required just two separate electrolytes/eluents and all steps were controlled by voltage rather than pressure. This approach would be helpful if this procedure were to be ported to a μTAS format or to any platform where a pump is not typically included. Both Zhang *et al*. and Vizioli *et*

al. achieved similar RSD values for migration time and peak area: generally less than 5%. However, Vizioli *et al*. reported greater column-column reproducibility.

In a different approach, Yone *et al*. prepared an IMAC monolithic column by attaching iron protoporphyrin IX to monoliths which they prepared by γ-irradiation of a solution of GMA and diethylene glycol dimethacrylate [56]. These monoliths were able to extract angiotensin I by either coordination of histidine groups with the iron chelate or alternatively by π-π stacking of tyrosine or phenylalanine residues with the protoporphyrin itself. The selectivity of the material was confirmed by the fact that an alternative peptide that had no histidine or aromatic groups was not able to be extracted. The angiotensin I sample was introduced into the capillary by pressure and the monolith was then washed for 4 minutes in the separation buffer which consisted of 50 mmol/L phosphate buffer adjusted to pH 7 with HCl. The peptide was released from the monolith by a pressure-driven plug of low pH buffer with 25% acetonitrile, followed by a CE step. The system gave a 10,000 fold improvement in the limit of detection compared to a standard hydrodynamic injection. However, Yone *et al*. did not demonstrate the separation of angiotensin I from any other analytes during the CE step.

1.5 Conclusion

Polymer monoliths are being used for all of the major types of affinity chromatography and they are applied in a wide variety of platforms for a growing range of applications. The numerous successful application demonstrations clearly show that polymer monoliths have sufficient surface area to be effective affinity chromatography sorbents and this factor need not be considered an impediment to widespread adoption of this technology.

Researchers frequently refer to the advantages of polymer monoliths with regards to mass transport, mechanical strength and permeability. However, for affinity chromatography, the stand-out feature of polymer monoliths is perhaps not their performance. Rather, it may be the convenience and scalability of the *in situ* synthesis, which facilitates preparation of columns of any shape and size. In some cases, the ease-of-synthesis was probably the *only reason* that the researchers chose to work with polymer monoliths as opposed to using other types of sorbent. This aspect of polymer monoliths has made them popular research-enabling tools; they are probably the most convenient class of sorbent for testing new separation formats and new chemistry for novel selectivity.

Methacrylate monoliths are the most popular type of monolith due to their favourable morphology, well documented and relatively simple synthesis methods, as well as their relatively low hydrophobicity [2]. Methacrylate monoliths also offer the significant advantage of the fact that they can be spatially defined within the desired section of a microchannel or capillary through simple photomasking. Poly(GMA-*co*-EDMA) monoliths are a very popular choice for affinity chromatography monoliths, particularly those with immobilised protein ligands. However, their popular may be partly the result of a self-fulfilling cycle in which they are assumed to be the most appropriate polymers due to their ubiquity in the literature. It would be helpful if there were more reports that involved direct comparison of the performance of various types of polymer monoliths, as well as other classes of sorbent including silica monoliths. It would also help to see performance comparisons with the less common types of polymer monolith such as those based on poly(TRIM) and epoxy resins. These chemistries have received surprisingly little attention despite having been successfully

demonstrated in a few reports. Numerous successful approaches to ligand immobilisation have been demonstrated and this is another source of confusion which would benefit from more direct experimental comparison.

1.6 References

1. Potter, O. G., Hilder, E. F., *J. Sep. Sci*. 2008, *31*, 1881-1906.
2. Tetala, K. K. R., van Beek, T. A., *J. Sep. Sci*. 2010 *33*, 422-438.
3. Mallik, R., Hage, D. S., *J. Sep. Sci*. 2006, *29*, 1686-1704.
4. Josic, D., Clifton, J. G., *J. Chromatogr., A* 2007, *1144*, 2-13.
5. Thurman, E. M., Mills, M. S., *Solid-Phase Extraction: Principles and Practice*, ed. J.D. Winefordner. 1998, New York: Wiley-Interscience.
6. Li, C., Lee, K. H., *Anal. Biochem*. 2004, *333*, 381-388.
7. Jmeian, Y., El Rassi, Z., *Electrophoresis* 2008, *29*, 2801-2811.
8. Jmeian, Y., El Rassi, Z., *J. Proteome Res*. 2007, *6*, 947-954.
9. Varilova, T., Madera, M., Pacakova, V., Stulik, K., *Curr. Proteomics* 2006, *3*, 55-79.
10. Xu, Y., Cao, Q., Svec, F., Frechet, J. M. J., *Anal. Chem*. 2010, *82*, 3352-3358.
11. Rieux, L., Niederlander, H., Verpoorte, E., Bischoff, R., *J. Sep. Sci*. 2005, *28*, 1628-1641.
12. Allen, D., El Rassi, Z., *Electrophoresis* 2003, *24*, 3962-3976.
13. Svec, F., *J. Chromatogr., B* 2006, *841*, 52-64.

14. Kovarik, P., Hodgson, R. J., Covey, T., Brook, M. A., Brennan, J. D., *Anal*. *Chem*. 2005, *77*, 3340-3350.

15. Hodgson, R. J., Brook, M. A., Brennan, J. D., *Anal*. *Chem*. 2005, *77*, 4404-4412.

16. Feng, S., Pan, C., Jiang, X., Xu, S., Zhou, H., Ye, M., Zou, H., *Proteomics* 2007, *7*, 351-360.

17. Vlakh, E. G., Tennikova, T. B., *J*. *Sep*. *Sci*. 2007, *30*, 2801-2813.

18. Viklund, C., Svec, F., Frechét, J. M. J., *Chem*. *Mater*. 1996, *8*, 744-750.

19. Wang, S., Zhang, R., *Anal*. *Chim*. *Acta* 2006, *575*, 166-171.

20. Stulik, K., Pacakova, V., Suchankova, J., Coufal, P., *J*. *Chromatogr*. *B* 2006, *841*, 79-87.

21. Svec, F., *J*. *Sep*. *Sci*. 2005, *28*, 729-745.

22. Roberts, M. W. H., Ongkudon, C. M., Forde, G. M., Danquah, M. K., *J*. *Sep*. *Sci*. 2009, *32*, 2485-2494.

23. Svec, F., Peters, E. C., Sykora, D., Frechet, J. M. J., *J*. *Chromatogr*. *A* 2000, *887*, 3-29.

24. Yu, C., Davey, M. H., Svec, F., Frechet, J. M. J., *Anal*. *Chem*. 2001, *73*, 5088-5096.

25. Nischang, I., Brueggemann, O., Svec, F., *Anal*. *Bioanal*. *Chem*. 2010, *397*, 953-960.

26. Nischang, I., Svec, F., FreÌ• chet, J. M. J., *Anal*. *Chem*. 2009, *81*, 7390-7396.

27. Rogeberg, M., Wilson, S. R., Greibrokk, T., Lundanes, E., *J. Chromatogr. A*, *1217*, 2782-2786.

28. Chen, J.-L., Lin, Y.-C., *J. Chromatogr. A*, *1217*, 4328-4336.

29. Oleschuk, R., Shultz-Lockyear, L., Ning, Y., Harrison, D. J., *Anal. Chem.* 2000, *72*, 585-90.

30. Baryla, N. E., Toltl, N. P., *Analyst* 2003, *128*, 1009-1012.

31. Saunders, K. C., Ghanem, A., Hon, W.-B., Hilder, E. F., Haddad, P. R., *Anal. Chim. Acta* 2009, *652*, 22-31.

32. Bencina, K., Podgornik, A., Strancar, A., Bencina, M., *J. Sep. Sci.* 2004, *27*, 811-818.

33. Vlakh, E., Ostryanina, N., Jungbauer, A., Tennikova, T., *J. Biotechnol.* 2004, *107*, 275-284.

34. Okanda, F. M., El Rassi, Z., *Electrophoresis* 2006, *27*, 1020-1030.

35. Pflegerl, K., Podgornik, A., Berger, E., Jungbauer, A., *J. Comb. Chem.* 2002, *4*, 33-37.

36. Mallik, R., Jiang, T., Hage, D. S., *Anal. Chem.* 2004, *76*, 7013-7022.

37. Bedair, M., El Rassi, Z., *J. Chromatogr. A* 2004, *1044*, 177-186.

38. Bedair, M., El Rassi, Z., *J. Chromatogr. A* 2005, *1079*, 236-245.

39. Pan, Z., Zou, H., Mo, W., Huang, X., Wu, R., *Anal. Chim. Acta* 2002, *466*, 141-150.

40. Hahn, R., Podgornik, A., Merhar, M., Schallaun, E., Jungbauer, A., *Anal. Chem.* 2001, *73*, 5126-5132.

41. Dhal, P. K., Vidyasankar, S., Arnold, F. H., *Chem*. *Mater*. 1995, *7*, 154-162.

42. Rohr, T., Hilder, E. F., Donovan, J. J., Svec, F., Fréchet, J. M. J., *Macromolecules* 2003, *36*, 1677-1684.

43. Feng, S., Yang, N., Pennathur, S., Goodison, S., Lubman, D. M., *Anal*. *Chem*. 2009, *81*, 3776-3783.

44. Satterfield, B. C., Stern, S., Caplan, M. R., Hukari, K. W., West, J. A. A., *Anal*. *Chem*. 2007, *79*, 6230-6235.

45. Manz, A., Graber, N., Widmer, H. M., *Sens*. *Actuators, B* 1990, *B1*, 244-8.

46. Anonymous Promotional Article, *Proteomics* 2005, *5*, 1738.

47. Liu, C.-H., Ma, W.-L., Shi, R., Zhang, B., Ou, Y.-Q., Zheng, W.-L., *Br J Biomed*. *Sci*. 2003, *60*, 22-5.

48. Mao, X., Luo, Y., Dai, Z., Wang, K., Du, Y., Lin, B., *Anal*. *Chem*. 2004, *76*, 6941-6947.

49. Yu, C., Xu, M., Svec, F., Frechet, J. M. J., *J*. *Polym*. *Sci*. *Part A: Polym*. *Chem*. 2002, *40*, 755-769.

50. Yang, Y., Li, C., Lee, K. H., Craighead, H. G., *Electrophoresis* 2005, *26*, 3622-3630.

51. Bedair, M., Oleschuk, R. D., *Analyst* 2006, *131*, 1316-1321.

52. Armenta, J. M., Gu, B., Humble, P. H., Thulin, C. D., Lee, M. L., *J*. *Chromatogr*. *A* 2005, *1097*, 171-178.

53. Armenta, J. M., Gu, B., Thulin, C. D., Lee, M. L., *J*. *Chromatogr*. *A* 2007, *1148*, 115-122.

54. Vizioli, N. M., Rusell, M. L., Carbajal, M. L., Carducci, C. N., Grasselli, M., *Electrophoresis* 2005, *26*, 2942-2948.

55. Zhang, L., Zhang, L., Zhang, W., Zhang, Y., *Electrophoresis* 2005, *26*, 2172-2178.

56. Yone, A., Rusell, M. L., Grasselli, M., Vizioli, N. M., *Electrophoresis* 2007, *28*, 2216-2218.

2 Polymer Monoliths for Boronate Affinity Chromatography

2.1 Introduction

Boronate affinity chromatography (BAC) is typically used for highly selective separations of cis-vicinal coplanar diols and is suitable for a wide range of applications in both research and clinical diagnostics. Compounds containing 1,2 and 1,3 cis diol groups are selectively bound on boronate stationary phases. The mechanism of the binding interaction is widely explained as the reversible formation of anionic cyclic boronate esters as shown in Figure 2.1, however some aspects of this mechanism are still under investigation [1].

The boronate ligand also has strong affinity for nitrogen-containing Lewis bases in aprotic solutions thus enabling trapping of nucleosides and other metabolites in non-aqueous solvents [1, 2].

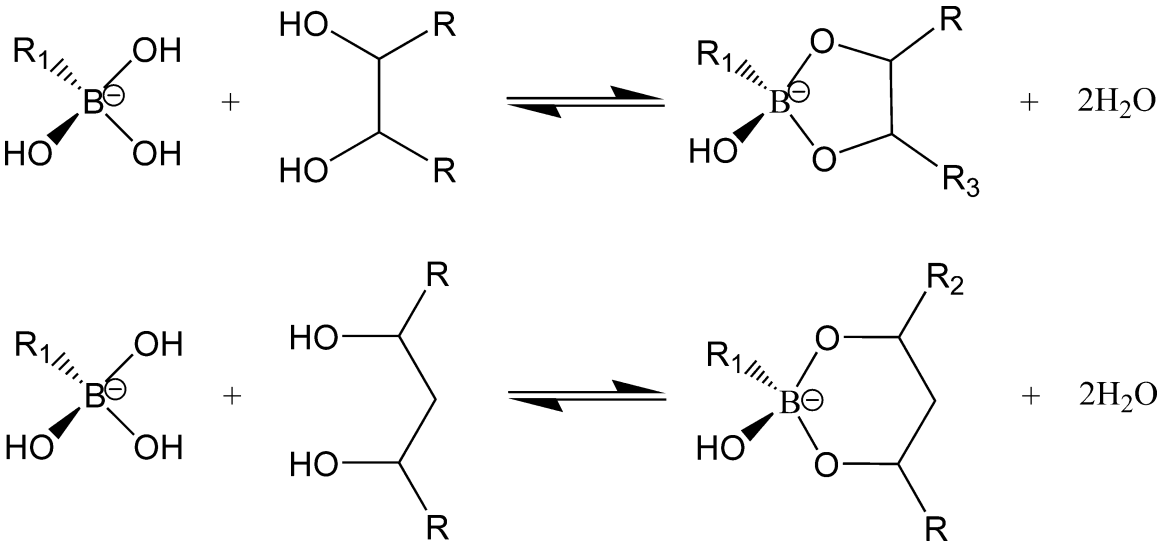

Figure 2.1 – Popular model of the interaction between boronate groups and cis 1,2 and 1,3 diols, based on the formation of cyclic boronate esters.

Highly selective solid phase extraction of diols is the most important application of BAC. This is typically carried out as an off-line sample preparation step for the purposes of sample cleanup or enrichment. Common applications include extractions of nucleosides [1-4], nucleotides [5], catecholamines [6-8], and glycated proteins from blood and tissue samples [9-11], as well as extraction of glycated peptides from tryptic digests [12-14]. The boronate affinity interaction can also be used as a complement to lectin affinity chromatography for the extraction of glycosilated proteins, and this is often seen as the most exciting potential application for BAC [15]. Numerous other applications were described in a recent review [16] and further information is available in the *Encyclopedia of Separation Science* [17].

The majority of boronate affinity extractions are currently practiced using a handful of commercially available boronate affinity sorbents. Two of the most popular sorbents are Affigel 601 beads (Bio-Rad, Hercules, CA, USA), which are based on slightly crosslinked porous polyacrylamide, and phenylboronic acid substituted agarose (GE Life Sciences, Uppsala, Sweden). Whilst these products set the standard in terms of capacity and selectivity, they are soft swollen polymers and therefore can only be used for off-line sample preparation under very low pressure conditions such as gravity driven flow. The literature presents several examples of phenylboronate sorbents based on non-porous agarose beads [11], chitosan [18], carboxymethylcellulose [8], and wall coatings for open tubular formats [19]. Rigid highly crosslinked macroporous polymer-based packing materials such as ProSphere™ Boronate (Alltech Associates Inc., Deerfield, IL, USA) [1] and TSK Boronate-5PW Gel (Tosoh Bioscience LLC, Tokyo, Japan) [20] as well as phenylboronate functionalised silica beads [4, 5, 7]

can be packed in HPLC columns and used at higher flow rates and back pressures. One interesting and recent addition to this list is a boronate functionalised highly ordered particulate mesoporous silica material, however this material was not packed and was instead employed by suspension incubation and centrifugation [21].

As discussed in the previous chapter, porous polymer monoliths afford a number of advantages compared to particulate stationary phases and there is therefore a compelling case for the development of monolithic materials for solid phase extraction [22, 23]. First, the relatively high porosity and convection dominated mass transport in polymer monoliths reduce flow-resistance allowing them to be used with high linear flow rates whilst maintaining separation efficiency, potentially leading to more rapid extraction procedures than would be achieved with packed particle stationary phases. Meanwhile, the *in situ* preparation of polymer monoliths within a column, capillary or channel, may in many cases be more facile than packing particulate media. Furthermore, polymer monoliths can also be patterned with a variety of functionalities by photoinitiated grafting processes, allowing a single monolith to perform a sequence of functions in an analysis process [24, 25], which could be particularly useful in the complex and integrated microscale analytical devices (μTAS) that have been touted as heralding a new age of affordable point-of-care diagnostic devices [26, 27]. Together, these advantages could all be highly relevant to BAC in miniaturized systems. The work described in this chapter was carried out in order to address the fact that there was no report nor method for a porous monolithic boronate affinity stationary phase in the literature when this research project commenced.

This chapter introduces methods for the preparation of polymer monolith boronate sorbents using poly(butyl methacrylate-*co*-ethylene dimethacrylate) as the starting monolith which is prepared by a rapid and convenient photoinitiated polymerization. A layer of poly(glycidyl methacrylate) is then formed on the pore surface by means of a recently demonstrated two-step photografting process [24, 28]. The work described in this chapter builds on previous investigations by the author into boronate affinity monoliths that were undertaken in an undergraduate project [29] and which later formed part of a paper that was published in *The Analyst* (Cambridge, UK) [30]. In that report, polymer monoliths were formed by thermal polymerisation of a copolymer of glycidyl methacrylate and ethylene dimethacrylate. The monoliths were then functionalised by reaction with 4-hydroxyphenylboronic acid in the presence of triethylamine and acetonitrile. Some monoliths were first modified using a 1-step photoinitiated grafting step prior to functionalisation in which a layer of glycidyl methacrylate was formed on the pore surface. The grafting procedure resulted in an increase in ligand density which was observed as a doubling in the selective retention factor of ribonucleosides.

The polymer monoliths developed in this PhD project and described in this chapter are copolymers of butyl methacrylate as opposed to the glycidyl methacrylate monoliths described in that work. The switch to butyl methacrylate copolymers was made because the butyl methacrylate copolymer is a superior substrate for the new photografting methods described in this chapter which are dependant on the presence of methylene hydrogens [24]. Furthermore, whilst irreversible blockages were frequent both during and after the preparation and functionalisation of the glycidyl methacrylate copolymer materials, this problem

was hardly ever encountered when working with the butyl methacrylate copolymer based material reported herein. In addition to functionalisation methods of the epoxide groups using 4-hydroxyphenylboronic acid (HPBA) [30], a new functionalisation approach employing reaction with an aqueous solution of aminomethylphenylboronic acid (AMPBA) was trialed. The loading capacity and selectivity of these monoliths was investigated by applying them to BAC of nucleosides and glycated peptides, continuously monitored by UV absorbance and ESI-MS detection.

2.2 Experimental

2.2.1 Equipment

Polyimide coated and PTFE coated fused silica capillaries were purchased from Polymicro Technologies (Phoenix, Arizona, USA). Capillaries with the UV-transparent PTFE coating was used for the monolithic capillary columns and for the section of capillary that was inserted into the UV absorbance detector.UV irradiation was performed using an OAI Model 30 deep UV collimated light source (San Jose, CA, USA) fitted with a 500 W HgXe lamp. The intensity was adjusted to 11.5 mW/cm^2 using an OAI Model 306 UV power meter with a 260 nm probe head.

Micrographs were taken using a S-4300 SE/N Scanning Electron Microscope (Hitachi High Technologies America, Pleasanton, CA, USA). Prior to characterisation by scanning electron microscopy, monolithic columns were washed first with water, then with methanol and dried by purging with air. The capillaries were cut at two different points and sputtered with gold to a layer thickness of 20 nm.

2.2.2 Reagents

Butyl methacrylate (BuMA) 99%, ethylene dimethacrylate (EDMA) 98%, glycidyl methacrylate (GMA) 97%, 3-(trimethoxysilyl)propyl methacrylate 98% (with 1 % methanol), decanol >99%, cyclohexanol 99%, 2,2-dimethoxy-2-phenylacetophenone 98% (DMPAP), benzophenone 99%, methanol (Chromasolv Plus for HPLC 99.9%), diethylenetriaminepentaacetic acid dianhydride 98%, toluene >99%, 4-hydroxyphenylboronic acid (HPBA), sodium bicarbonate 99.7%, sodium phosphate (dibasic) 99%, HCl (37% in water, 99.999%), eleven nucleoside test mix and HEPES 99.5% were purchased from Sigma-Aldrich (St Louis, MO, USA). Reagent grade triethylamine and HPLC grade acetone 99.6% were obtained from Fischer Scientific (Hampton, NH, USA). 4-Aminomethylphenylboronic acid hydrochloride (AMPBA·HCl) was received from Combi-Blocks (San Diego, CA, USA) and sodium carbonate 99.5%, sodium phosphate (monobasic) >98%, ammonium hydroxide solution 28-30% and glacial acetic acid 99.7% were from EMD Chemicals (Gibbstown, NJ, USA) while LC-MS grade acetonitrile was from Riedel de Haan (Seelze, Germany).

Pepstatin A 79%, Phe-Gly-Phe-Gly, 2-deoxcytidine monohydrate 99% and 2-deoxyguanosine 99% were purchased from Sigma-Aldrich. Cytidine 99% and guanosine 99% were from Fluka, (St Louis, MO, USA).

2.2.3 Preparation of Monolithic Capillary Columns

The polymerisation mixture for the preparation of poly(BuMA-*co*-EDMA) monoliths was adopted from previous work [31] and the conditions were selected to afford a monolithic structure with a pore size of about 1 μm. The polymerisation mixture comprised of 42.9 wt % decanol, 16.9 wt % cyclohexanol,

15.9 wt % EDMA, 23.9 wt % BuMA and 0.4 wt % 2,2-dimethoxyacetophenone. A single batch of this mixture was used for all monoliths described in this report. This solution was de-oxygenated by sonication and purging with nitrogen gas for 10 minutes prior to infusion into 100 μm i.d. PTFE-coated fused silica capillaries that had been vinylized on the inner wall using a process described elsewhere [31]. Free radical polymerisation was then initiated by exposing the capillaries to UV light for 15 min at a distance of 32 cm from the collimating lens. Lamp intensity was set so that the intensity in the centre of the collimated region was 11.5 mW/cm^2. The capillaries were then removed and the porogens were washed out by flushing the capillary with methanol at a flow rate of 30 μL/hr for several hours.

2.2.4 Grafting of Monolithic Capillary Columns

A previously reported two-step sequential photoinitiated grafting including activation and polymerization [24, 28] was adapted to functionalise the pore surface of the monoliths. A solution of 5% benzophenone in methanol was sonicated and purged with nitrogen for 5 min. This solution was then pumped through the monolithic capillary columns using a syringe pump for at least 30 min. The ends of the capillaries were then sealed with rubber septa and exposed under the UV light for 120 s at an intensity of 11.5 mW/cm^2. Following this, the capillaries were flushed with methanol for 30 min. Next, a solution of 0.079 g of glycidyl methacrylate was made up to 5 mL in water then sonicated and purged with nitrogen for 5 min. This solution was pumped through the pre-activated monolithic capillary columns for 30 min. The ends of the capillaries were then sealed with rubber septa and irradiated with the UV light for 60 s using the same

conditions as above. The capillary columns were then washed with methanol for several hours.

2.2.5 Functionalisation of Capillary Columns

Two types of solutions were prepared for two alternative functionalision reactions. The first, similar to that described in the previous communication in *The Analyst* [30] was composed of 0.069 g HPBA, 0.22 mL of triethylamine and 0.75 g acetonitrile. This reaction solution is based on previous experience in immobilizing para-hydroxy aromatic compounds [32]. The second solution consisted of 0.0154 g of AMPBA·HCl dissolved in a buffer that was prepared from 0.40 mol/L sodium carbonate with 0.10 mol/L sodium bicarbonate. This choice of reaction solution is based on the experiences of colleagues with immobilizing amines in high pH aqueous solutions [33]. The respective functionalisation solutions were briefly sonicated to completely dissolve the phenylboronate reagents. The solutions were then purged with nitrogen for 5 min and pumped through the monolithic columns at a flow rate of 0.3 µL/min for 18 h whilst being heated to 60 °C in a column oven. The columns were then washed for several hours using the mobile phase before they were used for chromatography.

2.2.6 Chromatography

LC-UV experiments and back pressure measurements were performed using an Agilent 1200 Series Capillary Pump G1376A, an Agilent A/D Converter 35900E and a Linear™ UVIS-205 Detector (Santa Clara, CA, USA). The monolithic capillary columns were trimmed to 15 cm and attached directly to the injection valve. The other end of the column was attached by a zero dead-volume PEEK

union (Upchurch Scientific, Oak Harbor, WA, USA) to a 100 cm long 75 µm I.D. PTFE coated fused silica capillary. The detection beam passed through the PTFE coated capillary at 5.0 cm after the PEEK union, creating a dead volume of 221 nL between the end of the monolithic column and the point of detection. All breakthrough experiments were conducted at 1.00 µL/min using a 0.50 mol/L HEPES buffer adjusted to pH 9.0 using NaOH. The sample loop consisted of 2.0 m of 100 µm I.D. polyimide coated capillary. This large volume was necessary for the breakthrough experiments. 2-Deoxycytidine (0.50 mmol/L) and cytidine (0.50 mmol/L) solutions in the HEPES buffer were loaded into the sample loop prior to the breakthrough experiments.

LC-MS work was carried out using an Agilent 1200 Series Nano Pump G2226-90010 connected through the microspray ESI to micrOTOF-Q MS (Bruker Daltonik, Bremen, Germany). The settings used were: nebulizer; 0.4 bar, drying gas; 4 L/min, drying temperature; 190 ° C, ESI voltage; 4 kV, end plate offset; 500V, positive ion mode with an m/z range of 150 – 450 for the nucleoside analysis and 300 – 800 for the peptides. The monolithic capillary column was trimmed to 15 cm and attached directly to the injection valve. At the distal end the column was attached via a zero-dead-volume PEEK union to a 40 cm long 25 µm I.D. polyimide coated fused silica capillary that was plumbed into the ESI MS source. The pump was operated continuously at 1.00 µL/min using a 0.10 mol/L ammonium hydroxide buffer adjusted to pH 9.0 using acetic acid. The sample loop consisted of 50 cm of 100 µm I.D. polyimide coated fused silica capillary and was used both for the loading and introduction of samples as well as for the loading and introduction of washing and desorption buffers.

Three different injection and elution programs were used: Program A: Sample injection began at 6 s and continued until 60 s. The column was then washed in 0.1 mol/L ammonium acetate adjusted to pH 9 until 105 s at which time the eluent was switched to 0.1 mol/L acetic acid adjusted to pH 4 with ammonium hydroxide.

Program B: Sample injection began at 6 s and continued until 60 s. The column was then washed with 0.10 mol/L ammonium acetate adjusted to pH 9 until 80 s. A plug of a 1:1 mixture of acetonitrile with 0.10 mol/L ammonium acetate pH 9 was then flushed through the column (using a large sample loop) until 140 s, at which point the eluent was switched back to the ammonium acetate buffer. At 160 s the eluent was changed to 0.10 mol/L acetic acid adjusted to pH 4.

Program C: Sample injection began at 6 s and continued until 120 s. The column was then washed with 0.10 mol/L ammonium hydroxide adjusted to pH 9 until 180 s at which time the eluent was switched to 0.10 mol/L acetic acid adjusted to pH 4.

A 6-port injection valve, model MXP7980-000 from Rheodyne (Rohnert Park, CA, USA) was operated via relay contacts for the LC-UV work and via manual control for the LC-MS work.

2.2.7 Preparation of glycated peptide

Glycated peptide standards were prepared by an adaptation of the procedure reported by Brock *et al*. [34]. Phe-Gly-Phe-Gly (2.4 mg) was dissolved in 1.0 mL of a solution containing 0.40 mol/L D-glucose, 1 mmol/L diethylenetriaminepentaacetic acid and phosphate buffer at pH 7.4 (0.152 mol/L Na_2HPO_4 and 0.048 mol/L NaH_2PO_4). This solution was vortexed and purged

with nitrogen for 2 min. 500 μL of the solution was then transferred to an Eppendorf vial and 1 drop of toluene was added. The solution was then re-purged with nitrogen for 10 s before the vial was capped and placed in an airtight plastic container from which the air was displaced by nitrogen. This container was then held in a water bath at 37 °C for 24 h. The Phe-Gly-Phe-Gly and glycated Phe-Gly-Phe-Gly were then extracted in a C18 Bakerbond™ cartridge (Mallinckrodt Baker, Griesheim, Germany), eluted with 50% aqueous acetonitrile containing 0.1% formic acid and these standards were then frozen for storage. A sample solution was prepared by diluting one part of this eluted fraction with 50 parts of 0.10 mol/L ammonium hydroxide buffer adjusted to pH 9 with acetic acid.

2.3 Results

2.3.1 Physical characterization

Physical characterisation of the polymer monoliths is important in assessing the success of the various synthesis and functionalisation steps. The SEM image (Figure 2.2, top) show a poly(BuMA-*co*-EDMA) monolith with good attachment to the inner capillary wall, which is maintained even after the monolith has been photografted and functionalised (Figure 2.2, bottom). The structure of the monoliths appears to be quite uniform across the cross-section, although there does appear to be a slight change in globule shape at one end of each cross-section compared to the other. It is not clear whether this slight change is a genuine feature of the monoliths (perhaps an effect of the orientation during photoinitiation) or whether it is merely an artifact of the capillary cutting procedure that was used to expose the cross-sections.

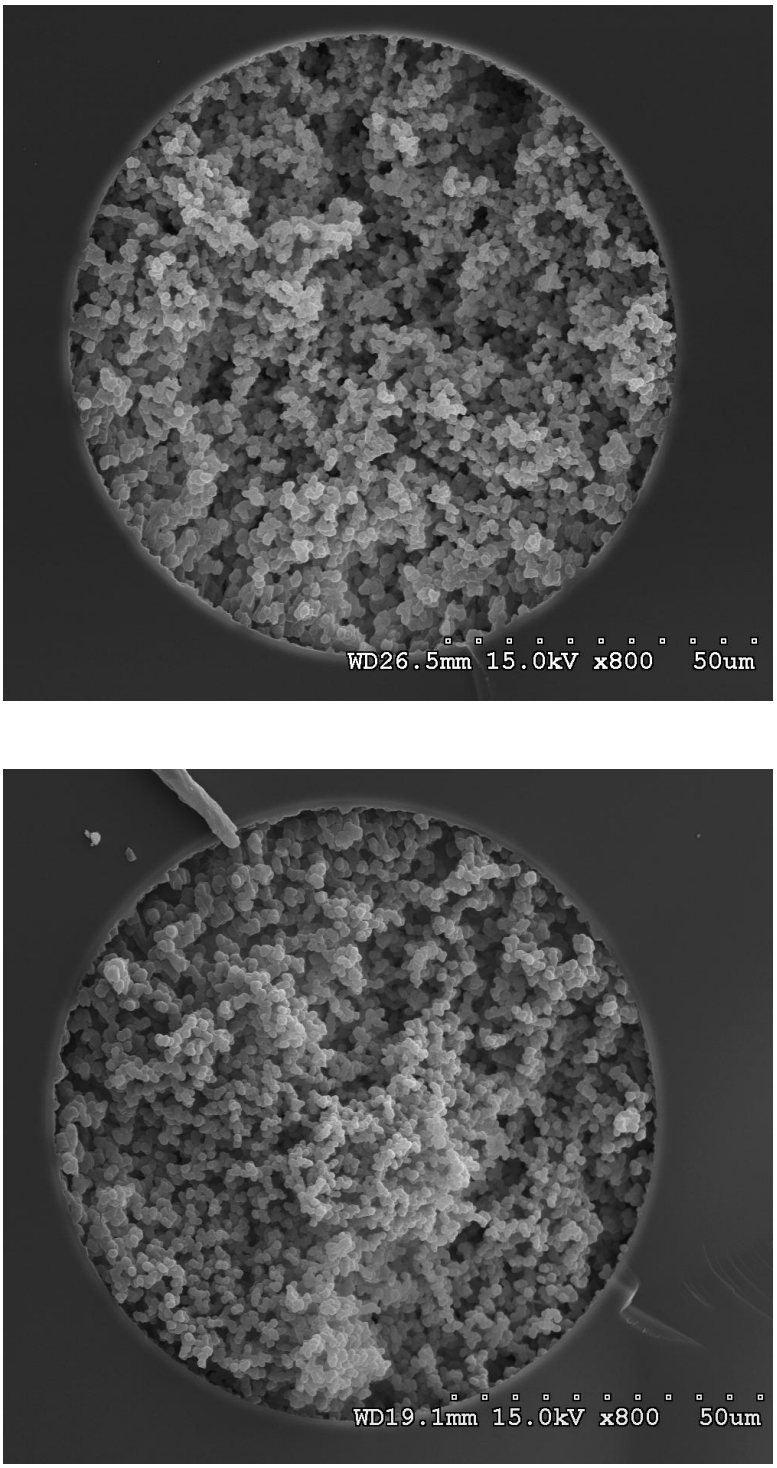

Figure 2.2 – Scanning electron micrographs of cross-sections of unmodified poly(BuMA-co-EDMA) monolith (top) and a HPBA reacted, poly(GMA) grafted poly(BuMA-co-EDMA) monolith (bottom).

The SEM images of the original and functionalised, grafted monoliths presented in Figure 2.2 do not show significant differences in the structure of the monolith on the micrometre scale. However, at greater magnification (Figure 2.3) it can be seen that there is a difference in the fine structure at the surface of individual microglobules. Specifically, the surface texture of the grafted monolith (bottom) is smoother with less obvious roughness on the sub 100 nm scale. This must result from the fact that surface is covered with a layer of functionalised poly(glycidyl methacrylate). While this layer is presumably solvated in the solvent, it may create a featureless structure after the solvent is removed during sample preparation for SEM.

In spite of the fact that the functionalised grafted layer is difficult to observe in SEM micrographs, it had a profound effect on flow-resistance during LC operation when the grafted polymer chains are solvated. Figure 2.4 shows pressure drop as a function of flow rate for grafted monoliths functionalised with HPBA and AMPBA, respectively. The resistance to flow of the HPBA monolith in 50 mmol/L pH 9 HEPES buffer is already rather high and increases by a factor of more than three when pure water is used as the mobile phase. In addition, it requires several hours to reach a stable back pressure after the mobile phase was changed. This suggests that swelling of the grafted layer depends on ionic strength of the solvent. Such a large difference in flow resistance also implies that a large quantity of boronate functionalised polymer is present, forming a layer which has a thickness after swelling that is commensurate with the pore size. It is likely that this significant swelling results from conversion of the epoxides to ionizable groups including the boronate functionalities which result from coordination of the boron to OH^- ions in the alkaline buffer. There is evidence

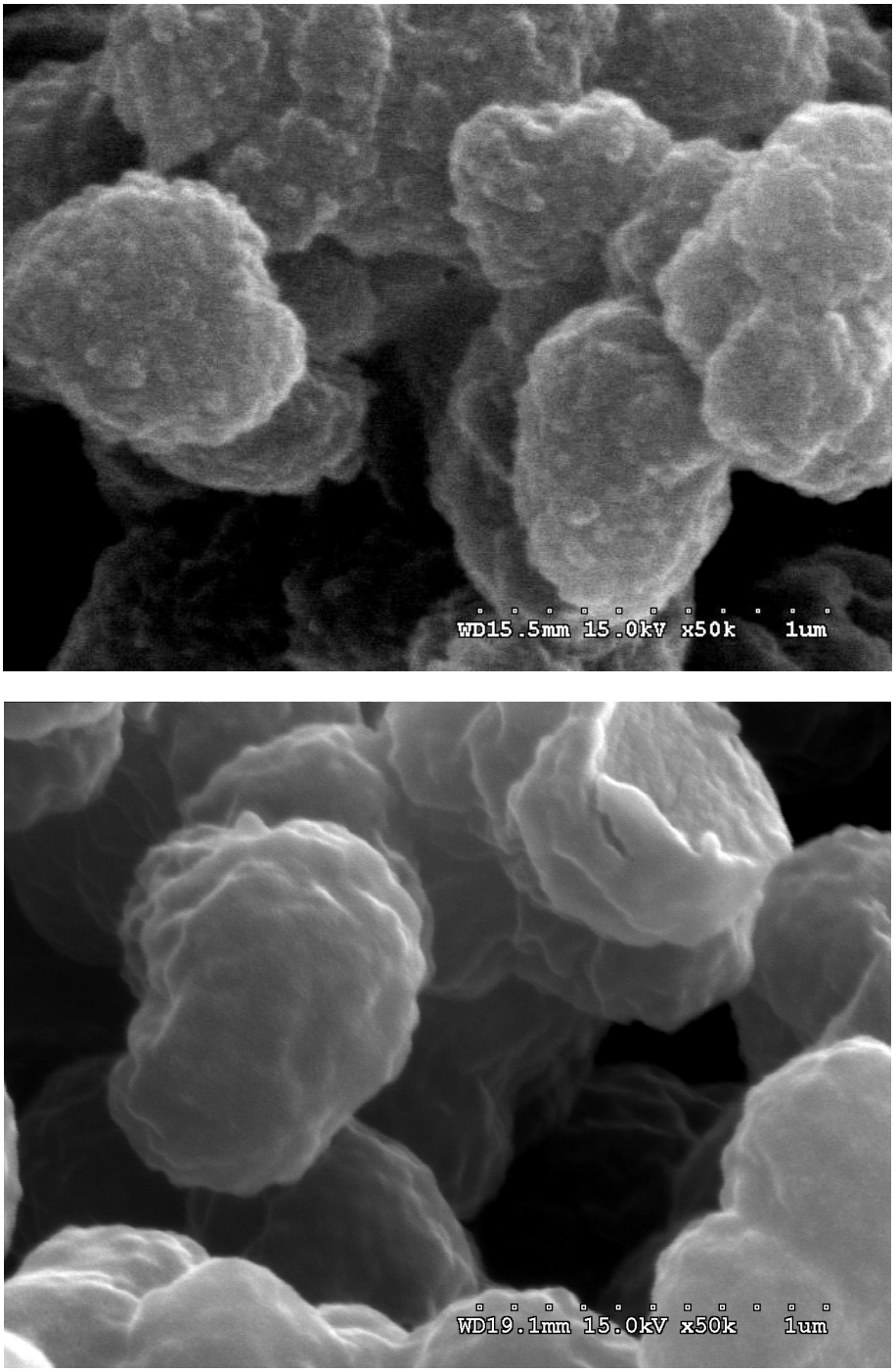

Figure 2.3 – Close-up scanning electron micrographs of unmodified poly(BuMA-co-EDMA) monolith (top) and a HPBA reacted, poly(GMA) grafted poly(BuMA-co-EDMA) monolith (bottom).

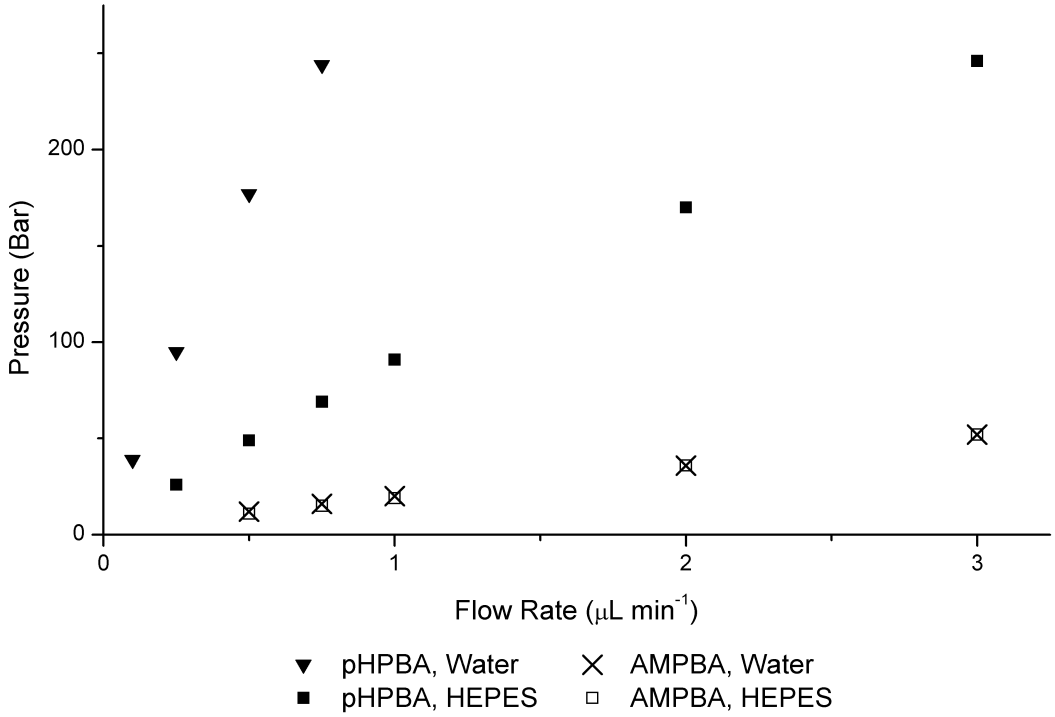

Figure 2.4 – Effect of flow rate on back pressure in monolithic columns modified with HPBA and AMPBA. Conditions: Monolithic capillary column: 15 cm x 100 μm I.D., mobile phase: water and 50 mmol/L HEPES adjusted to pH 9 with NaOH.

that the reaction used can also lead to nucleophilic ring-opening substitution by triethylamine resulting in quaternary ammonium cations [30]. Swelling caused by either or both of these two ionizable groups then explains why higher resistance to flow is encountered in water, which has much lower ionic strength than the buffer. Figure 2.5 illustrates the proposed swelling effect on the grafted, HPBA functionalised monoliths. Ionic strength dependant swelling of solvated charged polymers is known as the "polyelectrolyte effect" [35].

In contrast, back pressure exhibited by the monolith functionalised with AMPBA does not change no matter what aqueous solution is used. This suggests that the reaction of AMPBA with the epoxide rings is not very efficient and the monolith does not contain too many ionizable functionalities. This difference may explained by poor wetting of the poly(GMA) layer by aqueous carbonate buffer used for the AMPBA reaction thus affording a lower conversion of epoxide groups. The glycidyl groups in the poly(GMA) are hydrophobic and may form an impenetrable layer during the functionalisation process so that only the outermost epoxide groups are available for conversion. The poorly-functionalised poly(GMA) layer does not exhibit an ionic strength dependant conformation change effect because it has only a relatively small number of charged groups.

2.3.2 Chromatographic characterisation

Figure 2.6 shows breakthrough curves for unretained 2-deoxycytidine and the selectively retained cytidine using three HPBA monoliths operated at a flow rate of 1.00 μL/min. The first two cytidine breakthroughs are from two monoliths that were grafted and functionalised in tandem, whereas the breakthrough at ~ 7.5 minutes was observed for a monolith that was grafted and functionalised separately from freshly prepared grafting and functionalisation solutions. Whilst

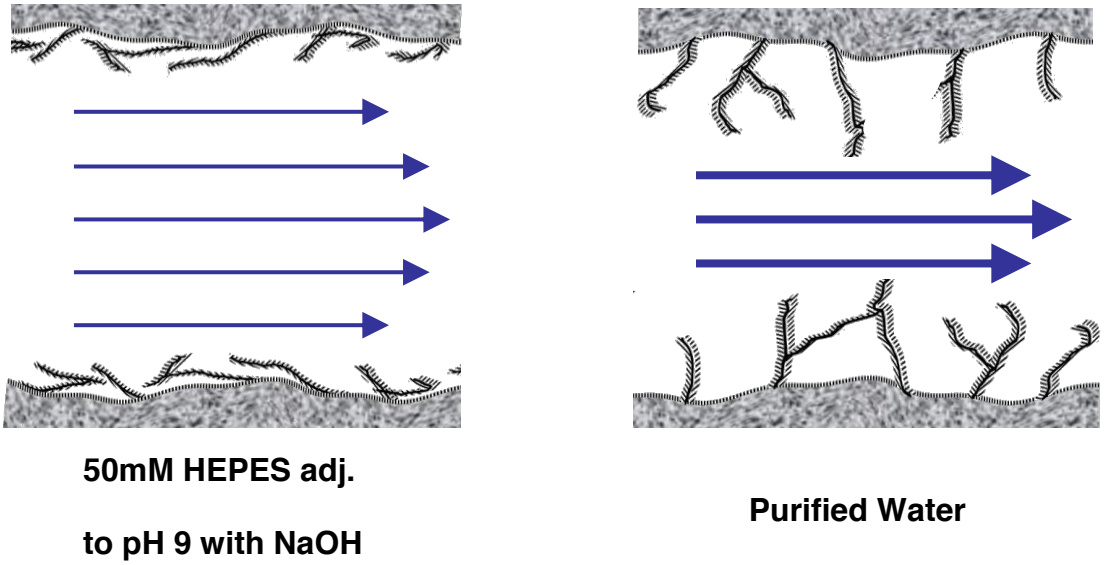

Figure 2.5 – Artistic impression of swelling in the grafted, functionalised layer on the globule surface of the monoliths.

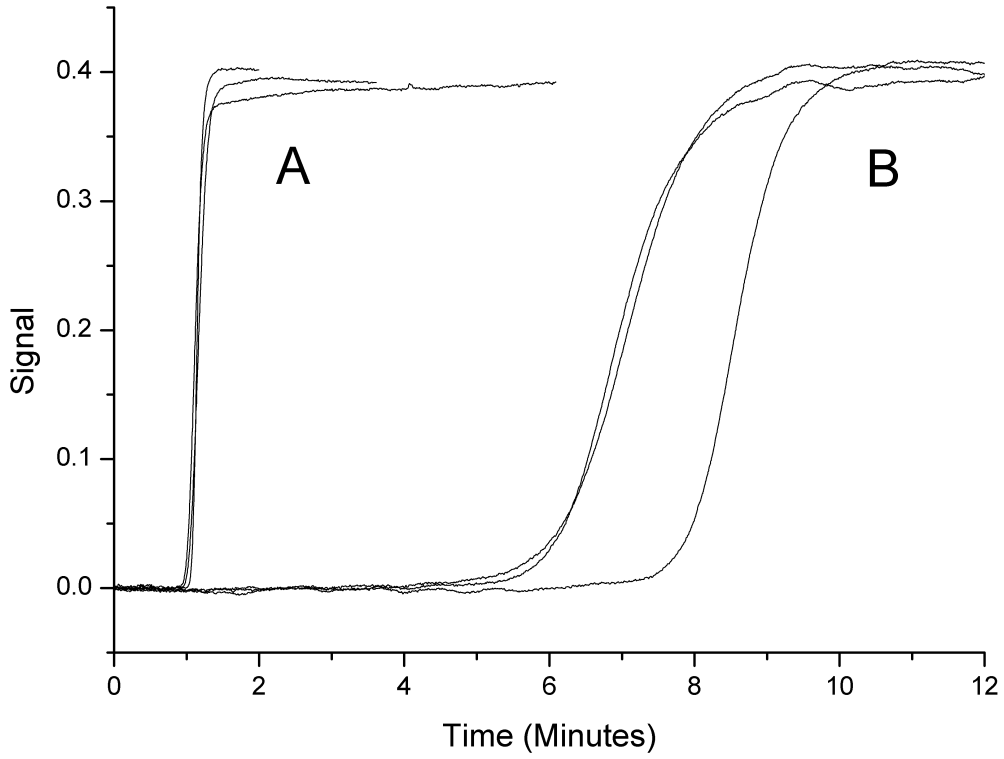

Figure 2.6 – Breakthrough curves for 0.50 mmol/L 2-deoxycytidine (A) and cytidine (B) dissolved in 0.50 mol/L HEPES buffer adjusted to pH 9 with NaOH. Conditions: Monolithic column 15 cm x 100 µm I.D., flow rate 1 µL/min, UV detection at 280 nm.

the plan had been to use thiourea as a void marker, it was found that 2-deoxycytidine actually eluted slightly earlier than thiourea and therefore 2-deoxycytidine breakthrough curve was chosen as void time. The dead volume of 221 nL between the end of the column and the detector has been subtracted from the breakthrough curve data for the purpose of calculating numerical chromatographic properties. The three HPBA monoliths used in the measurements have an average void of 0.822 ± 0.015 µL, suggesting a porosity of 70%. This is is higher than the 60% porosity that might be expected based on the content of porogens in the polymerisation mixture, most likely because of the shrinkage typical of polymerisations of vinylic monomers. Taken at 5 % of breakthrough, the HPBA monolithic colums have an average cytidine capacity of 2.7 ± 0.5 nmol or 2.3 ± 0.5 µmol/mL. This value compares well with 3-aminophenylboronic acid polymer resin available from Sigma-Aldrich that has a specific capacity of 10 µmol/mL for ribose [36]. It is worth noting that the capacity of the HPBA monoliths was determined using cytidine which is a relatively large and sterically hindered analyte compared to ribose; the capacity for ribose would most likely be higher.

The AMPBA functionalised monolith had a significantly lower capacity of 0.04 nmol of cytidine, equivalent to a specific capacity of just 0.03 µmol/mL. Although it had initially been expected that the aliphatic amine group of AMPBA would be a more potent nucleophile than the phenoxide generated from HPBA, this hypothesis was not supported in the result. The difference may also be due to the poor wetting achieved with the aqueous AMPBA grafting solution compared to the acetonitrile solution used for the HPBA reaction. This is the same

explanation that was proposed above for the difference in swelling of the two differently functionalised grafted layers.

The breakthrough curves for cytidine were recorded at flow rates of 0.25, 0.50, 1.0 and 2.0 μL per minute, corresponding to linear flow velocities of 4.6, 9.2, 18 and 36 cm min^{-1}, respectively. As can be seen in Figure 2.7, there was very little variation in loading capacity when measured at 50% of breakthrough for these different flow rates. This reflects the rigidity of the monolith and suggests that the availability of functional groups in the grafted layer is not significantly altered by the increase in flow rate and pressure. On the other hand, the breakthrough zones are broader at higher flow rates and this suggests that the rate of mass transport plays a dominant role in chromatographic performance at these flow velocities.

2.3.3 Demonstration of BAC-MS of urinary nucleosides

The general selectivity of the HPBA functionalised monolith for nucleosides was demonstrated by trapping and releasing eleven different nucleosides in a commercial test mixture. The monolithic column was directly connected to an ESI-MS system to afford identification of the various nucleosides. Figure 2.8 shows extracted ion chromatograms corresponding to the nine different expected masses of the 11 nucleosides in the test mix (two pairs of nucleosides shared the same mass). At least 9 nucleosides were successfully trapped in pH 9 buffer and eluted in tight bands at the expected time by introduction of pH 4 buffer. The problem of insufficient $[M+H]^+$ signals for some nucleosides was alleviated by monitoring the sodium adducts.

Likely applications of the monolith require selective retention of the nucleosides in the presence of a complex sample matrix. Human urine is likely to be the most

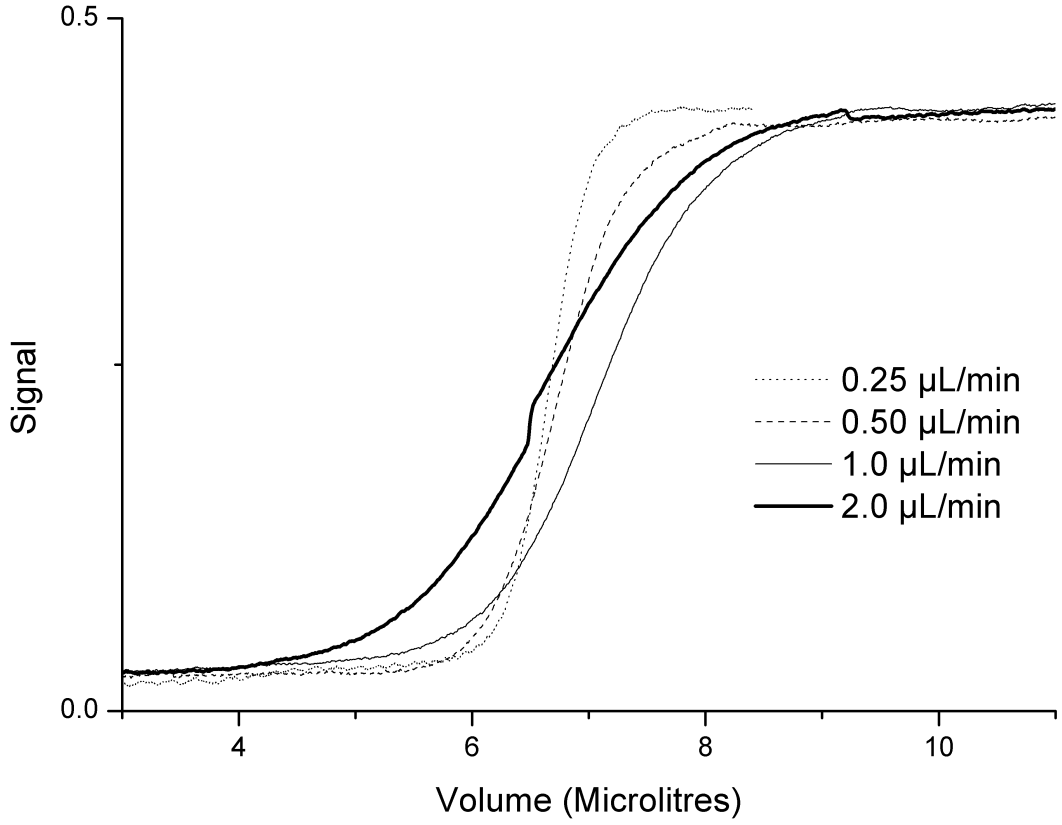

Figure 2.7 - Breakthrough curves for 0.5 mM cytidine at four different flow rates.

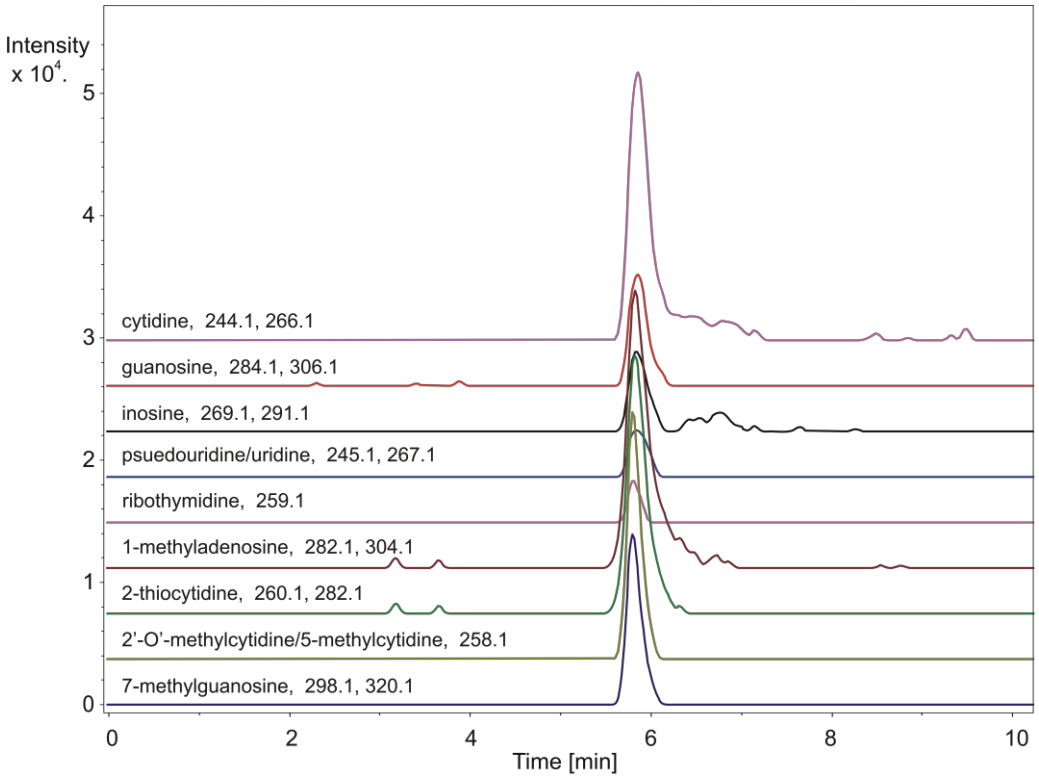

Figure 2.8 – Extraction of nucleosides from a test mixture by a HPBA monolithic capillary column using program C (see materials and methods section). Conditions: column size 15 cm x 100 µm ID, flow rate 1.00 µL/min. Mass range windows were ± 0.05. The concentration of nucleosides in sample was approximately 1 µg/mL.

important sample matrix for diagnostic analysis because urinary nucleosides are gaining attention as biomarkers for cancer and AIDS [37, 38]. They are typically present at low concentrations and it is therefore highly advantageous to selectively enrich them.

The nucleoside text mix was mixed 1:1 with human urine. Due to concerns about the potentially contaminating effect of the high sodium content of the urine and the nucleoside test mix on the MS equipment, it was necessary to dilute the mixture of urine and nucleoside standard by a factor of 50 for this experiment, yielding final nucleoside concentrations in the range of 0.1 to 1.0 μg mL^{-1}. This large dilution would not be necessary in the most likely applications (BAC-LC-MS) which could involve an additional switching valve to direct the unretained components such as sodium ions to waste before they reach the HPLC column.

The numerous metabolites in the urine provide for a complex mass spectrum including many compounds that were retained at the high pH, high ionic strength buffer and which were released with the low pH buffer, thereby confounding the detection of the nucleosides. Therefore, a washing step with 1:1 acetonitrile-buffer was performed after the extraction step to elute some of the signal-occluding matrix compounds before the low pH buffer was used to elute the nucleosides. As shown in Figure 2.9, this washing step results in the elution of a large amount of hydrophobic material, affording a significantly cleaner spectrum for the low pH eluted fraction. Nevertheless, the low pH fraction was still very complex and many of the nucleosides were obscured by large unidentified compound signals, although a clear guanosine signal with correct mass was observed at the expected time. The total ion chromatogram is also shown in Figure 2.9, demonstrating that guanosine is indeed cleared from the non-retained

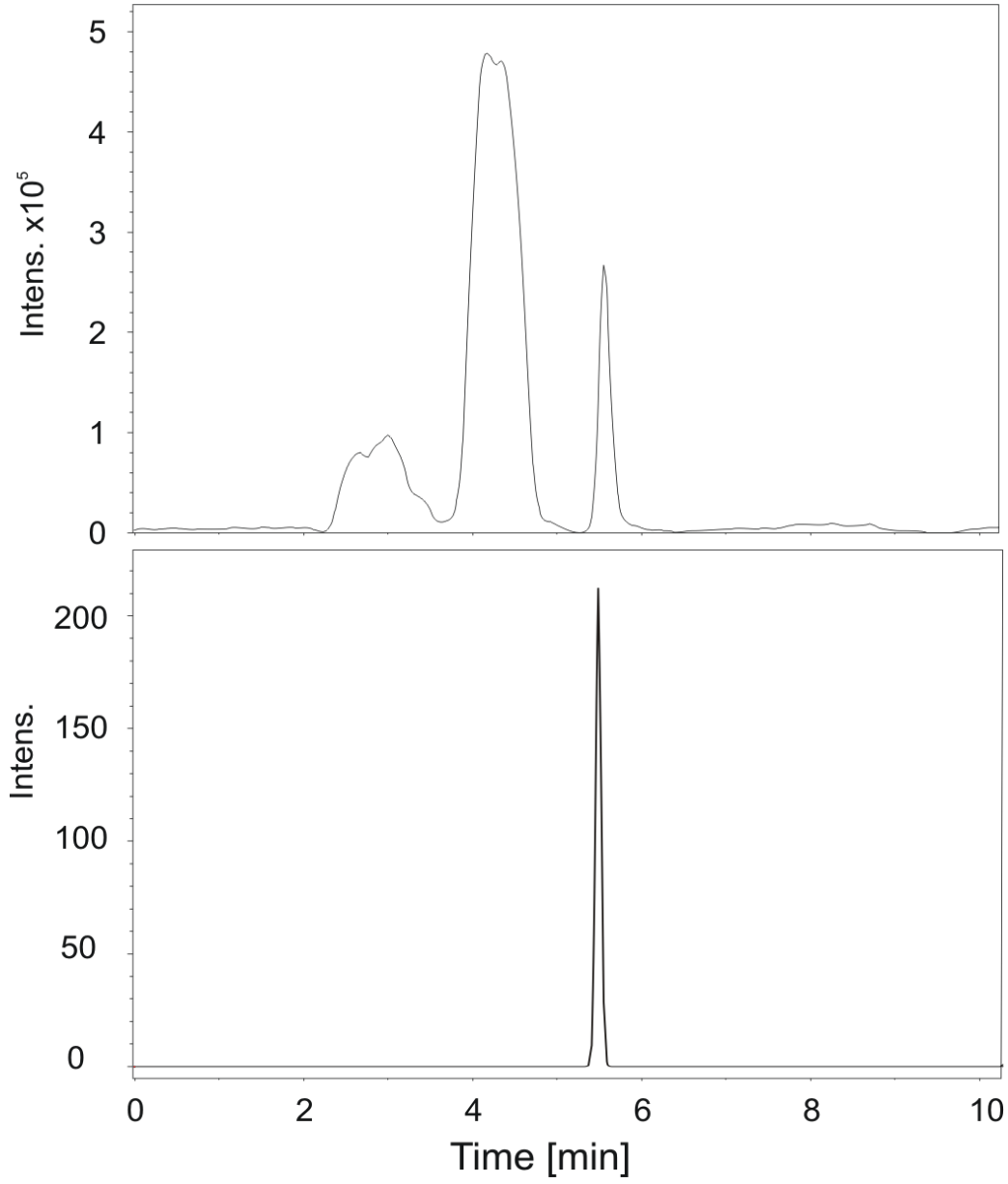

Figure 2.9 – Extraction from urine sample spiked with 0.25 µg guanosine (2% urine and 2% nucleoside test mix in 0.10 M pH 9 ammonium acetate buffer) using program B (see experimental section). Top: Total ion chromatogram. Bottom: Guanosine extracted ion chromatogram, proton and sodium adducts (284.1 ± 0.5 and 306.1 ± 0.5).

contaminants and more hydrophobic contaminants in the nucleoside test mix. The difficulty in detecting all of the nucleosides by this method is not particularly surprising given the complexity of the urine sample and the possible effects of ion suppression of the weakly ionisable nucleosides, the inevitable fouling of the ESI-MS source with sodium during this experiment, as well as the likelihood of signal occlusion by the numerous unidentified metabolites, some of which may be unidentified boronate-interacting analytes from the urine. Furthermore, the ESI-MS detection was performed in the presence of 100 mM buffer which is likely to reduce sensitivity as compared to the ionisation that could be achieved in typical reversed phase eluents such as acetonitrile-water solutions with only 0.5% formic acid.

2.3.4 Demonstration of BAC-MS for glycated peptide

Glycated peptides are produced when sugars or their derivatives reduce amino or guanidine groups in blood or tissue proteins [39] and their accumulation has been linked to age-related disorders including Alzheimer's disease [40], cardiovascular disease [41] and also to diabetes-related pathologies [42]. Glycation by D-glucose gives a so-called "Amadori-product" [39] which bears a cis co-planar vicinal diol, allowing retention of many glycated peptides and proteins by BAC as has previously been demonstrated for off-line sample cleanup and enrichment [9, 12, 13]. No commercially available glycated peptide standards could be found, therefore the synthetic method of Brock *et al*. [34] was used to create a standard containing both glycated and non-glycated peptide Phe-Gly-Phe-Gly in order to clearly demonstrate the selectivity of the monolith for compounds with the Amadori product diol. Working with the glycated and non-glycated form of the same peptide allows great certainty in attributing selective retention to the diol

interaction as opposed to the other types of interaction that may occur on a boronate column [16]. The glycation reaction proceeds by reduction of the n-terminus of the peptide, followed by rearrangement to form an Amadori product glycated peptide [39].

The phenylboronate column was attached to an ESI-MS source to facilitate detection and identification of the peptides. Ammonium acetate buffers were used for MS-compatibility, with a high pH buffer being used for adsorption and a low pH buffer being used for elution as is typical for BAC [4]. Figure 2.10 shows how both peptides are retained in the pH 9 buffer and are eluted in the low pH buffer, with the glycated peptide retained more strongly due to its interaction with the phenylboronate groups. The fact that the non-glycated peptide was also retained in the pH 9 buffer indicated that there was a significant degree of pH dependant non-specific interaction. Peptstatin A, a short hydrophobic peptide that lacks an N-terminus, was then injected in order to investigating this phenomenon further, The Pepstatin A was strongly retained by the column. However, it was efficiently eluted by a plug of a 1:1 mixture of acetonitrile and pH 9 ammonium hydroxide buffer. These results suggest that the non-specific interactions are of a reversed phase or hydrophobic interaction nature. In the case of the short peptide Phe-Gly-Phe-Gly (and its glycated counterpart), this interaction was sufficiently reduced in the low pH and lower ionic strength of the pH 4 acetic acid buffer to allow elution.

The glycated peptide separation was redesigned to take the hydrophobic interaction into account. After the binding step, the non-glycated Phe-Gly-Phe-Gly was eluted by a plug of 50% acetonitrile in pH 9 buffer whilst the glycated peptide was retained by its interaction with the phenylboronate moieties. The

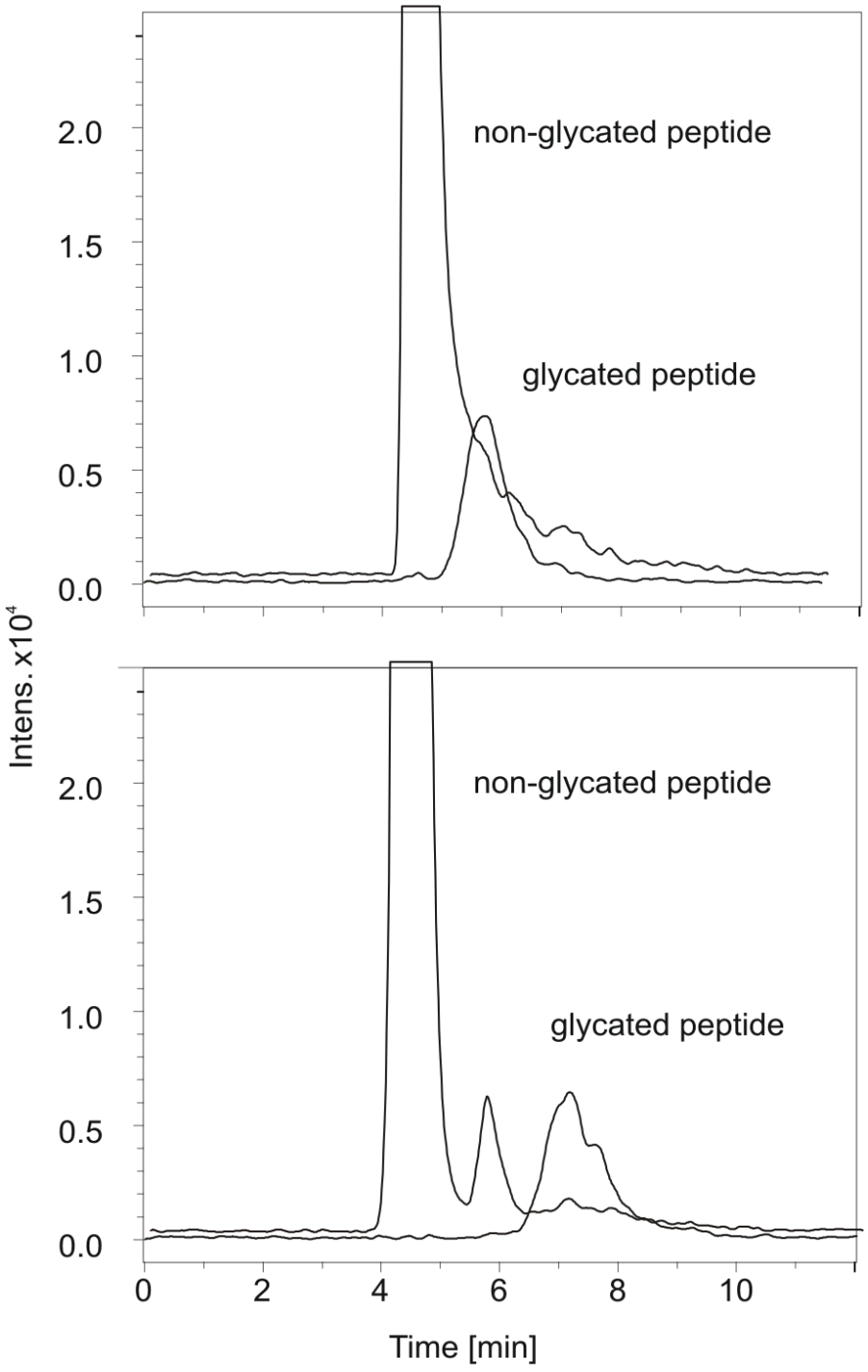

Figure 2.10 – Capillary LC-MS separation of non-glycated peptide phe-gly-phe-gly (mass range 427.2 ± 0.2) from glycated peptide (mass range 589.2 ± 0.2) on a HPBA monolithic capillary column. Conditions: column size 15 cm x 100 µm ID, flow rate 1.00 µL/min. The top separation used elution program A and the bottom separation used program B (see Section 2.2.6).

glycated Phe-Gly-Phe-Gly was then eluted by the low pH buffer, resolved from the non-glycated peptide, as shown in Figure 2.10 (bottom).

Whilst several other groups have performed BAC extractions of glycated peptides and proteins [9, 12, 13], there was no report of a selective trapping of a glycated peptide on a monolith when this work was carried out, nor had there been any report of a separation of a glycated peptide in a microscale system. In addition, this may have been the first BAC of glycated peptides that was carried out on-line to ESI-MS.

2.4 Discussion

The poly(BuMA-*co*-EDMA) monoliths are effective and rigid scaffolds for grafting and functionalisation with good wall attachment, whist the 2-step poly(GMA) photografting method appears to be a robust method for creating a layer than can be modified with nucleophiles containing phenylboronate groups.

The HPBA reaction was much more effective than the AMPBA reaction in terms of creating a high BAC binding capacity, due either to differences in nucleophilicity of the reagents or to the different wetting of the grafted layer achieved in the different reaction solvent systems. Whilst the HPBA monolith swells considerably in low ionic strength buffer, this will not give rise to any problems if appropriate binding/eluting protocols are used.

The poly(BuMA-*co*-EDMA) monoliths grafted with GMA and modified with HPBA selectively retain glycated peptides and also show some ability to trap and release nucleosides from real life samples such as urine. They also exhibit the useful features of high permeability, high pressure resistance and the ease with which they are prepared *in situ*. These functionalised monoliths are therefore

good candidates for on-line microscale boronate affinity chromatography in microfluidic systems. They could have potential application as a preconcentration and sample cleanup columns hyphenated online to an LC-ESI-MS system, as has previously been demonstrated with several other types of microscale monolithic extraction columns [22] and also with some particle-packed BAC columns [2, 4]. It is likely that the monoliths could be scaled down to smaller dimensions if required to form part integrated microscale analysis systems.

At this stage of development the columns exhibit non-specific interactions that might pose a challenge to their application to complex biological samples. A combination of the boronate extraction with LC separation in reversed phase or HILIC mode will likely enhance the detection ability of ESI-MS by providing further separation of the analytes from other low-pH eluted compounds and also by preventing contamination of the ESI-MS source with sodium salts. If the non-specific adsorption is still found to be problem then there are several possible avenues to address this. These include optimisation of the mobile phase properties such as pH, ionic strength, fraction of organic modifiers, or even by the inclusion of a detergent as has previously been demonstrated for reducing non-specific adsorption of proteins on BAC sorbents [19]. In addition, a layer of poly(ethylene glycol methacrylate) can be photografted on the pore surface within the monolith itself, a technique that has proven very successful in reduction of non-specific adsorption of proteins [24].

2.5 Recent Boronate Affinity Monoliths

Since the completion of this work, a few other groups have reported alternative syntheses and applications for boronate affinity polymer monoliths.

Gillespie *et al*. demonstrated an interesting alternative synthesis of a monolithic boronate sorbent based on a poly(butyl methacrylate-*co*-ethylene dimethacrylate) monolith grafted with (polyethyleneglycol)methacrylate and poly(4,4-dimethyl-2-vinylazlactone) and then reacted with *m*-aminophenylboronic acid. However, this monolith was in fact used to demonstrate a new approach to probing the pK_a of monoliths and the authors did not yet demonstrate any selectivity or separation with the monolith. It is therefore not possible to make an assessment of the capabilities of this monolith for BAC.

Ren *et al*. from Nanjing University, China, used a direct approach of co-polymerising a vinylphenylboronic acid with ethylene dimethacrylate [43]. The author of this thesis previously attempted to form monoliths this way during an earlier project [29], but the approach was abandoned because it was difficult to control the porosity of the monolith using the typical porogens of 1-dodecanol, 1-decanol and cyclohexanol. In contrast, Ren *et al*. succeeded because they identified ethylene glycol and diethylene glycol as more appropriate porogens for this polymerisation mixture. The resulting monolith had a high surface area of 47.73 m^2/g. This monolith functioned well at pH 9 with a catechol capacity of 10.8 μmol/mL, about 4 times higher than the HPBA functionalised monolith capacity for cytidine. In making this comparison it is important to note that cytidine is a significantly larger and more sterically hindered molecule than catechol. Therefore it seems reasonable to conclude that this monolith behaves, in broad terms, similarly to the HPBA monolith in terms of capacity. Ren *et al*. also showed that inclusion of fluoride ions in the mobile phase can increase retention factor on monolithic BAC stationary phases, with 50 mM NaF increasing the retention of catechol almost by a factor of two.

The poly(VPBA-*co*-EDMA) monolith described by Ren *et al*. suffered from one of the same limitations that were suffered by the HPBA monolith described in this thesis: non-specific interactions [43]. Reversed phase interactions were shown to be prevalent on the monolith by injecting a homologous series of alkyl benzenes which eluted in the typical order expected of reversed phase chromatography.

This issue of non-specific interactions was subsequently addressed in their next paper on BAC monoliths [44]. Their approach to this problem was to replace the crosslinking monomer agent (originally EDMA) with N,N'methylenebisacrylamide, which is a significantly more hydrophilic monomer. Remarkably, this substitution did not cause a significant change in binding capacity for catechol, despite the new monolith having only quarter of the surface area of their earlier, more hydrophobic version. Retention factors of the akyl benzene series were reduced by roughly 70% compared to the EDMA version.

Ren *et al*. used the improved monolith for specific capture and release of a set of glycoproteins. The monoliths showed good specific binding of glycoproteins versus non-glycoproteins, which were not strongly retained. The protocol required a very strong ionic strength binding phase of 250 mM ammonium acetate (pH 8.5) to minimize the electrostatic repulsion between the negatively charged groups on the proteins and the negatively charged boronate groups. Unfortunately, the selectivity of this monolith was not demonstrated in the presence of a complex sample matrix, and it is therefore not yet possible to make conclusions about its potential for application to real samples. Nevertheless, the selectivity of the monolith for glycoproteins appears to be very good and this

approach remains as one of the best characterized and most promising approaches to designing a BAC monolith for that glycoprotein separations.

Rather than improving on this design or demonstrating it for real separation applications, Ren *et al*. instead introduced a new epoxy type polymer monolith for BAC in 2009 [45]. They formed an amine reagent by coordinating m-aminophenylboronic acid to hexamethylenediamine (B-N coordination), and used tris(2,3-epoxypropyl)isocyanurate as the epoxy reagent. It was hoped that the resulting monolith would retain its boron-nitrogen coordinated state, making it a so-called "Wuff-type boronic acid" which may be more effective at lower pH values. The material did indeed perform well at the relatively low pH of 7.0, with a loading capacity for catechol of 1.56 μmol mL^{-1}. This value is not that much lower than the loading capacity for cytidine observed for the grafted HPBA monolith at pH 9. Indeed, the material compared very favourably with other BAC materials in terms of its function at pH 7. However, the selective retention of monolith was demonstrated only for adenosine and catechol and the monolith was not exposed to any complex sample matrices, so it remains unknown whether this synthesis approach could make monoliths suitable for real applications.

Chen *et al*. took an approach similar to that originally taken by Ren *et al*. They prepared monoliths by direct radical copolymerisation of 3-acrylamidophenylboronic acid and EDMA [46]. They also identified the difficulty of finding an appropriate solvent porogen system for boronic acid monomers, which they solved by using PEG 20 000, a reagent that is commonly associated with monoliths formed by condensation polymerisation. The monolith was not used in online mode but rather was used for offline sample preparation by selective extraction of diols. Whilst the selectivity for ribonucleosides over

2-deoxyribonucleosides was demonstrated conclusively, the enrichment factors were not particularly high and there were significant amounts of 2-deoxyribonucleosides in the eluate. Whilst Chen *et al*. did not calculate a breakthrough capacity for their monolith, they did estimate a capacity of 185 μg (0.69 μmol) of adenosine per mL of monolithic column volume.

Chen *et al*. did however, achieve a significant milestone by demonstrating their monolith for off-line extraction for glycopeptides from a tryptic digest. Using the monolith for sample enrichment prior to MALDI-TOF-MS, they showed that they could selectively enrich glycopeptides from a tryptic digest of glycoprotein Horse Radish Peroxidase (HRP). Furthermore, by applying their monolith to a mixture of HRP and BSA, they showed excellent selective enrichment of the glycoprotein whilst the BSA was washed out in the flow-through. However, given the large number of potential interactions occurring on the monolith, including ion exchange and reversed phase, as well as the wide range of glycans that might be targeted, Chen *et al*. would need to show selective enrichment of a wider range of glycoproteins from more complex matrices before any conclusions are drawn as to the potential of this material for off-line sample enrichment of real samples. Despite the fact that the material was used only for offline extraction, the author of this thesis can think of no reason why the same sorbent could not be used for online sample enrichment.

Conclusions and future directions in the development of polymer monoliths are presented in the final chapter of this thesis.

2.6 References

1. Tuytten, R., Lemiere, F., Esmans, E. L., Herrebout, W. A., vanderVeken, B. J., Maes, B. U. W., Witters, E., Newton, R. P., Dudley, E., *Anal. Chem.* 2007, *79*, 6662-6669.

2. Tuytten, R., Lemiere, F., VanDongen, W., Witters, E., Esmans, E. L., Newton, R. P., Dudley, E., *Anal. Chem.* 2008, *80*, 1263-1271.

3. Zheng, Y., Xu, G., Yang, J., Zhao, X., Pang, T., Kong, H., *J. Chromatogr. B* 2005, *819*, 85-90.

4. Hagemeier, E., Kemper, K., Boos, K.-S., Schlimme, E., *J. Chromatogr.* 1983, *282*, 663-669.

5. Glad, M., Ohlson, S., Hansson, L., Månsson, M.-O., Mosbach, K., *J. Chromatogr.* 1980, *200*, 254-260.

6. Hansson, C., Agrup, G., Rorsman, H., Rosengren, A. M., Rosengren, E., *J. Chromatogr.* 1978, *161*, 352-5.

7. Kemper, K., Hagemeier, E., Ahrens, D., Boos, K. S., Schlimme, E., *Chromatographia* 1984, *19*, 288-91.

8. Soga, T., Inoue, Y., *J. Chromatogr. B* 1993, *620*, 175-181.

9. Zhang, Q., Tang, N., Schepmoes, A. A., Phillips, L. S., Smith, R. D., Metz, T. O., *J. Proteome Res.* 2008, *7*, 2025-2032.

10. Caines, P. S., Thibert, R. J., Draisey, T. F., Foreback, C. C., Chu, J. W., *Clin. Biochem.* 1989, *22*, 285-7.

11. Hjertén, S., Li, J.-P., *J. Chromatogr. A* 1990, *500*, 543-553.

12. Frolov, A., Hoffmann, R., *Ann*. *N*. *Y*. *Acad*. *Sci*. 2008, *1126*, 253-256.

13. Zhang, Q., Tang, N., Brock, J. W. C., Mottaz, H. M., Ames, J. M., Baynes, J. W., Smith, R. D., Metz, T. O., *J*. *Proteome Res*. 2007, *6*, 2323-2330.

14. Takátsy, A., Böddi, K., Nagy, L., Nagy, G., Szabó, S., Markó, L., Wittmann, I., Ohmacht, R., Ringer, T., Bonn, G. K., Gjerde, D., Szabó, Z., *Anal*. *Biochem*. 2009, *393*, 8-22.

15. Monzo, A., Bonn, G. K., Guttman, A., *Anal*. *Bioanal*. *Chem*. 2007, *389*, 2097-2102.

16. Liu, X.-C., *Sepu* 2006, *24*, 73-80.

17. Scouten, W. H., *Immobilized Boronates/Lectins*, in *Encyclopedia of Separation Science*, I.D. Wilson, Editor. 2000, Academic Press: Sydney. p. 273-277.

18. Matsumoto, M., Shimizu, T., Kondo, K., *Sep*. *Purif*. *Technol*. 2002, *29*, 229-233.

19. Bossi, A., Castelliti, L., Piletsky, S. A., Turner, A. P. F., Righetti, P. G., *J*. *Chromatogr*. *A* 2004, *1023*, 297-303.

20. Reid, T. S., Gisch, D. J., *J*. *High Resolut*. *Chromatogr*. 1989, *12*, 249-50.

21. Xu, Y., Wu, Z., Zhang, L., Lu, H., Yang, P., Webley, P. A., Zhao, D., *Anal*. *Chem*. 2009, *81*, 503-508.

22. Potter, O. G., Hilder, E. F., *J*. *Sep*. *Sci*. 2008, *31*, 1881-1906.

23. Svec, F., *J*. *Chromatogr*. *B* 2006, *841*, 52-64.

24. Stachowiak, T. B., Svec, F., Frechet, J. M. J., *Chem*. *Mater*. 2006, *18*, 5950-5957.

25. Peterson, D. S., Rohr, T., Svec, F., Frechet, J. M. J., *Anal*. *Chem*. 2003, *75*, 5328-5335.

26. Tudos, A. J., Besselink, G. A. J., Schasfoort, R. B. M., *Lab Chip* 2001, *1(2)*, 83-95.

27. Minc, N., Viovy, J.-L., *Comptes Rendus Physique* 2004, *5*, 565-575.

28. Ma, H., Davis, R. H., Bowman, C. N., *Macromolecules* 2000, *33*, 331-335.

29. Potter, O. G., *Porous polymer monoliths for microscale boronate affinity chromatography (Honours Thesis)*. 2005: University of Tasmania.

30. Potter, O. G., Breadmore, M. C., Hilder, E. F., *Analyst* 2006, *131*, 1094-1096.

31. Rohr, T., Hilder, E. F., Donovan, J. J., Svec, F., Fréchet, J. M. J., *Macromolecules* 2003, *36*, 1677-1684.

32. Hutchinson J. P., Hilder E. F., Shellie R. A., Smith J. A., Haddad P. R., *Analyst* 2006, *131*, 215-21.

33. Krenková, J., Bilkova, Z., Foret, F., *J*. *Sep*. *Sci*. 2005, *28*, 1675-1684.

34. Brock, J. W. C., Hinton, D. J. S., Cotham, W. E., Metz, T. O., Thorpe, S. R., Baynes, J. W., Ames, J. M., *J*. *Proteome Res*. 2003, *2*, 506-513.

35. Graham, S., Cormack, P. A. G., Sherrington, D. C., *Macromolecules* 2004, *38*, 86-90.

36. *Technical Information Bulletin AL-102; Boric Acid Gel for Column Chromatography*. 1978, Aldrich Chemical Company, Inc.: Milwaukee, WI.

37. Dudley, E., Tuytten, R., Lemiere, F., Esmans, E. E., Newton, R. P., *Collect*. *Symp*. *Ser*. 2008, *10*, 229-233.

38. Nakano, K., Nakao, T., Schram, K. H., Hammargren, W. M., McClure, T. D., Katz, M., Petersen, E., *Clin*. *Chim*. *Acta* 1993, *218*, 169-183.

39. Cho, S. J., Roman, G., Yeboah, F., Konishi, Y., *Curr*. *Med*. *Chem*. 2007, *14*, 1653-71.

40. Takeuchi, M., Yamagishi, S.-I., *Curr*. *Pharm*. *Des*. 2008, 14, 973-8.

41. Misciagna, G., De Michele, G., Trevisan, M., *Curr*. *Pharm*. *Des*. 2007, 13, 3688-95.

42. Nawale, R. B., Mourya, V. K., Bhise, S. B., *Indian J*. *Biochem*. *Biophys*. 2006, 43, 337-344.

43. Ren, L., Liu, Z., Dong, M., Ye, M., Zou, H., *J*. *Chromatogr*. *A* 2009, 1216, 4768-4774.

44. Ren, L., Liu, Y., Dong, M., Liu, Z., *J*. *Chromatogr*. *A* 2009, 1216, 8421-8425.

45. Ren, L., Liu, Z., Liu, Y., Dou, P., Chen, H.-Y., *Angew*. *Chem*., *Int*. *Ed*. 2009, 48, 6704-6707.

46. Chen, M., Lu, Y., Ma, Q., Guo, L., Feng, Y.-Q., *Analyst* 2009, 134, 2158-2164.

3 Conception and Proof-of-Principle of Photochemical Eluent Control

3.1 Introduction

3.1.1 Eluent Composition Gradients for Liquid Chromatography

One of the most significant challenges for the miniaturisation of chromatography is the problem of creating temporal eluent composition gradients in systems with flow rates in the order of one microlitre per minute and lower.

Temporal eluent composition changes are ubiquitous in traditional scale HPLC, especially in reversed phase, hydrophilic interaction and ion exchange chromatography. The main purpose of these changes, which are often termed "mobile phase gradients", is that they facilitate the separation of sample components that have a wide range of retention behaviours in a single run [1, 2]. In a typical program, the eluting strength of the mobile phase is gradually increased throughout the run. Therefore, weakly retained components are eluted and resolved during the early part of the gradient, whilst analytes with a higher affinity for the stationary phase are eluted during the "strong" part of the gradient. Under the right conditions [1], gradient elution allows the determination of a wider range of sample components in a shorter time and with better detection limits than would be possible with isocratic separations. Meanwhile, affinity chromatography methods are dependant on eluent composition changes to efficiently desorb selectively bound analytes from the column after the undesired components have been eluted.

The most common types of mobile phase change are those of ion concentration, organic solvent ratio, pH, as well as concentration changes of more specialised molecules for affinity chromatography [3, 4]. Smooth composition changes are usually refereed to as “smooth gradients” or simply “gradients”, whilst abrupt changes in composition are called “step gradients”.

The control of eluent gradients in traditional scale chromatography benefits from a mature technology: programmable gradient piston pumps that combine the liquids from two or more eluent stock bottles at variable ratios. For ease-of-discussion, the two different stock liquids will henceforth be referred to as A and B. Whilst the main advantage associated with gradient pumps is their ability to form eluent composition gradients, they can also provide advantages for isocratic elution chromatography. This is because they allow near-instantaneous selection of a new isocratic eluent with any desired proportion of A versus B (and sometimes “C” and “D”), which can save a lot of time during method development.

There are several distinct pump designs that can be used to control the proportion of A and B in the eluent. The most common approaches can be categorised into whether mixing occurs at low pressure upstream of the pump or at high pressure downstream of the pump(s). Interested readers can find system schematics and descriptions by referring to the manuals of either the Agilent 1200 Series Quaternary Pump [5] or the Agilent 1200 Series Binary Pump [6] which respectively provide examples of these two approaches. Whilst these approaches are very effective for operation at flow rates of several hundreds of microlitres per minute and higher, they suffer from the difficulties of microfluidic mixing,

pumping at low flow rates and the increased significance of dead volumes when they are applied to microfluidic gradient chromatography.

3.1.2 Eluent Composition Gradients for Miniaturised Chromatography

Whilst there are a variety of ways of achieving gradient microscale flows by combining A and B, only two significantly distinct approaches are used by the leading chromatographic equipment manufacturers. The first approach is based on the high-pressure mixing design mentioned above in which flow is combined in a mixer downstream of two pumps (fed by A and B, respectively). This is the method utilised by the Agilent 1200 series capillary pumps (Figure 3.1), which pumps at several hundreds of microlitres per minute. The flow is then split down to the microscale by use of an "intelligent" flow splitting device which is situated downstream of the mixer. The system relies on feedback from a flow sensor near the outlet to determine how fast to operate the pumps and to determine the appropriate settings for the variable flow splitting device. One of the difficulties with these complex systems is that there is typically a substantial dwell volume between the formation of the gradient and the flow splitting mechanism which can be a significant challenge to effective operation at low flow rates [7]. Another issue is the fact that only a tiny fraction of liquid A and B is used for chromatography; almost all of the liquid in the eluent bottles is shunted off to waste after mixing, making it very difficult to recycle.

An alternative approach is employed by the Dionex RSLC nano system, which uses a microfluidic mixer to directly combine two microfluidic flows from two pumps that are fed by A and B respectively. This system, which can be called a "splitless flow" method, requires pumps and flow sensors with very low flow rate

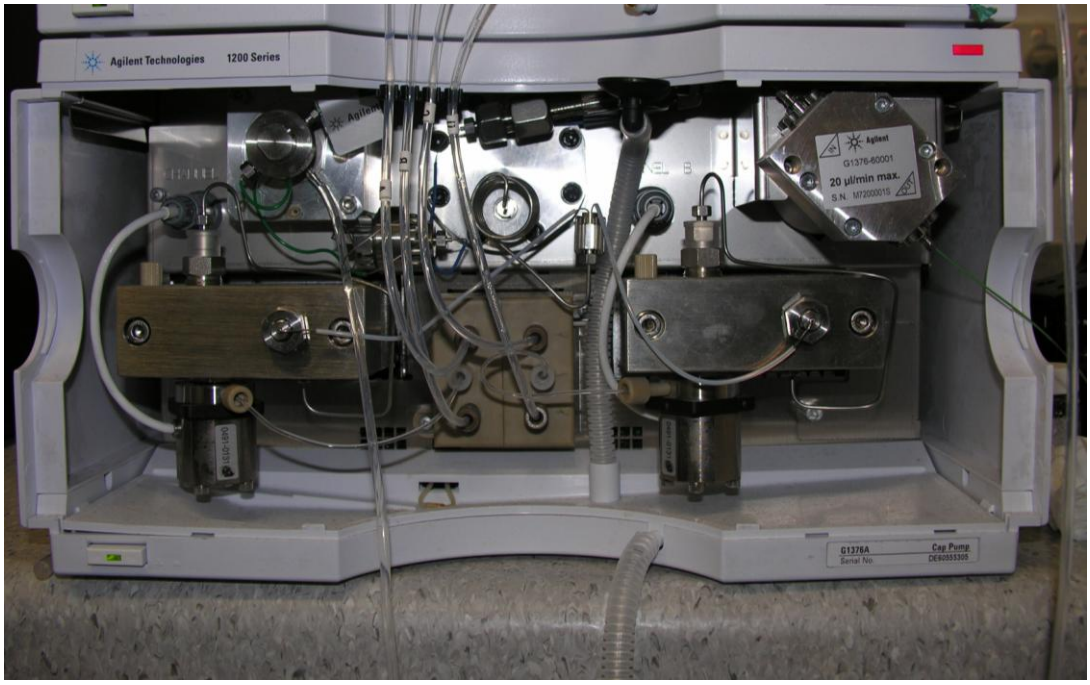

Figure 3.1 – Agilent 1200 series capillary pump which can be used for microscale gradient chromatography. Other pumps with comparable capability are of a similar size and have broadly equivalent components. This pump was used (in non-gradient mode) throughout the experiments in this chapter and in the following two chapters to provide a steady source of microscale fluid flow.

capability. Whilst this approach resolves the issue of the gradient delay and reagent waste, the system performance degrades significantly at lower flow rates and at low percentages of %A or %B because it pushes the limits of capability of the pump and flow rate sensing components [7]. For example, to produce a steady 20 nL/min flow rate with 5% A and 95 % B, such a system would require that the pump fed by A would operate at only 1 nL/min, which is an extremely low flow rate for a high pressure mechanical pump.

Both of these manufacturer-favoured gradient pumping systems can lead to concentration and pressure fluctuations because of difficulties with coordinating both pumps during the pump cycles, and further microfluidic design features may be required to ameliorate this effect [8].

Whether or not the performance limits of such designs are of concern depends on the specifics of the intended application. However, even when the performance is sufficient, these approaches still have the disadvantage of requiring precision mechanical equipment with many degradable parts. As such, instruments based on these designs are expensive and take up a similar amount of bench space as a traditional bench top HPLC gradient pump. It is very difficult to imagine how such systems could be physically miniaturized or integrated into smaller, portable devices.

3.1.3 Alternative approaches

It is possible to create temporal gradients for miniaturized chromatography by combining multiple flows *without* the use of microfluidic high pressure gradient piston pumps. However, most of these approaches suffer from some significant limitations.

For example, the idea of combining flows from worm-drive syringe pumps filled with A and B is appealing due to its simplicity. However, approaches that rely on syringe pumps to create high pressures are likely to fail because of the high relative volume of the syringes when compared to microfluidic channels. Indeed, this approach is rarely used even in isocratic chromatography because the compressibility of the large volume of liquid in the syringe makes it difficult to control the flow rate in such systems, which are unable to cope with changes in back pressure. Even the simple act of starting the pumping system can take a significant amount of time because the liquid in the syringe first needs to be pressurised. Syringe pump driven chromatography becomes even more problematic when a gradient is attempted [9].

One class of approaches involves pre-filling a small internal diameter tube with a pre-formed gradient of eluent. For example, Ishii *et al*. devised a method in which B is gradually added and mixed into a vessel filled with 100% A whilst a fraction of the liquid in that vessel is continuously drawn into a 0.5 mm ID tube. The tube, which eventually holds a gradient of A with increasing %B, can then be installed in a chromatography system. Other researchers have developed variations on this idea by pre-forming the gradient using a dual syringe pump [10] or a low pressure gradient pump [11]. Recently, Deguchi *et al*. used a more automated and sophisticated adaptation of this approach to make a gradient delivery system that could conceivably compete with the manufacturer-favoured approaches described above [12]. Their method relied on a commercial gradient pump (which could be a traditional scale or capillary scale pump) to form the desired eluent gradient, which was continuously pumped into an injection loop on a 10 port valve. There were two of these injection loops so that the eluent from

the gradient pump was captured regardless of whether the pump valve was in "position 1" or "position 2". While one loop was filled, the other loop was pumped into a chromatography system using a nanoflow isocratic pump, and the cycle repeated at up to 4 times per minute. Due to the difference in pump speeds, only a small fraction of the eluent in each loop was actually pumped into the chromatography system by the nanoflow pump. However, the system was still able to generate adequately smooth gradients. The main drawback of these "preformed gradient" approaches are their mechanical complexity, which might make them expensive or difficult to miniaturise.

Zhang and Roper [13] used two microfluidic diaphragm pumps that consisted of 3 pressure valves each to create temporal composition gradients for cell perfusion studies. Repeatedly opening and closing these pressure valves in a programmed sequence generated flow, whilst the down time between each sequence repetition determined the average flow rate for that pump. By varying the down time between the two pumps in a complimentary fashion, gradients of A and B could be formed downstream with the help of a microfluidic mixing structure. Whilst this approach worked quite well for the low pressure application of cell perfusion studies, it is doubtful whether such as system would satisfy the very high pressure and flow rate precision requirements of high resolution chromatography.

A microfluidic device prepared by Xie *et al*. used electrolysis to generate gases which pushed liquid through the system [14]. The device was able to operate at very low flow rates and could also generate gradients. The system was limited to a pressure of only 100 psi, though higher pressures may be possible with improved chip design. However, the fact that the system relies on pressurised gasses means that it may be difficult to control the flow rate and any system based

on this design is likely to be highly sensitive to changes in back pressure. Furthermore, the system could not pump indefinitely because the gas chambers eventually filled up.

Lazar and Karger demonstrated an alternative approach that uses an electroosmotic pumping system [15]. Their system used two electroosmotic pumping modules (channels) that each consisted of numerous small-diameter channels. When a potential difference was applied across the length of these channels, an electroosmotic flow was induced, the rate of which depended on the applied voltage. Combining two flows of A and B from two separate electroosmotic pumps allowed the generation of smooth gradients in concentration from A to B. The device was designed so that there would be no potential difference across any component of the device except for the pumping modules themselves, thereby avoiding any problems that might have resulted from the application of voltages in the separation channels. The main drawbacks of this approach are the general drawbacks of electroosmotic pumping: its high sensitivity to the chemical composition of the eluent and the potential for back-flow leakage through the middle of the channels. Whilst the pumps could operate at an impressively low 10 nL/min, the system had a maximum demonstrable pressure capability of only 80 psi. Such a low pressure might be sufficient for limited applications in solid phase extraction or chromatography with very low back pressure monolithic stationary phases. However, the vast majority of high resolution microscale chromatography applications require much higher pressures, often in the thousands of psi range.

One of the more promising approaches is that demonstrated by Brennen *et al*. [7]. They designed a microfluidic chip which can produce smooth gradients by

carefully combining a sequence of flows of pure A followed by pure B. The chip worked by splitting the flow into a series of 20 parallel channels of different lengths which are recombined downstream. Initially, these so-called "timing channels" are pre-loaded with pure A. When the gradient is required, pure B is pumped through the chip, progressively filling each timing channel, starting with the shortest one. Therefore, at the recombination point, the combined flow is initially 100% A, with a staggered increase in %B as each timing channel is progressively filled. Band broadening processes were harnessed downstream of the point where the channels recombine to convert the staggered concentration changes into a smooth gradient. Such a chip can be used to reduce the gradient dwell volume, and would also allow for a far simpler (and perhaps cheaper and smaller) pump design upstream. However, this approach has a significant drawback in terms of programmability because each new gradient elution profile (e.g. linear versus convex)_would require a new gradient chip.

3.1.4 Electrolytic Eluent Generation

All of the methods of creating eluent gradients discussed thus far have involved combining at least two different liquids (often called stock solutions) through adjective or diffusive processes. However, there is an entirely distinct approach that has found tremendous application for one class of chromatography. In the past decade, Dionex Corporation developed electrolytic eluent generation for ion chromatography applications, which had been pioneered by Strong *et al*. in 1991 [16, 17]. This method relies on electrolysis of water and migration of ions across a semi-permeable membrane to create eluents with variable concentrations of KOH, H_2CO_3 or methanesulfonic acid determined by the applied electric current. Electrolytic eluent generation provides extremely pure eluents and has the

advantage that the instrument operator needs only to top up the system with deionised water rather than prepare their own eluents which is thought to be an important source of error and irreproducibility in chromatography [17].

However, electrolytic eluent generation is a complex approach in terms of instrument design. In addition to electrodes, the system requires a semi-permeable membrane connected to a reservoir of concentrated acid or base [17], which can limit the maximum back pressure of the system. Furthermore, O_2 and H_2 are produced during electrolysis and must be removed in a degassing unit downstream of the eluent generator, anda mixing unit is required to homogenize the concentration across the axial dimension of the flow. Given the continued interest in miniaturising and integrating chromatography systems into smaller and even portable instrumentation, these design requirements may pose significant challenges.

Electrolytic eluent generation has to date been largely been restricted to 100% aqueous eluents and the potential for electrochemical oxidation or reduction precludes the use of some of the organic modifiers, buffers, complexing agents and ion pair reagents that are required by many types of chromatography. These limitations may be the reason that electrolytic eluent generation has been used primarily for inorganic ion chromatography rather than biological applications that typically require more than a simple acid or base concentration gradient in otherwise pure water. Figure 3.2 summarises the disadvantages and advantages of electrolytic eluent generation versus high pressure gradient pump systems.

High Pressure Gradient Mixing:

Combining 2 or more stock solutions by advective/diffusive processes

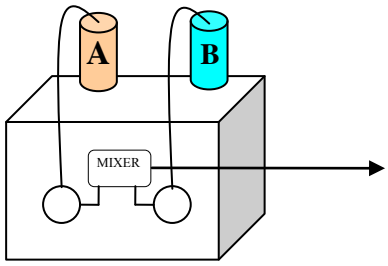

- Requires: separate fluid reservoirs, mixers, multiple pressure sources, precision flow sensors
- Difficult to make small instruments
- Expensive and high maintenance
- Performance degrades at lower flow rates because of dependance on precision mechanical processes

Electrolytic Eluent Generation:

Electrolysis of water in presence of acid/base via a semipermeable membrane

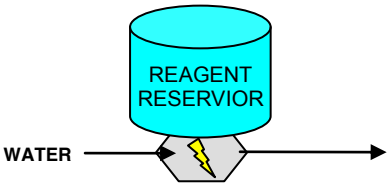

- Limited to producing gradients of KOH, LiOH, NaOH, (bi)carbonate, as well as methane-sulfonic acid
- Incompatible with most organic additives
- Produces gases which must be removed
- Requires reagent reservoir
- Pressure limited by membrane

FIGURE 3.2 – Limitations of the two major manufacturer-favoured approaches to controlling eluent composition to create mobile phase gradients.

3.1.5 Photochemical eluent control

If a liquid contains appropriate photochemical reagents, then its composition can be altered *in situ* without combining it with separate liquids. Given that the liquid might be used as a chromatography eluent, it is clear that photochemistry could be used to control the composition of a mobile phase over time. The obvious design would be to pump the eluent through a photoreaction cell upstream of the sample injector in a chromatography system.

A report by Salamoun and Slais in 1990 describes a system in which a mercury lamp was used to activate hydrogen peroxide in an eluent containing formate buffer, resulting in conversion of formate to carbonate in a low flow rate system (50 µL/min) [18]. This gave a modest increase in the pH of the eluent which was used for pH dependant reversed phase chromatography. Given the difficulty of varying the intensity of this type of lamp, their system instead relied on partially occluding the light with a piece of black paper in order to control the extent of the photochemical reaction. This approach may have only limited potential for miniaturisation due to the heat generation and the significant size of the lamp. Furthermore, the highly reactive hydrogen peroxide could potentially interfere with the sample and some types of stationary phase chemistry. It is perhaps due to these limitations that the work by Salamoun and Slais has not been developed further and has been cited only three times.

On the other hand, the use of compact, variable intensity light sources focussed on the photoreaction cell would allow quantitative control over the extent of the photochemical reaction as the eluent passes through the cell. For ease of

discussion, this concept will henceforth be refereed to as "photochemical eluent control".

The appeal of photochemical eluent control is that it suggests a completely non-mechanical means of controlling eluent composition. Intuitively one might expect that the relative ease of producing a photochemical eluent system versus a mechanical one will become more significant for smaller systems. This is because the mechanical components become less robust and more difficult to implement at smaller scales. In contrast, the photochemical approach is expected to *benefit* from miniaturisation because the lower flow rates would allow the use of lower light outputs and smaller (therefore thinner) photoreaction cells which are more efficient than larger ones because of improved transmission of light throughout cell. Therefore, the concept of photochemical eluent control is well worth exploring as a way of making eluent composition gradients for miniaturised systems with microfluidic chromatography and solid phase extraction.

Proof-of-concept for this approach is demonstrated in this chapter using the example of cation exchange chromatography. Desyl chloride was used as a photoreagent that undergoes photolysis to release HCl when exposed to UV radiation [19, 20], providing a source of H_3O^+ which is a common competing ion for cation exchange chromatography. Appropriate sources of UV irradiation could include various types of lamps or lasers. However, given the emphasis on potential miniaturisation, light emitting diodes (LEDs) were deemed to be the most appropriate radiation source because they are cheap and compact. Furthermore, they give relatively stable output intensities which can be easily controlled by increasing or decreasing the applied electric current [21].

3.2 Experimental Section

3.2.1 Eluent

The eluent used was 50% w/w acetonitrile (HPLC grade, BDH, Darmstadt, Germany) in water. The eluent also had 2.0 mmol/L desyl chloride (DeCl) which was purchased from Alfa Aesar, UK, and 0.24 mmol/L HCl which was from Sigma-Aldrich, St Louis, MO, USA.

3.2.2 Capillary Pump

Eluent flow was controlled by an Agilent 1200 series capillary pump G1376A (including 1200 series vacuum degassing unit G1379B). The reported flow rate of 2.3 μL/min was confirmed by collecting eluent to measure output volume over time.

3.2.3 Photoreaction cell

The photoreaction cell was a 3 cm section of 1.0 mm ID polyimide coated fused silica tube (Polymicro Technologies, AZ, USA). The polyimide coating was burned off the tube in the section that was exposed to radiation. An Araldite epoxy adhesive (Selleys, Australia) was used to join the photoreaction cell with fused silica capillary at either end. The cell was rested in a small v-shaped fold of steel to hold it in place and to reflect backward any radiation that was transmitted through the cell.

3.2.4 LEDs

Three UVTOP-39BL 270nm and one UVTOP-39BL 290nm LEDs (Sensor Electronic Technology, Inc., Columbia, SC, USA) were connected in series and were powered by a supply with a variable current limiting system with a

maximum of 24 mA that was prepared in-house. Two of the LEDs were attached to an XYZ stage whilst two were attached to a metallic brace. The LEDs were then focussed directly onto the photoreaction cell from approximately 20 mm above so that they irradiated separate zones along the length of the cell.

3.2.5 Separation Column

The separation column was prepared by packing a 25 cm of 330 μm ID PEEK tubing with SCS1 low capacity weak cation exchange packing material baring carboxylate functional groups supported on polymer-coated mesoporous silica particles with a diameter of 4.5 μm (Dionex Corporation, Sunnyvale, CA, USA).

3.2.6 Suppressor Column

The suppressor column was prepared by forming a porous polymer monolith based on that described by Preinerstorfer *et al*. [22]. The composition of the reaction mixture was 30% w/w cyclohexanol (99%, Merck)), 30% w/w 1-dodecanol (98%, Sigma-Aldrich), 24% w/w glycidyl methacrylate (97%, Aldrich) and 16% w/w ethylene dimethacrylate (98%, Aldrich) with 1% w/w AIBN (Sigma-Aldrich). The polymerisation mixture was sonicated and purged with nitrogen for 10 minutes and then were infused into a length of 250 μm ID polyimide coated fused silica capillary (Polymicro Technologies, Phoenix, AZ, USA) which had been vinylised on the inner surface by a widely used method [23].

Quaternary ammonium groups were then formed by reacting the column with triethylamine (98%, Fluka) at 30 μL/hr in a column heater at 70°C for 2 hours and at 60 degrees C for 6 hours based on several reports of amine functionalisation of materials with pendant glycidyl groups [22, 24].

3.2.7 Capacitively coupled contactless conductivity detection

An eDAQ conductivity detector module (eDAQ Pty Ltd, Australia) was operated directly downstream of the suppressor column on 75 µm ID polyimide coated fused silica capillary with 363 µm outer diameter (Polymicro, Phoenix, AZ, USA). The data was recorded using a Powerchrom A/D convertor with Powerchrom V2 Software (eDAQ Pty Ltd, Australia). The eDAQ settings for the cation exchange chromatography were 100V amplitude, 1200 KHz and headspace gain was switched on. All experiments were performed at 25°C.

3.2.8 Photochemical reagent performance measurements

A simpler set up was used for these experiments which did not require the separation or suppressor columns. The conductivity detector was operated on a section of 75 µm ID polyimide coated capillary directly downstream from the six port injector (Rheodyne MXP-7980, IDEX, Northbrook IL) which led to waste. In order to get a linear response for the calibration curve the eDAQ settings were changed to 60 V amplitude and 800 kHz with no offset and no headspace gain. A linear calibration with $R^2 = 0.9991$ was generated by spiking the eluent with different concentrations of HCl. This calibration allowed conversion of the conductivity scale into a [HCl] scale. A discussion on the assumptions involved in making this conversion can be found in Section 4.5.3.

3.3 Results and Discussion

The photochemical eluent control system was set up as shown in Figure 3.3, although the separation and suppressor columns were not included initially. The capillary pump system included a vacuum degassing module which removed dissolved oxygen from the eluent. The vacuum degasser may be considered to be

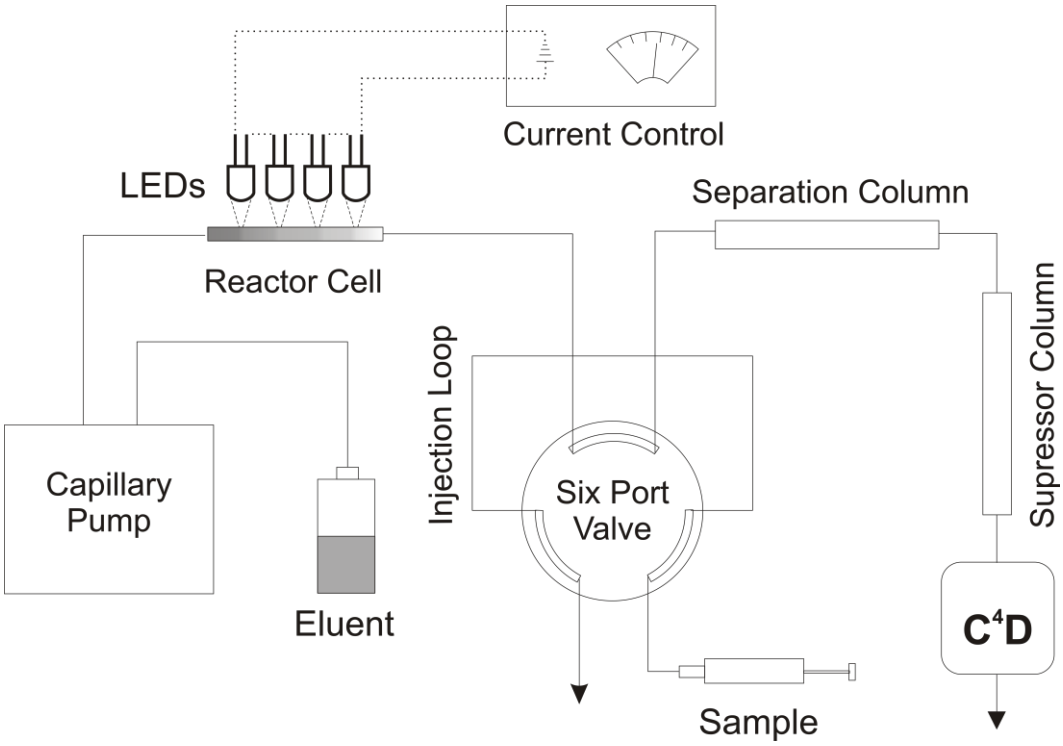

Figure 3.3 – Photochemical eluent generation apparatus. For inorganic cation exchange chromatography experiments the scheme used was exactly as shown above, and used three 270 nm LEDs and one 290 nm LED. Whilst it was known that DeCl has a reasonable level of absorbance these wavelengths (as discussed in Chapter 4) this mix of LEDs was used simply because this was the set of LEDs available to the author at the time of the experiment. The system included a Rheodyne MXP-7980 injection valve. For the reversed phase chromatography experiments in chapter 5 there was no suppressor column or C4D detector – the system was instead hyphenated directly to ESI-MS (Agilent 6320 Ion Trap). The reversed phase chromatography experiments only used only one LED with a wavelength maximum of 310 nm.

quite important because the photochemical reactions of desyl chloride may involve excited triplet state intermediates [19, 20] and it is likely that these may be sensitive to the presence of molecular oxygen [25]. A 1.0 mm ID fused silica tube that was plumbed between the capillary pump and the injection valve served as a UV-transparent photoreaction cell. Three 270 nm LEDs and one 290 nm LED were connected in series to an adjustable power supply and their beams were focused onto the reaction tube (Figure 3.4). The single 290 nm LED was included because it was hoped that it would transmit radiation deeper into the reaction chamber given that desyl chloride absorbs less at this wavelength. The eluent was 2.0 mmol/L Desyl Chloride with 0.2 mmol/L HCl in 50% w/w acetonitrile-water, which was pumped at a rate of 2.3 μL/min. The 0.2 mmol/L HCl was added in order to keep the pH of the eluent below 3.7 at all times. This constant low pH is important during the chromatography experiments because it ensures that the weak cation exchange separation column remains in the H_3O^+ form at all times, expediting its equilibration and minimising the build up of contaminating cations on the column even when the LEDs are switched off.

The conductivity of the reacted eluent was measured over time using a capacitively coupled contactless conductivity detector (C^4D). The results were recorded whilst the LED current was altered and the results are presented in 3.5 (solid line). The conductivity signal has been converted to the concentration of photochemically generated HCl by calibrating the conductivity meter with standards of HCl in 50% w/w acetonitrile-water. These values do not include the 0.2 mmol/L HCl that was used to adjust the pH of the eluent. This conversion from conductivity to concentration relies on the assumption that H_3O^+ and Cl^- were the only ionic photoproducts, which is a reasonable assumption given that

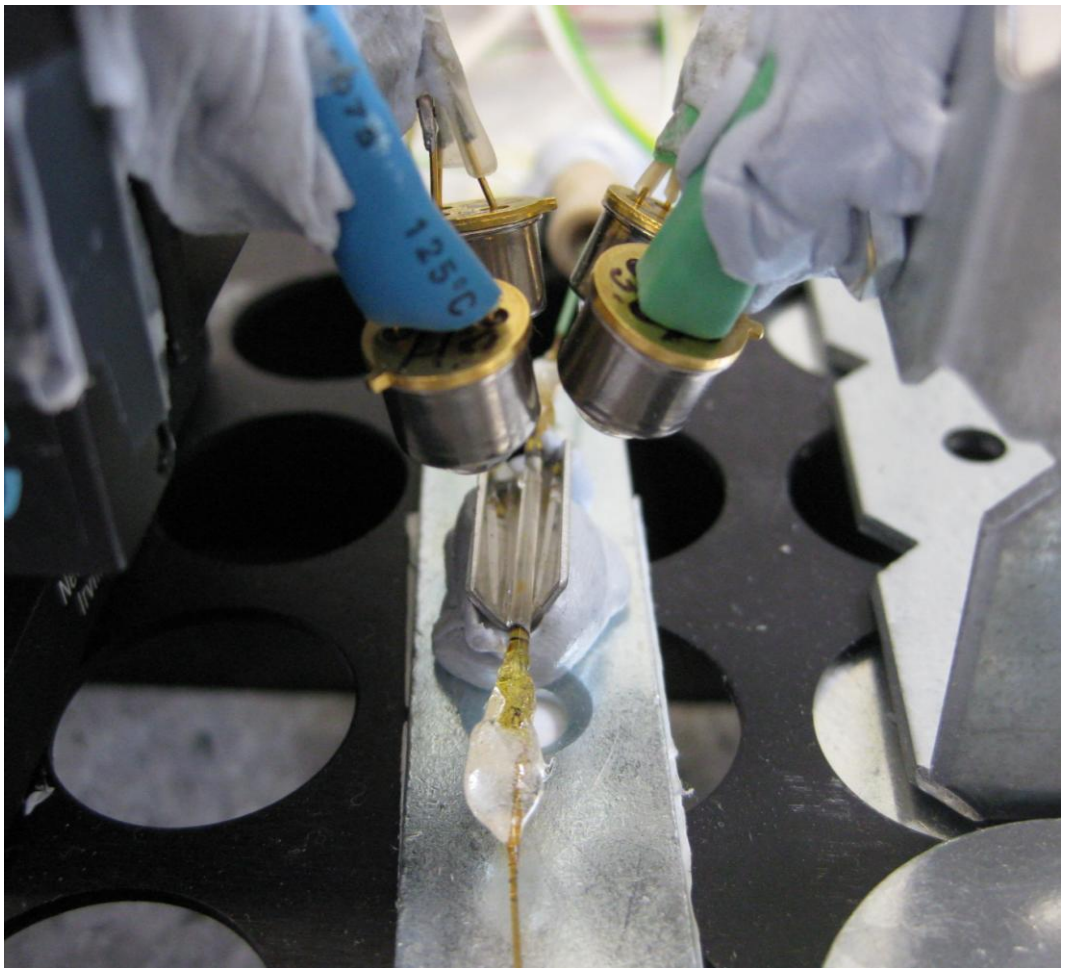

Figure 3.4 – The photoreaction cell, irradiated by four LEDs. The 1 mm internal diameter fused silica reaction tube can be seen in the centre, attached to the downstream 380 µm outer diameter capillary using an epoxy adhesive. To the left is an XYZ stage that allowed control over the position of two LEDs on the left. To the right some metal brackets that were used to support and position the two LEDs on the right.

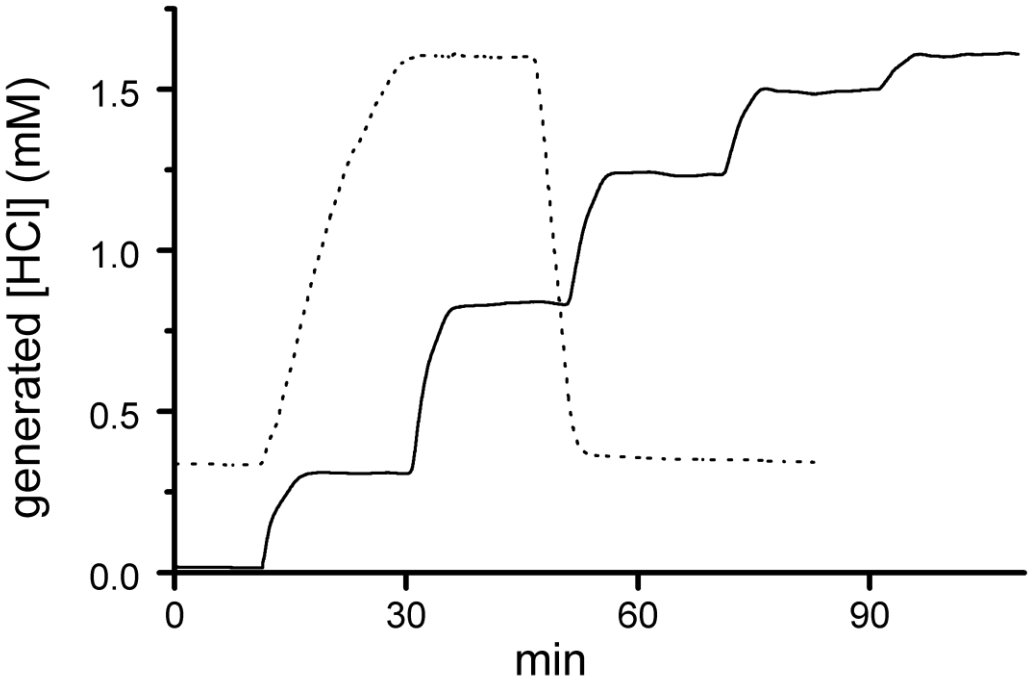

Figure 3.5 – Photochemical control of cation exchange chromatography eluents. Solid line: a series of isocratic eluent profiles with different LED currents. 0 min, 0 mA; 10 min, 5 mA; 30 min, 10 mA; 50 min 15 mA; 70 min, 20 mA; 90 min 23.7 mA. Dotted line: Typical gradient elution program. 0 min, 5 mA. 10 min, 7 mA, increasing by 2 mA every two minutes until 26 minutes at which time the current was held at 23 mA. At 45 minutes the current was reset to 5 mA. A 1.0 mm ID fused silica tube served as a UV-transparent photoreaction cell. Three 270 nm LEDs and one 290 nm LED were connected in series to an adjustable power supply and their beams were focussed onto the photoreaction cell. 2.0 mmol/L desyl chloride with 0.2 mmol/L HCl in 50% w/w acetonitrile-water was pumped through the cell at a rate of 2.3 μL/min.

no other conceivable photoproducts are likely to have been charged in the acidic solution (pH < 3.7).

Increasing the LED current in steps of 5 mA gave corresponding increases in generated [HCl]. There was a delay of approximately 1 minute after increasing the current before any effect was observed due to the dead volume between the irradiated zone and the conductivity detector. This was followed by an increase in [HCl] that occurred over the course of 6 minutes due to the time required for the eluent to move through the irradiated zone in the photoreaction cell. The volume of the irradiated zone was calculated to be 12 μL, accounting for most of this time (the volume of flow in 6 minutes is 14 μL). Hydrodynamic band broadening may also play a small role.

The response was not linear; the increase in generated [HCl] from 5 mA to 10 mA was roughly twice as large as the increase in generated [HCl] from 15 mA and 20 mA. There are several potential causes for this deviation from linear response. Some non-linearity is likely to result from the changing concentrations of desyl chloride and its photoproducts at different LED currents. As the current is increased, the concentration of unreacted desyl chloride decreases whilst the competing absorption of radiation by organic photoproducts becomes more and more significant. Some absorbing photoproducts may be inert whilst others may themselves undergo acid-releasing photolysis [20]. Another potential explanation for this non-linearity is the fact that the radiation intensity is likely to vary considerably throughout the cross-section of the photoreaction cell due to the imperfect emission pattern, refraction, reflection and absorption by desyl chloride and its photoproducts. Therefore it could be that some regions of the cross-section have achieved full conversion at moderate LED currents and that further

increases in current lead to photolysis in smaller and smaller regions of the photoreaction cell cross section. Finally, some non-linearity is probably due to the fact that LED radiation output is not perfectly correlated with current [21]. The maximum achievable [HCl] with the system used was 1.6 mmol/L, representing a yield of 80%.

Generation of smooth gradients of competing ion concentration is considered desirable for ion chromatography. A typical ion chromatography gradient elution profile was demonstrated by adjusting the LED current in a series of steps lasting 2 minutes each (Figure 3.5, dashed line). In principle it would be possible to program the LED current in any fashion to create any desired elution profile in this concentration range, subject only to the maximum gradient steepness allowed by the volume of the irradiated zone. This will be discussed more in the following chapter.

The photochemical eluent generation system was incorporated into a microscale cation-exchange chromatography system with suppressed conductivity detection, as depicted in Figure 3.3. This system used the same flow rate and liquid as that described above, with the liquid now functioning as the chromatography eluent. A standard mix of 0.2 mmol/L $CaCl_2$, 0.4 mmol/L $CsNO_3$ and 0.6 mmol/L LiCl in 50% w/w acetonitrile-water was used throughout these experiments, with manually timed partial loop injections lasting 20 seconds.

The LED current was switched to 20 mA, which was expected to generate 1.5 mmol/L HCl based on the calibration. Under these conditions lithium was eluted after 18.9 minutes whilst caesium and calcium co-eluted 5 minutes later (Figure 3.6, top). Reducing the LED current to 8 mA to generate approximately 0.7 mmol/L HCl resulted in a longer separation with full resolution of each cation.

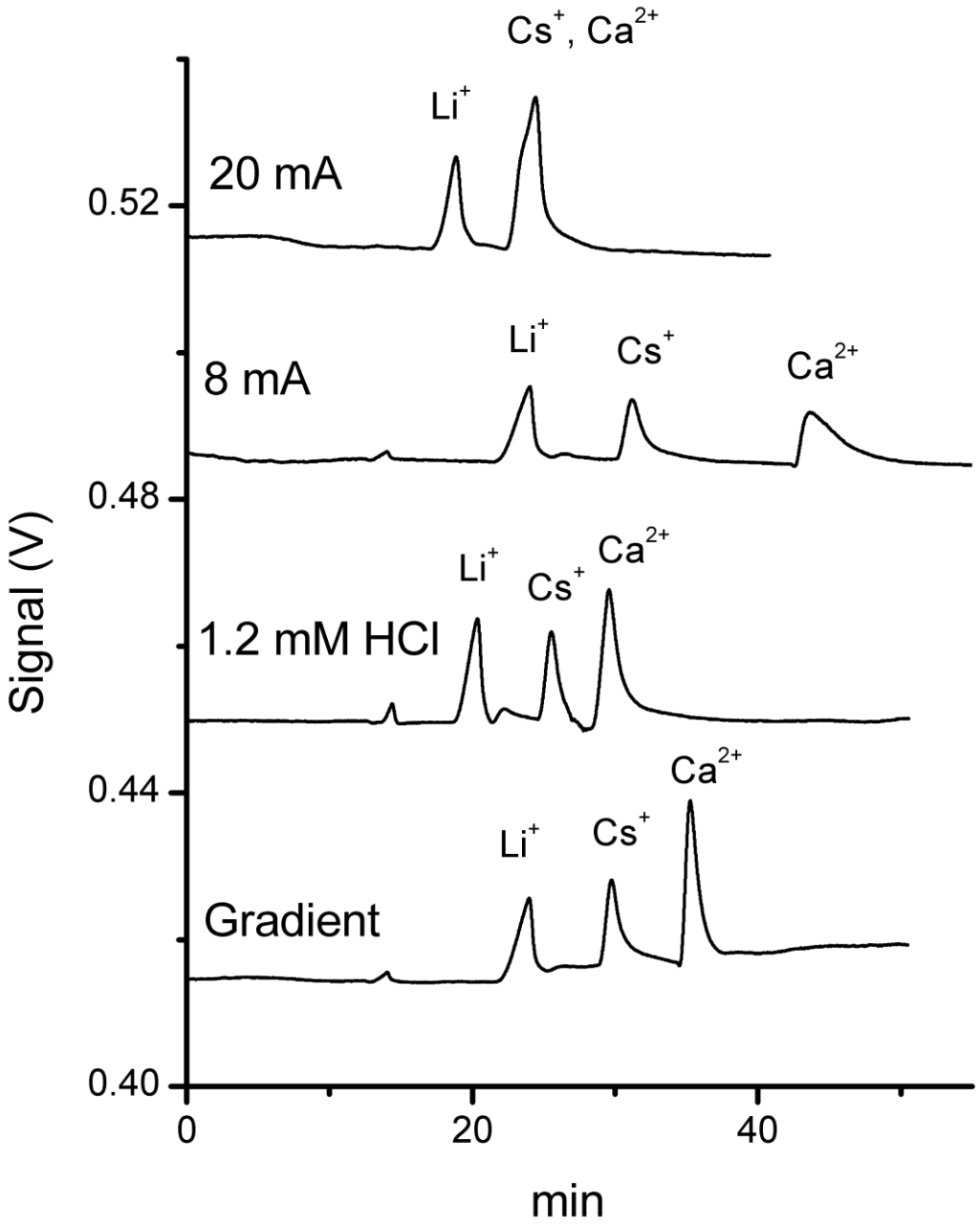

Figure 3.6 – Cation exchange chromatograms using photochemical generation of HCl to control eluent strength. Top and second: isocratic chromatograms. Second from bottom: Control chromatogram with 1.2 mmol/L HCl added to the eluent. Bottom: Chromatogram with photochemically generated eluent gradient. LED current initially 8 mA, then at 6 min increased to 10 mA and continued to increase by 2 mA every 3 minutes until 21 minutes when the current was turned up to 20mA and held at this level for the remainder of the separation.

The retention factors of lithium and caesium increased by a factor of approximately two under these conditions. The calcium retention factor was increased more significantly, by a factor of 3, as expected for divalent species in ion-exchange chromatography. As a control, the separation was run with 1.2 mmol/L HCl spiked into the eluent (in addition to the 0.2 mmol/L HCl for pH adjustment) with the LEDs switched off, resulting in a similar separation with intermediate retention times (Figure 3.6, second from bottom). This confirms that the photochemical eluent generation system operates as expected and effectively generates isocratic H_3O^+ eluents for ion chromatography. Finally, a gradient elution program was performed by increasing the LED current from 8 mA to 20 mA in a series of steps lasting 3 minutes each. As expected for gradient elution programs, the peak shape (especially for calcium) was improved whilst resolution was maintained (Figure 3.6, bottom).

The run-to-run reproducibility of the photochemical eluent generation system was demonstrated by running the gradient program 3 times. Figure 3.7 shows that there was quite good reproducibility between the three runs: retention time RSD was 1% for all three analytes. The run-to-run reproducibility depends on maintaining a constant flow rate, temperature and injection procedure. The injection procedure is likely to be the primary source of error in this case because of the limited precision of human-controlled partial loop injection. Another factor which may affect reproducibility is LED beam alignment, which may have undergone very slight drift throughout the hours required for this experiment. Both of these sources of error were particular to the apparatus used in this proof-of-principle experiment. They could be ameliorated by including an automated injection system and by improving the sturdiness of the LED support structure.

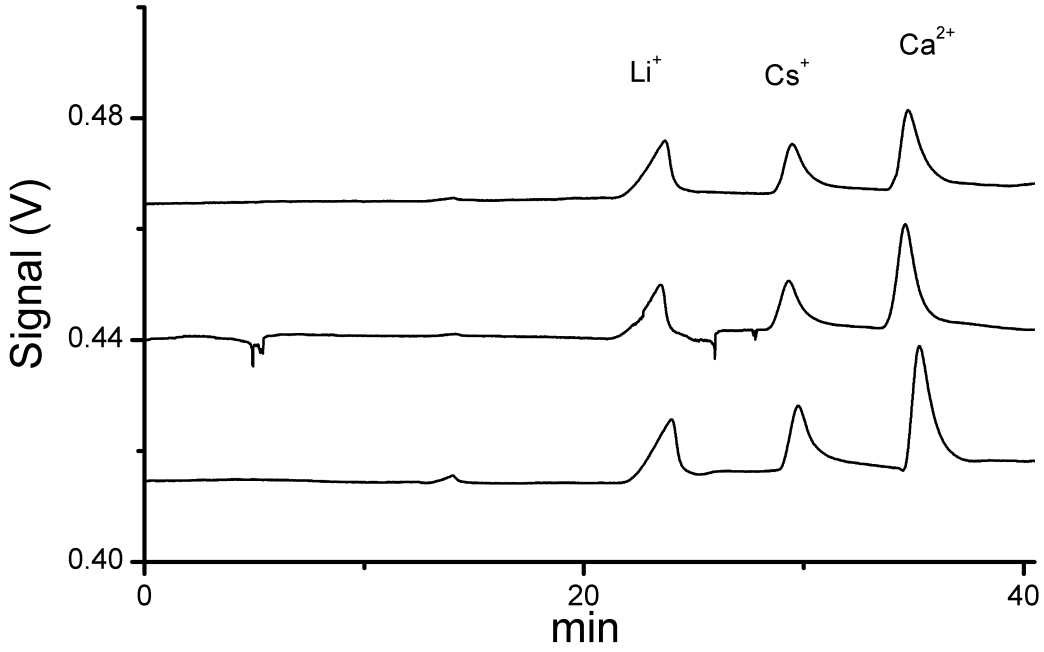

Figure 3.7 – Demonstration of the run-to-run reproducibility of the proof-of-principle photochemical eluent control system. These separations use the gradient program described in Figure 3.6.

3.4 Conclusions

The proof-of-principle experiments described above demonstrate that photochemical eluent control can be used as the basis for a programmable eluent composition control system for both isocratic and gradient chromatography. At this stage, however, the demonstration is limited to the specific case of cation exchange chromatography with suppressed conductivity detection. In the following chapters, theoretical aspects of photochemical eluent control will be developed, alternative photochemicals will be compared, and additional applications and modes of chromatography will be explored.

Perhaps the most important finding that arises from the work described in this chapter is that compact UV LEDs are sufficiently powerful light sources to make a useful concentration change in a microscale chromatography eluent. Given that the apparatus used was at a very early prototype stage, the ability to generate up to 1.6 mmol/L of the desired chemical (HCl) is promising, though higher concentrations would be desired for greater utility. The separation quality, though mediocre, should not be of major concern. Whilst the separation efficiency was not very high, this can be most likely be attributed to the fact that the separation was performed with a separation column and suppressor column that were not well suited to the flow rate and eluent composition that was used.

The use of compact, low temperature light sources and tailored photochemicals as demonstrated in this thesis may be a more practical approach and far more amenable to miniaturized portable devices than the method of Salamoun and Slais [18]. Therefore, it may be that photochemical eluent control has only recently

become practical, given that high power compact UV LEDs have become available relatively recently.

The photochemical eluent control approach is nearly unique in its ability to create precision compositional changes in a flowing liquid *in situ,* without combining multiple liquids. The only comparable technology that comes to mind is electrolytic eluent generation, described in the introduction to this chapter. However, the electrolytic approach has more design requirements and at present seems to be incompatible with most organic solutions and solutes.

3.5 References

1. Papadoyannis, I. N., Georga, K. A., *Encycl*. *Chromatogr*. *(3rd Ed.)*, *2*, 1032-1034.

2. LaCourse, W. R., *Chromatography: Liquid: Instrumentation*, in *Encyclopedia of Separation Science*, I.D. Wilson, Editor. 2000, Academic Press: Oxford. p. 670-676.

3. Varilova, T., Madera, M., Pacakova, V., Stulik, K., *Current Proteomics* 2006, *3*, 55-79.

4. Mallik, R., Hage, D. S., *J*. *Sep*. *Sci*. 2006, *29*, 1686-1704.

5. Agilent, 1200 Series Quaternary Pump User Manual, Edition July 2008, Agilent Technologies, Waldbronn, Germany

6. Agilent 1200 Series Binary Pump SL User Manual, Edition February 2009, Agilent Technologies, Waldbronn, Germany

7. Brennen, R. A., Yin, H., Killeen, K. P., *Anal*. *Chem*. 2007, *79*, 9302-9309.

8. Hartmann, D. M., Nevill, J. T., Wyrick, D., Votaw, G. A., Crenshaw, H. C., *Lab Chip* 2009, *9*, 2332-2338.

9. Martin, M., Guiochon, G., *J. Chromatogr*. 1978, *151*, 267-89.

10. Davis, M. T., Stahl, D. C., Lee, T. D., *J. Am. Soc. Mass Spectrom*. 1995, *6*, 571-7.

11. Eschelbach, J. W., Jorgenson, J. W., *Anal. Chem*. 2006, *78*, 1697-1706.

12. Deguchi, K., Ito, S., Yoshioka, S., Ogata, I., Takeda, A., *Anal. Chem*. 2004, *76*, 1524-1528.

13. Zhang, X. Y., Roper, M. G., *Anal. Chem*. 2009, *81*, 1162-1168.

14. Xie, J., Miao, Y., Shih, J., He, Q., Liu, J., Tai, Y.-C., Lee, T. D., *Anal. Chem*. 2004, *76*, 3756-3763.

15. Lazar, I. M., Karger, B. L., *Anal. Chem*. 2002, *74*, 6259-6268.

16. Strong, D. L., Dasgupta, P.K., Friedman, K., Stillian, J.R., *Anal. Chem*. 1991, *63*, 480-486

17. Liu, Y., Srinivasan, K., Pohl, C., Avdalovic, N., *J. Biochem. Bioph. Meth*. 2004, *60*, 205-232.

18. Salamoun, J., Slais, K., *J. Chromatogr*. 1990, *522*, 205-11.

19. Sheehan, J. C., Wilson, R. M., *J. Am. Chem. Soc*. 1964, *86*, 5277-81.

20. Sheehan, J. C., Wilson, R. M., Oxford, A. W., *J. Am. Chem. Soc*. 2002, *93*, 7222-7228.

21. UVTOP Technical Data, Sensor Electronic Technology, Inc. (Columbia, SC, USA), <http://www.s-et.com/datasheet/SET_UVTOP_Catalog.pdf> (2009), accessed on 28th of August 2010.

22. Preinerstorfer, B., Bicker, W., Lindner, W., Lämmerhofer, M., *J. Chromatogr. A* 2004, *1044*, 187-199.

23. Rohr, T., Hilder, E. F., Donovan, J. J., Svec, F., Fréchet, J. M. J., *Macromolecules* 2003, *36*, 1677-1684.

24. Yang, C.-P., Ting, C.-Y., *J. Appl. Polym. Sci*. 1993, *49*, 1019-1029.

25. Turro, N. J., *Modern Molecular Photochemistry*. 1991, Sausilito, California: University Science Books. 589-593.

4 Photochemical Eluent Control: Technical Considerations and Optimisation of Acid Generation

4.1 Introduction

In the previous chapter, the concept of photochemical eluent control was introduced and demonstrated. The proposed advantages of this approach all stem from the fact that it allows a completely non-mechanical means of controlling eluent composition; eluent concentration is ultimately controlled by an applied electric current. It also seems to have potential advantages over the other current controlled method, electrolytic eluent generation, in terms of design simplicity and flexibility. However, the capabilities of photochemical eluent control need to be explored more thoroughly before any predictions can be made as to whether these advantages can translate into realistic practical applications.

Photochemical eluent control is an application of flow photolysis in microfluidic systems, a process which has previously been explored in a theoretical study [1] and also in a practical demonstration [2]. However, these investigations were concerned with the application of flow photolysis to the control of very rapid concentration changes in the micromolar range for the purpose of studying the effects of metabolites on cells on microfluidic platforms. Exploring the technical aspects of photochemical eluent control requires a different perspective because it involves much higher concentration changes and because it does not require ultra-fast composition switching times. The only known report of a photochemical reaction to control eluent composition which precedes this project (Salamoun and

Slais [3]) used a completely different approach which may not be suitable to miniaturised chromatography, and in any case did not include a significant discussion on the technical or theoretical aspects of the idea. Therefore, this chapter explores some of the technical aspects of photochemical eluent control from first principles, whilst attempting to anticipate various problems and limitations. The second half of this chapter extends this exploration into a practical study by testing and comparing the performance of several classes of photochemical reagent in order to develop a significantly improved acid generation flow photolysis system.

4.2 Design Aspects

The design aspects of a photochemical eluent control system include the reaction cell materials and geometry as well as the type and arrangement of the light sources.

4.2.1 Light generation and delivery

As stated in the previous chapter, LEDs are an excellent light source for photochemical eluent control because they are inexpensive, compact, generate very little heat, and their output intensity is easily controlled across a wide range by the applied current [4]. All methods described in this thesis rely on ball lens LEDs which are focussed on the eluent as it flows through the reaction cell. However, in principle there is no need to have such a complicated system. It might be better if the LED material could be directly next to, or surround, the reaction cell. This type of arrangement was recently demonstrated by Ren *et al*. who developed a microfluidic chip with an array of capillary electrophoresis channels using fluorescence detection. Their system included an excitation LED

which was tightly integrated into the chip without the need for a lens [5]. Whilst such schemes might give improvements in terms of size, robustness and efficiency of photochemical eluent generation systems, they were not tested in this project because they would have required the development of a far more complicated and expensive prototype.

Alternative light sources such as lasers and various types of lamp all suffer from disadvantages such as increased cost, size, heat generation, or difficulty in controlling intensity. However, they would have to be considered for those applications with light requirements which surpass the limitations of LEDs. For example, many classes of photochemical reaction require a wavelength lower than 240 nm, which is below the current limit of commercially available compact LED technology [6]. Fortunately, LED technology is expected to improve over time, and shorter wavelength LEDs are already in development [7].

4.2.2 Reaction Cell Geometry

The yield of the photochemical reaction is dependant on the dimensions of the photoreaction cell because this affects how much of the emission profile of the LED can be captured. For the UVTOP LEDs used in the experiments described in this thesis, the emission profile was a 2 x 2 mm square-like shape at the best focal range. The depth of the reaction cell from the angle of incidence can limit the photolysis reaction because light is absorbed by the reagent and its photoproducts as it penetrates through the solution, reducing the intensity at greater depths inside the cell. This effect could potentially reduce the photochemical reaction yield for cells with greater thickness (depth). On the other hand, increased reaction cell depth also results in an increase in the cross-sectional area of the photoreaction cell. The cross-sectional area determines the

relationship between volumetric flow rate and linear flow velocity, which in turn determines how long (in seconds) the reagent will be exposed as it passes through the irradiated zone in the reaction cell. Therefore there is a competing effect in which an increased reaction cell depth may increase the photochemical reaction yields.

The volumetric flow rate also controls the maximum yield by affecting the linear flow velocity through the cell. However, it is not an appropriate parameter for optimisation because it is usually chosen based on chromatographic considerations.

In principle, the reaction cell shape could be optimised, most likely to a wide but very shallow geometry. This would allow good penetration of light whilst capturing all of the LED emission pattern and providing a reasonable sized cross-sectional area to give a low linear flow velocity through the irradiated zone. Furthermore, the use of reaction cell with very shallow height would help prevent hydrodynamic band broadening by encouraging laminar flow, which could reduce the maximum achievable gradient slope. However, due to the competing effects of reaction cell geometry, any optimisation would be specific to the properties of the photochemical, the light intensity and emission pattern, and the desired volumetric flow rate. Therefore. the author determined to hold this parameter constant, preparing all reaction cells from short sections of 1 mm ID fused silica which were readily available.

The most obvious location for the reaction cell is upstream of the point of sample injection, as was the case in the system described in the previous chapter. This location has the advantage that the sample does not have to pass through the irradiated zone, where it might otherwise absorb the light that is intended for the

photochemical reagents or react with them whilst they are in their excited states. This approach also decreases the dead volume between the sample injector and the column compared to the alternative of having the reaction cell downstream of the injector. By contrast, the only advantage to having the reaction cell downstream of the injector would be that the eluent composition at the column could be adjusted more rapidly. Therefore, the author expects that having the reaction cell upstream of the point of sample injection would be the most desirable arrangement for most applications.

4.3 Photochemical Aspects

4.3.1 Photochemical system

A crucial step in designing a photochemical eluent control system is the identification of an appropriate photochemical system that could be incorporated into the eluent in order to effect the desired compositional change. The scope of potential photochemical systems is huge, varying from simple photolytic molecules that directly yield compounds of interest through to multicomponent system with photosensitisers and other reactants. For ease-of-argument, the discussion that proceeds assumes the simplest case where the photochemical system is merely a photolytic molecule in solution which undergoes an effectively irreversible reaction. Discussion on the different types of chemical composition change that could be achieved by various reactions is reserved for the next chapter.

Once a photochemical system has been identified which gives the right type of compositional change, the next concern is the quantitative extent of this composition change. Achieving the desired amount of eluent composition change

is likely to be a challenge due to the high concentration changes that are typically needed in gradient chromatography. The properties of the photochemical reagent are very important in this respect. The quantum yield for the desired photolysis reaction should be as high as possible, whilst the quantum yield for photochemical reactions leading to undesired side-products should be as low as possible. The performance of the reagent could also be influenced by the speed and quantum yields for the various photophysical processes that are possible after excitation as well the potential for any reversible photochemical changes which occupy the time of the photochemicals.

The effectiveness of the flow photolysis process is complicated by the absorbance of light as it penetrates the solution in the photoreaction cell. Therefore, the molar extinction coefficient of the photochemical has a more complicated effect. If it is too low, much of the light will pass through the cell and may be wasted, possibly resulting in insufficient photolysis. The use of reflective material around the cell could help alleviate that problem. On the other hand, if the molar extinction coefficient is too high, the light will be absorbed only in the outer portion of solution in the reaction cell, potential leading to reduced photolysis yields or radial variation in eluent composition.

4.3.2 Compatibility with Separation and Detection

Any eluent used in an HPLC system must be compatible with both the separation and the detection process. This sometimes creates challenges which are normally overcome by compromising the choice of eluent to meet the requirements of the detector. A well-known example of this is LC-ESI-MS, which requires that only volatile compounds be used in the eluent. Photochemical eluent control is likely

to present significant challenges of this kind because it imposes yet more requirements on the eluent system.

The first issue is that of solubility. The eluent may have certain requirements with regards to which solvents it includes for reasons of solubility of the photochemical and its products. The work described in the previous chapter exemplifies this, where it was necessary to use an eluent with a relatively high fraction of acetonitrile in order to dissolve DeCl. The inclusion of an organic modifier may be detrimental to some kinds of chromatographic separation and might not be compatible with some detection systems. Ideally, one would find photochemicals that are easily soluble in the solvent that is best suited to the most desirable separation column and detection methods. Otherwise, one would need to make compromises when deciding which detection methods and separation columns are to be employed.

The second issue is the potential detrimental effect of the photochemical reagent on separation and detection programs. One could imagine various types of incompatibility, including unwanted interactions between the photochemical reagent and the chromatography column. However, the most obvious and troubling problem that the author anticipates is the potential incompatibility of absorbance detectors with eluents that contain photochemicals. The absorbance of the photochemical (and its photoproducts) can give rise to complications if these compounds are absorbing at the same wavelength as the detector is measuring. In the worst case, they would absorb so much light that the detector loses much or all of its sensitivity to the analytes. Even if they absorb only weakly at the wavelengths measured by the detector, there is a possibility that

they would create a sloped baseline as they pass through the detector with a temporal concentration gradient.

The simplest way around this problem is to avoid using an absorbance detector. However, if absorbance detection is absolutely necessary, there might still be some ways to resolve this problem. The most obvious solution is to find alternative photochemicals which do not absorb at the wavelength of detection. This should be an effective solution for the determination of analytes which absorb in the visible region or the near UV. However, many of the most important analytes, including drugs, pollutants and inorganic ions and proteins require detection in the deep UV. Finding photochemical systems and appropriate light sources that can operate at sufficiently low wavelengths to permit the use of deep UV absorbance detectors might turn out to be very difficult. Other potential solutions to this problem are discussed in "Conclusions and Future Work".

4.4 Experimental

4.4.1 Reagents

HCl 37% and NaOH 98% were purchased from Sigma-Alrich, (St Louis, MI, USA). HPLC grade acetonitrile was purchased from BDH (Darmstadt, Germany). HBr 98% was from Aldrich (Milwaukee, WI, USA).

Desyl chloride 98% and 2-nitrobenzylchloride were purchased from Alfa Aesar (Heysham, UK). 2-Chloro-1-(2,5-dimethylphenyl)ethanone 95% was purchased from ChemBridge (San Diego, CA, USA). 4,5-Dimethoxy-2-nitrobenzyl bromide 97%, 2-bromo-4'-methoxyacetophenone 97% and 2-chloro-3'4'-dihydroxyacetephenone 97% were purchased from Aldrich. More details on these six photochemical reagents are presented in Section 4.5.2 "Chemical Data".

4.4.2 Measurement of Absorbance Spectrums

The absorbance spectrums of the six different photochemicals in 50% w/w acetonitrile-water were measured at concentrations of approximately 0.5 mmol/L using a cell width of 1 mm. These same solutions were used for the acid generation experiments described below. After they had been tested with all LEDs, the solutions were run through the reaction cell for several hours whilst being irradiated by the LED that gave the highest acid yield for that photochemical, respectively. The effluents were collected and the absorbance spectrums of these "processed" eluents were re-measured by the same method.

4.4.3 Determination of concentration of generated acid

The concentration of acid generated by the six different photochemicals at concentrations of 0.5 mmol/L and 15 mmol/L was determined as follows. Each photochemical, dissolved in 50% w/w acetonitrile-water, was pumped through the reaction cell at a flow rate of 1.6 µL per minute using an Agilent 1200 series capillary pump (Agilent Technologies, Santa Clara, CA) which included a degassing unit. The flow rate was confirmed by measuring the volume of liquid that was pumped through the system over several hours. The reaction cell was exposed to one single LED at a distance of 15 mm supplied by a current of 23 mA. Several 1 mm ID fused silica reaction cells were prepared in the same way as described in the previous chapter. A fresh reaction cell was used for the measurements on each new reagent to resolve the issue of reaction cell fouling (see Section 4.5). The experiment was repeated with up to six LEDs depending on the wavelength range of the absorbance spectrum of the photochemical. The six LEDs used were model type UVTOP-39BL, purchased from Sensor Electronic Technology, South Carolina, with wavelength maxima at 250 nm, 270 nm, 290

nm, 310 nm, 335 nm and 355 nm, respectively. Expected power outputs were unknown, 600, unkown, 600, 400, and 800 μW, respectively.

The concentration of generated acid was measured by conductivity using a C^4D cell (eDAQ, NSW, Australia) which was installed on a piece of 75 μm ID fused silica capillary (Polymicro, AZ, USA) downstream of the reaction cell and injection valve. The conductivity detector was calibrated using standards of HBr and HCl in 50% w/w acetonitrile-water. It was not possible to find a single set of detection settings that would allow determination of conductivity across the entire concentration range of the calibration, which covered more than two orders of magnitude. It was therefore necessary to calibrate the detector using two different sets of detection parameters for high and low ranges, respectively. The low sensitivity settings were: Head Space Gain = off, Frequency = 1000 KHz, Amplitude = 20 V, Offset = 0, Gain = 1. The high sensitivity settings were: Head Space Gain = off, Frequency = 600 KHz, Amplitude = 80 V, Offset = 0, Gain = 1. Calibration curves were not fitted across the entire calibration data set because the response of the C^4D was non-linear. Rather, two separate curves were fitted to each calibration set for the higher and lower values, respectively (except for the high sensitivity HBr calibration for which the high values curve was not needed), and it was necessary to use quadratic or cubic calibration curves to achieve an adequate fit. The calibration data and curves can be found in the appendix of this thesis. The curves are titled with four letter abbreviations. The first two letters denote whether the high sensitivity (HS) or low sensitivity (LS) settings were used, whilst the last two letters refer to whether the curve is fitted to the high values (HV) or low values (LV).

The photochemical solutions had low levels of conductivity prior to photolysis due either to contaminants in the manufacturer supplied reagents or partial premature photolysis under ambient conditions. In order to take this into account, the concentration of photochemically generated HCl or HBr was calculated as follows. First, the conductivity after photolysis was measured and this value was used to interpolate a preliminary value for the concentration of acid in the solution using the most appropriate calibration curve. Next, the baseline level of conductivity (LED turned off) was measured. This value was also used to interpolate a value for acid concentration from the most appropriate calibration curve, and this value was assumed to represent the contribution of conductive contaminants (including those produced by premature photolysis under ambient conditions) to the preliminary acid concentration score. The final acid concentration score (from this point onwards described as the concentration of "generated acid" or "acid yield") was calculated by subtracting the conductive contaminant score from the preliminary acid concentration score. The raw data for these measurements and calculations is presented in the appendix at the end of this thesis.

4.5 Results and Discussion

The system described in the previous chapter had a maximum yield of 1.6 mmol/L HCl using four LEDs operating at 2.3 μL/min using 2.0 mmol/L desyl chloride as the photochemical reagent. Whilst this served well as a proof-of-principle system, higher concentrations of acid would be desirable for many conceivable chromatography applications. Therefore, the primary objective in testing various photochemical reagents was to increase the maximum acid yield of the system. Meanwhile, the photochemical control system was altered to use just one LED at

a time. The LED was held in place firmly by a block of plastic with an appropriately shaped hole drilled into it such that the LED lenses would all rest in the same position near the bottom of the plastic, as shown in Figure 4.1. This way, different LEDs could be easily substituted in a consistent way, positioned 15 mm above the reaction cell. Finally, the flow rate was reduced to 1.6 μL/min to allow more time for exposure so as to partially compensate for the reduced number of LEDs.

4.5.1 Choice of Reagents

Whilst potential sources of acid-generating photochemical reagents (photoacids) could include chemicals from photolithography and photoinitiated polymerisation chemistry, the search was focussed on several families of photochemical that have been studied and developed for application to cell biology research where they are known as caged compounds [8] or photoremovable protecting groups [9]. These classes of photochemicals have already been selected by researchers in that field for their favourable properties of water stability as well as relatively high quantum yields from excitation at wavelengths varying between 250 nm up to the near UV range. This wavelength corresponds well to commercially available LEDs and also has the advantage that there is less background radiation in this range than at longer wavelengths, making these chemicals easier to store and more resilient against premature photolysis.

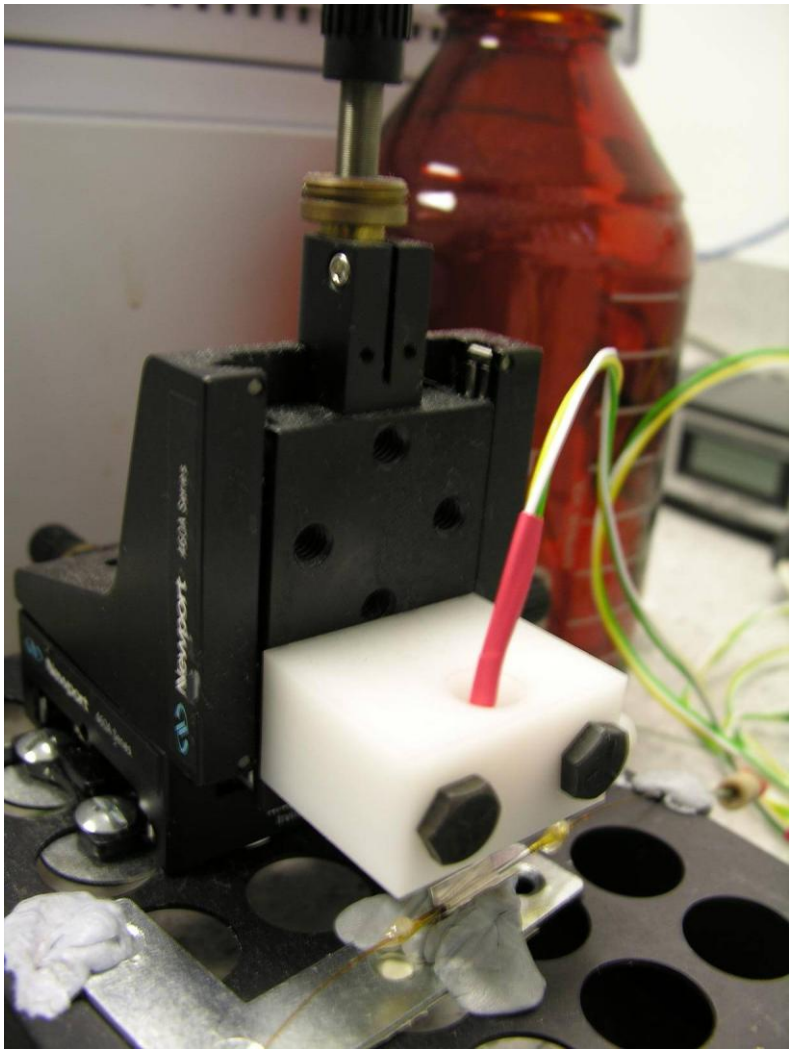

Figure 4.1 – Photochemical eluent control system using a single LED fixed in place with a plastic holder.

Whilst photochemicals from this class can react by a variety mechanisms [8, 9], the general overall outcome is shown in Equation 4.1.

Protecting Group-X → Photoproduct(s) + HX *Equation 4.1*

X is typically some sort of leaving group such as a phosphate or carboxylate ester and it is usually this group that is of interest to cell biology researchers. For example, X may be ATP or the c-terminus of a peptide. These photochemicals can also be used to generate acid, because X may also be a very weak base such as a halide. In that case, Equation 4.1 shows the release of one equivalent of strong acid into the system. The so-called "protecting group" part of these photochemicals can belong to one of several families that are identified by similar structure.

The author searched for commercially available reagents from the various families of photochemicals described in two reviews [8, 9] and determined to select only those with Cl or Br in the X position. Six candidate photochemicals were identified, as illustrated in Section 4.5.2, covering the most popular and best understood families of photochemical protecting group.

The first family is the benzoins, which includes desyl chloride from the work described in the previous chapter. Chemicals from this class can undergo a variety of reactions when exposed to UV radiation that can depend on the type of solvent used and the substitutions on the phenacyl ring [10], as well as the presence of cyclodextrins [11]. Fortunately, the net result of many of these

reactions is Equation 4.1. Benzoins with methoxy substituents in the meta position of the non-conjugated ring system have been reported to give the most controlled photoreaction, with one report giving a yield of 99.5% for HX and a substituted phenylbenzofuran photoproduct [12]. However, no commercial source could be found for a suitable methoxy substituted reagent. Therefore, it was decided that the completely unsubstituted benzoin that was used in the previous chapter, DeCl, would have to represent this class.

The second class of chemicals studied are the 2-nitrobenzyl family. This family includes the most popular commercially available photochemically caged compounds for cell biology studies [13]. The most common subtypes include 2-nitrobenzyl, represented here by 2-nitrobenzyl chloride (2NBC), and 4,5-dimethoxy-2-nitrobenzyl, which is represented in these experiments by 4,5-dimethoxy-2-nitrobenzyl bromide (DMNBB). Whilst a range of reaction mechanisms are possible for this family of photolabile compounds [14, 15], many of the best known reactions have the net result of Equation 4.1.

The third family of photochemicals studied are the phenacyl photoremovable protecting groups, first popularised by Sheehan and Umezawa in 1973 [16]. These chemicals are substituted benzenes with an acyl group attached, where the leaving group is bonded to the 2-carbon of the acyl moiety. A variety of mechanisms can result in Equation 4.1, and these are highly dependent on the substitutions on the ring [9]. The 4-methoxy pattern was the first to be studied [16] and it is represented in these experiments by 2-bromo-4'methoxyacetophenone (2B4MA). Somewhat more recently there has been interest in the 2,5-dimethyl substitution seems pattern which seems to give very good photolysis performance [17, 18]. The chloride substituted member of this

class, 2-chloro-1-(2,5-dimethylphenyl)ethanone (CDMEP), is investigated in this study. Another popular class is the 4-hydroxy substitution pattern [9]. Unfortunately, no suitable commercially available halogen substituted compound from this group could be found. The 3,4-dihydroxy substituted analogue, 2 chloro-3',4'-dihydroxyacetophenone (CDHAP), was acquired instead and served to represent this class, albeit imperfectly.

Section 4.5.2 "Chemical Data", beginning on following page, gives the name, abbreviation, molecular weight, supplier, and structural information of these chemicals, in addition to solubility and spectral data which are explained in later sections.

4.5.2 Chemical data

Name: Desyl Chloride, 98%

Abbreviation: DeCl

Molecular weight: = 230.69

Supplier: Alfa Aesar (UK)

Solubility in 50% w/w acetonitrile-water:

0.08 mol/L

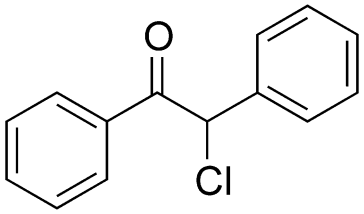

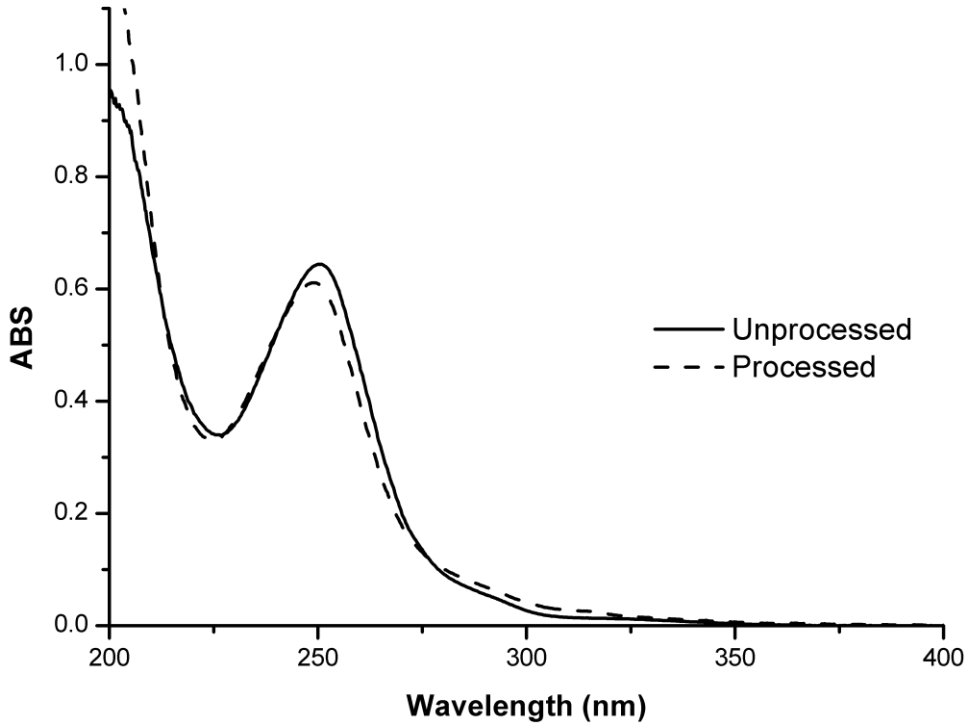

Spectrum of 0.50 mmol/L DeCl in 50% w/w acetonitrile-water.

Name: 2-nitrobenzylchloride, 98+%

Abbreviation: 2NBC

Molecular weight: = 171.58

Supplier: Alfa Aesar (UK)

Solubility in 50% w/w acetonitrile-water:

0.16 mol/L

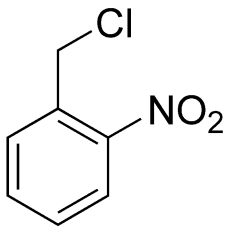

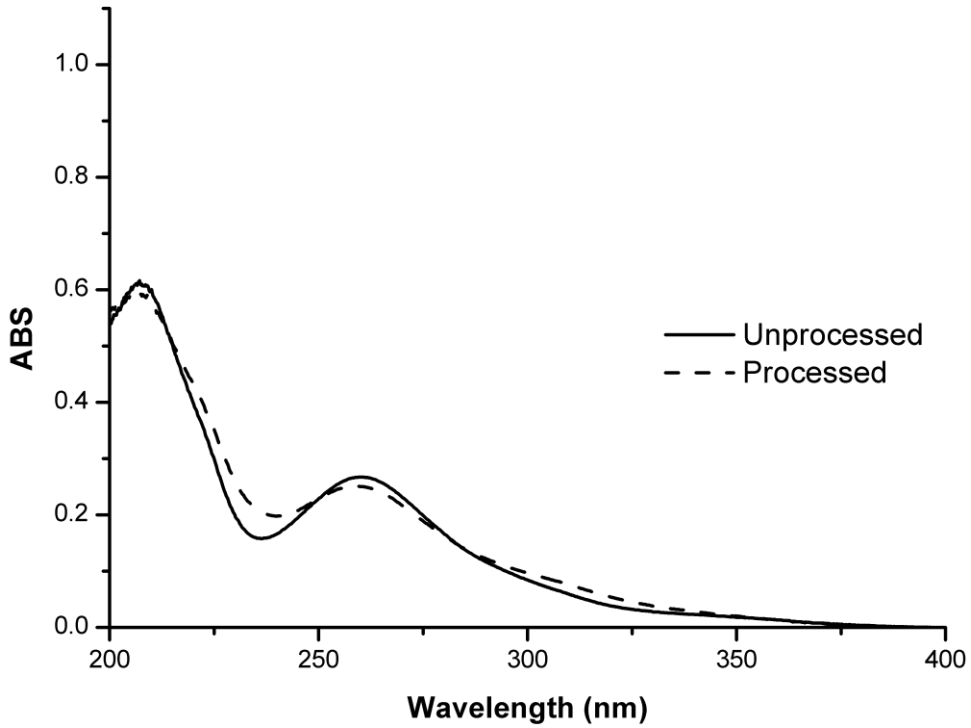

Spectrum of 0.51 mmol/L 2NBC in 50% w/w acetonitrile-water.

Name: 4,5-dimethoxy-2-nitrobenzyl bromide, 97%

Abbreviation: DMNBB

Molecular weight: = 276.09

Supplier: Aldrich, St Louis, MO, USA

Solubility in 50% w/w acetonitrile-water: 0.02 mol/L

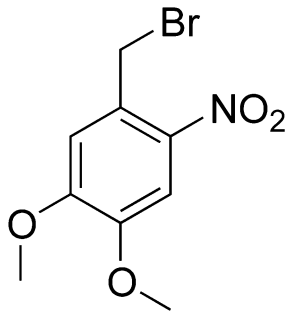

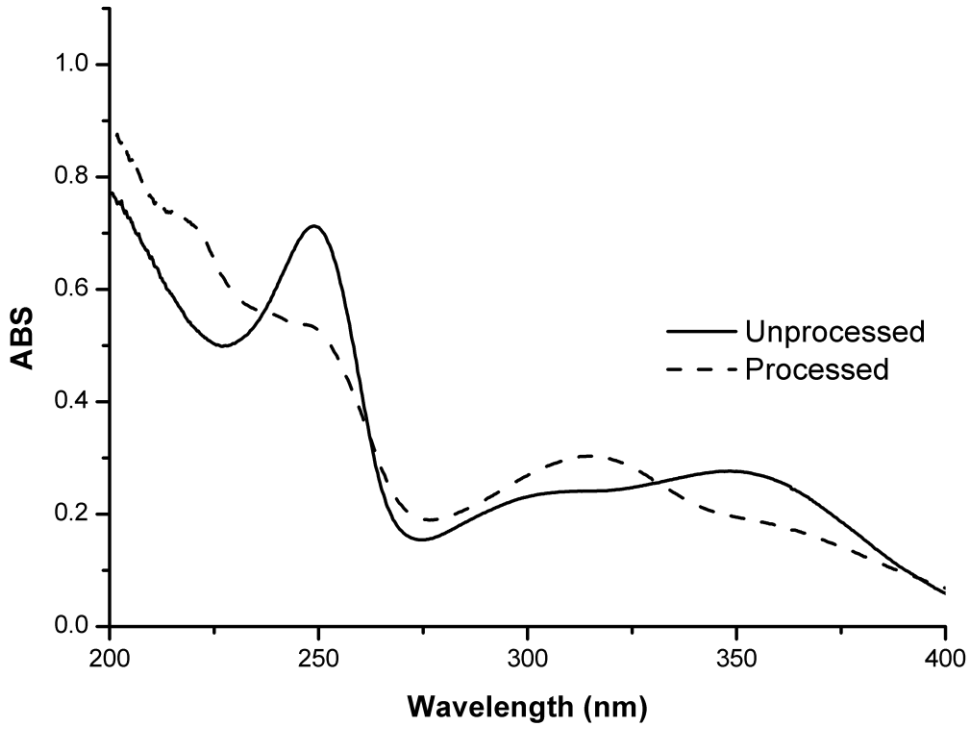

Spectrum of 0.50 mmol/L DMNBB in 50% w/w acetonitrile-water.

Name:

2-chloro-1-(2,5-dimethylphenyl)ethanone, 95%

Abbreviation: CDMEP

Molecular weight: = 183

Supplier: ChemBridge, CA, USA

Solubility in 50% w/w acetonitrile-water:

0.12 mol/L

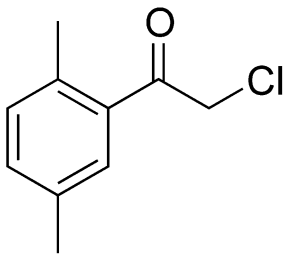

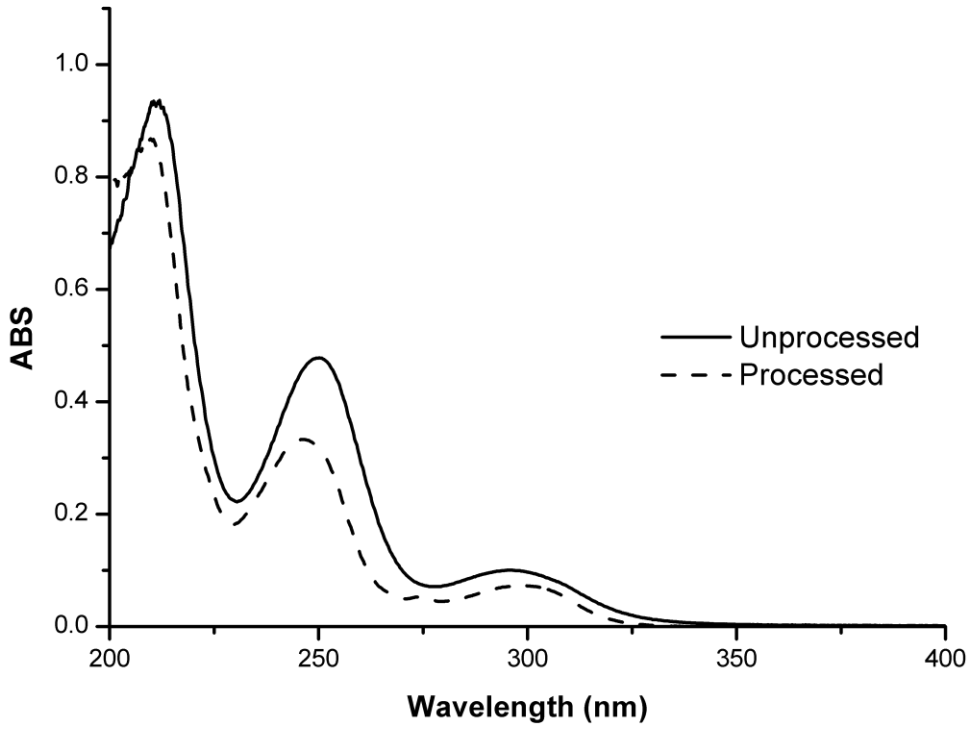

Spectrum of 0.63 mmol/L CDMEP in 50% w/w acetonitrile-water.

Name: 2-bromo-4'-methoxyacetophenone

97%

Abbreviation: 2B4MA

Molecular weight: = 229.07

Supplier: Aldrich, St Louis, MO, USA

Solubility in 50% w/w acetonitrile-water:

0.18 mol/L

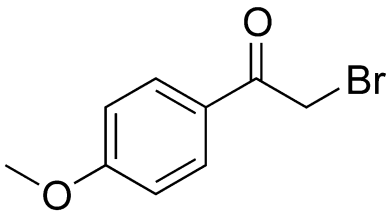

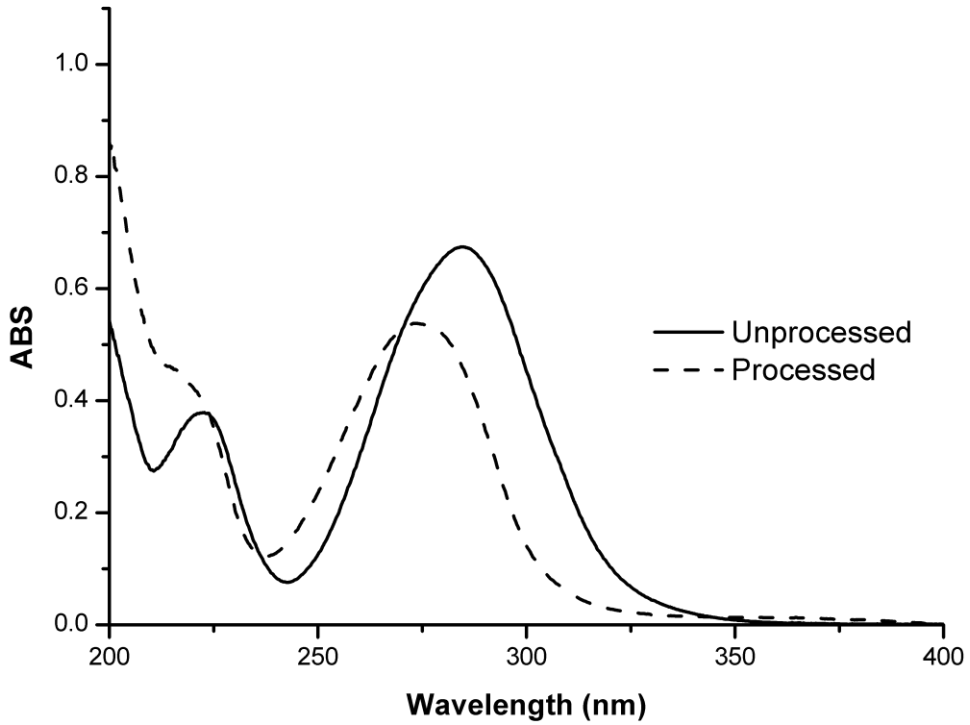

Spectrum of 0.52 mmol/L 2B4MA in 50% w/w acetonitrile-water.

Name: 2-chloro-3’4’-dihydroxyacetephenone, 97%

Abbreviation: CDHAP

Molecular weight: = 186.59

Supplier: Aldrich, St Louis, MO, USA

Solubility in 50% w/w acetonitrile-water:

0.26 mol/L

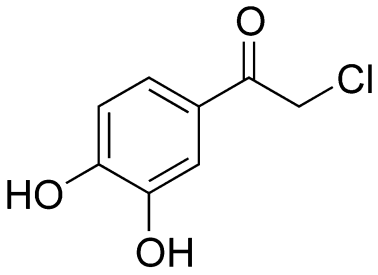

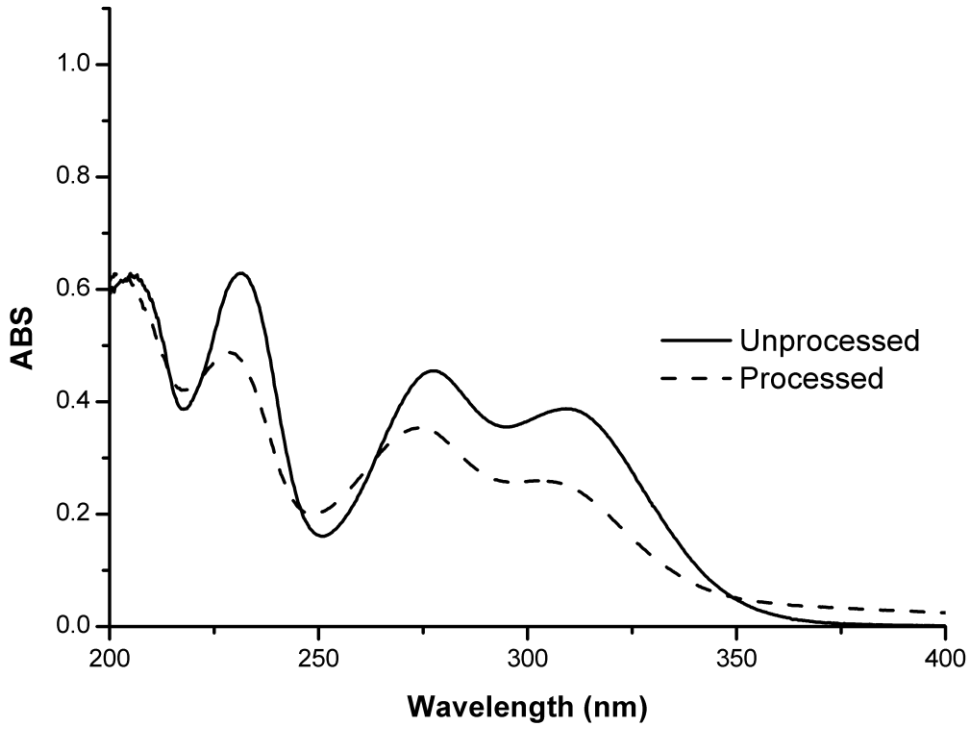

Spectrum of 0.50 mmol/L CDHAP in 50% w/w acetonitrile-water.

4.5.3 Acid generation

The six different photochemical reagents were tested at concentrations of approximately 0.5 mmol/L and also at higher concentrations of 15 mmol/L. The low concentration test reveals the photosensitivity of the reagents at different wavelengths in a surplus of light. This could be important information for designing and optimising a photochemical eluent control system involving these reagents. Meanwhile, the high concentration tests reveal the performance of the reagents in a situation where a very high portion of the incident light is being absorbed by the reagent, and where the photolysis process may be complicated by high concentrations of excited state chemicals and products. The high concentration test may be considered to be a more practical assessment of the capabilities of these reagents to generate meaningful compositional changes, although it is important to remember that the findings are specific to the reaction cell geometry, flow rate and LED type that was used in this study.

All of the reagents tested generated acid when exposed to UV light. The results have been compiled in Table 4.1 whilst the raw data is presented in the appendix of this thesis. CDMEP produced the most acid, generating 8.4 mmol/L using the 310 nm LED from a 15.0 mmol/L solution. The next best performer was DeCl which produced 4.4 mmol/L also from a 15.0 mmol/L solution when exposed to light from the 290 nm LED.

It should be noted that the acid concentration values in Table 4.1 are based on the assumption that HCl or HBr are the only ionised components in the mixture. This assumption is based on two proposals. The first proposal is that HCl or HBr are the expected photoproducts, as described above in the “choice of reagents” section. The second proposal is that the only other conceivable conductive

products are weak acids such as carboxylic acids. Given that the pH of the solution rapidly decreases after the first traces of photochemical are reacted, the weak acid products would be expected to exist primarily in their non ionised states which do not contribute to conductivity. To the extent that this effect might not hold true, the carboxylate anion products would be less conductive than Cl^- or Br^-, and therefore the measurements are likely to underestimate rather than overestimate the amount of acid produced.

The possibility of the formation of carboxylic acids is also the best explanation for the >100% yields observed for photolysis of 0.5 mmol/L solutions of CDHAP and 2B4MA. This hypothesis is supported by studies that have shown that photoremovable protecting groups from the 4-hydroxyphenacyl family in aqueous solutions can react to form carboxylic acid photoproducts after photolysis, effectively generating two acidic compounds from one starting molecule [19]. If this were happening to CDHAP and 2B4MA, it would account for the impossibly high values of [HCl] and [HBr] generated by those compounds, respectively. Given that these values assume that only HCl and HBr are generated (see above), the actual total values of acid would probably be somewhat higher, due to the lower conductance contribution expected by any conceivable carboxylic acid photoproducts compared to the conductance of HCl or HBr alone. This would also explain the relatively low values for the amount of acid generated by those compounds when their concentrations were increased to 15 mM; the conductance contribution of the carboxylic acid photoproducts would be increasingly suppressed at the lower pH values in these more concentrated solutions.

Whilst the results for each reagent compare the photolysis yields for six different wavelengths, they cannot be used to make definitive conclusions about the ideal

	Conc. mmol/L	Acid generated by LED (mmol/L) *250 nm*	*270 nm*	*290nm*	*310 nm*	*335 nm*	*355 nm*	Formation of residue on inside surface of photoreaction cell
2NBC	0.51	0.09	0.15	0.17	0.13	0.01	0.02	No residue
	15.0	0.28	0.60	**0.98**	0.92	0.30	0.74	No residue
DeCl	0.50	0.46	0.48	0.43	0.31	0.11	-	No residue
	15.0	1.2	2.6	**4.4**	3.9	1.7	-	Significant beige fluorescent residue
2B4MA	0.52	0.22	0.59	0.60	0.59	0.08	-	No residue
	15.1	0.38	0.77	**1.5**	1.4	0.63	0.27	Slight beige fluorescent residue
DMNBB	0.50	0.28	0.27	0.36	0.42	0.28	0.49	No residue
	15.0	0.50	0.69	0.55	1.1	0.55	**1.9**	Slight fluorescent purple residue
CDMEP	0.63	0.32	0.27	0.47	0.51	0.01	0.00	No residue
	15.0	1.1	2.6	6.6	**8.4**	1.2	0.32	Slight beige fluorescent residue
CDHAP	0.50	0.20	0.28	0.51	0.52	0.25	0.05	No residue
	15.0	0.47	1.3	**2.7**	2.1	1.2	0.85	Slight reddish residue

Table 4.1 – Acid generation data for 6 photochemicals at two different concentrations under 6 different LEDs. The conditions and methods are described in experimental section. The acid generation data is explained in Section 4.5.3 whilst the residue data is explained in Section 4.5.5.

wavelength for each reagent. Such an assumption would ignore the fact that each UVTOP-39-BL LEDs had a slightly different emission pattern and each is expected to have a slightly different light output. Whilst the table is a good guide to selecting the best LED from the set possessed by the author, it is only a rough guide for selecting the best wavelength for each reagent in general.

4.5.4 Absorbance spectra

Absorbance spectra of each reagent are presented on their respective information pages in Section 1.5.2 as the solid line (unprocessed). Photochemists might be interested to see the various absorption bands for each chemical in order to better understand the photochemistry of that reagent. However, from an analytical chemistry perspective it is the maximum wavelength of absorbance that is of most interest because it has strong implications for the compatibility of reagents with absorbance detection. All of the reagents had significant absorption up to a wavelength of at least 300 nm. This means that any photochemical control system using these reagents could reduce the sensitivity (perhaps significantly) of an absorbance detector operating at or below 300 nm. This is unfortunate because many of the most interesting analytes including proteins, peptides, inorganic ions, and metabolites absorb at or below this wavelength. Perhaps wider classes of photochemicals could be investigated in order to find reagents with shorter absorbance wavelengths. Other ways of dealing with the absorbance detector problem are discussed in "Conclusions and Future Work".

The absorbance spectrums of the reagent solutions after partial photolysis are also presented (dashed line). These spectra arise from the combined absorbance of the original reagents as well as their photoproducts. In the case of CDMEP, DMNBB and 2B4MA, there was a marked decrease in absorbance at the wavelength of

excitation. This means that these reagents may have an increased likelihood of achieving higher yields when compared to the other reagents, at least when they are used in high concentrations. This is because the excitation light will be transmitted through the solution more easily as photolysis progresses.

Another feature of interest is that the processed and unprocessed absorbance spectra cross over at points that are analogous to isosbestic points. If these points are stable across the full quantitative range of the reaction process (from zero conversion up to maximum photolysis), they are potentially useful. If an absorbance detector was used at these wavelengths there would be no baseline drift as the temporal concentration gradient went past the detector. However, the successful use of absorbance detectors with these photochemical systems would still depend on whether or not there could be sufficient transmission of light through the effluent in the detection cell at these wavelengths.

4.5.5 Miscellaneous Properties

All of the 6 reagents had adequate solubility in 50% acetonitrile-water. It was possible to make solutions with concentrations higher than 0.08 mol/L for all reagents except for DMNBB, which started to precipitate at 0.02 mol/L. On the other hand, all of the reagents were sparingly soluble in 100% water. The poor solubility of these reagents in water implies that there would be an upper limit on the fraction of water that could be used in a photochemical eluent control system that incorporates them. This is was an unfortunate finding because it places additional constraints on any photochemical eluent control system that would make use of these reagents.

All of the reagents except for 2NBC formed insoluble residues when they were irradiated at a concentration of 15 mmol/L which fouled the reaction cell by precipitating out onto the LED-facing part of the internal surface. Figure 4.2 is a photograph of the reaction cell residue generated by DeCl. Table 4.1 describes the nature of the various residues. The patches of residue on the inside of the reaction cell took several hours to form after which they seemed to reach a stable size. It is anticipated that such residues would cause problems in photochemical eluent control systems by absorbing or reflecting the excitation light before it reaches the eluent. Furthermore, some of the residues were fluorescent. This indicates that some of the reagents give fluorescent photoproducts which might need to be taken into consideration if the photochemical eluent control system is used with a fluorescence detector.

Fortunately, none of the reagents produced any observable residue when they were irradiated at a concentration of just 0.5 mmol/L. This suggests that for each reagent there should be maximum concentration, somewhere between 0.5 and 15 mmol/L, that can be used before the residue problem arises. It might also be possible to prevent the build up of the residue by using a different solvent mixture or reaction cell material.

4.6 Conclusions

CDMEP offers the best performance in terms of acid-generating photolysis. Whilst CDMEP did form a small amount of insoluble residue in the reaction cell when it was tested at a concentration 15 mM, the amount of residue was

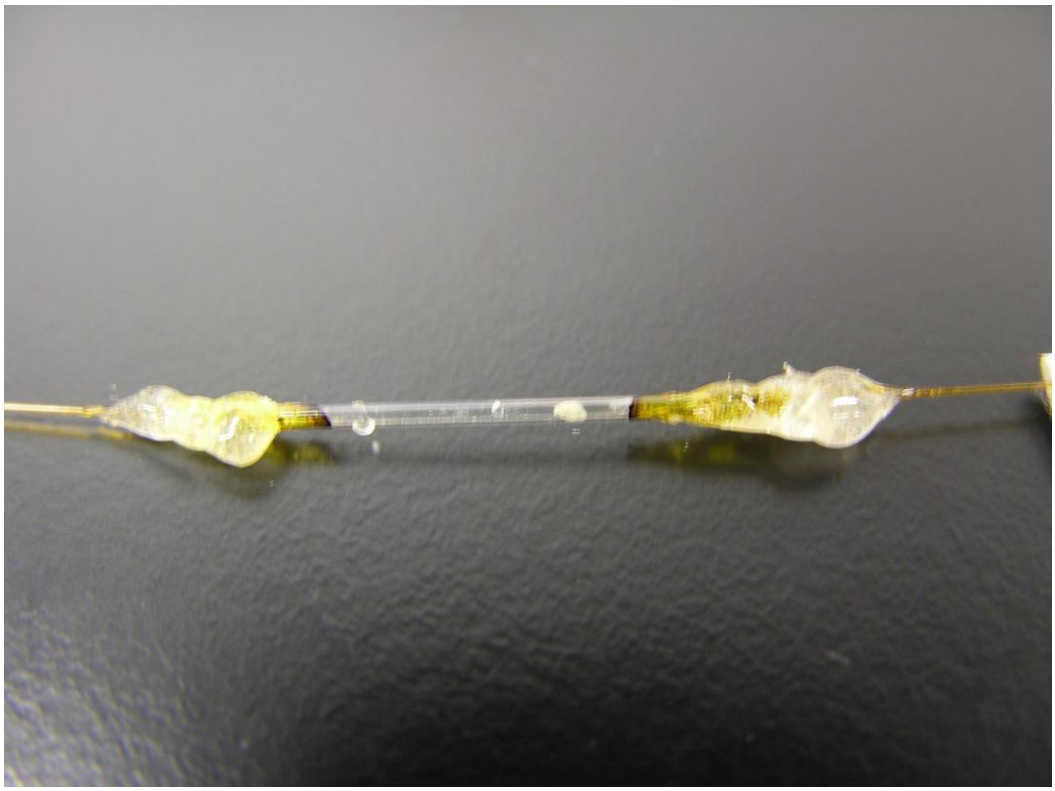

Figure 4.2 – The fused silica reaction cell after use. About 4/5ths of the way along the tube on the right hand side there is a zone of beige coloured material attached to the inner wall of the reaction tube. This material, which probably consisted of insoluble by-products of the photochemical reaction of desyl chloride, formed at the focal point of the 290 nm LED.

noticeably smaller than that formed by the second-best acid generator, DeCl. Therefore, CDMEP was determined to be the "most promising" photochemical candidate, although the successful use of this reagent may depend on finding conditions which completely suppress the build up of residue on the inside of the reaction cell.

It is important to note that the results do not allow any conclusion as to which reagent is the best for photochemical eluent control in general. Rather, the results are at least somewhat specific to the conditions used, such as reactor cell shape and LED strength. For example, there may have been a very different conclusion if more powerful light sources been used. In such conditions, it might be the case that all of the photochemicals would give fairly high yields. In such a scenario, 2NBC might have appeared to be the most promising chemical due to its lack of insoluble reaction residue.

The process of comparing the performance of various photochemical reagents has highlighted the importance of two of the aspects of designing a photochemical eluent control system that were mentioned in the introduction. First, it seems that the solubility of both the reagent and its products is likely to be a significant challenge. The second issue is that of absorbance detection. The fact that all of the reagents tested absorbed at 300 nm indicates that it might be very difficult to find reagents that would be compatible with absorbance detection at popular detection wavelengths.

Whilst these findings were cause for concern, the findings were quite favourable with regards to the ability to use photochemistry to make quantitatively significant composition changes in chromatography eluents. The top performance of 8.4 mmol/L HCl using just one LED (with CDMEP) is very large improvement on the

performance of 1.6 mmol/L HCl demonstrated in the previous chapter with DeCl with four LEDs. Given that this photochemical was identified after a relatively brief literature investigation with the additional constraint of commercial availability, there is every reason to assume that even better performing reagents could be identified or designed.

4.7 References

1. Bae, A., Beta, C., Bodenschatz, E., *Lab Chip* 2009, *9*, 3059-3065.
2. Beta, C., Wyatt, D., Rappel, W.-J., Bodenschatz, E., *Anal*. *Chem*. 2007, *79*, 3940-3944.
3. Salamoun, J., Slais, K., *J*. *Chromatogr*. 1990, *522*, 205-11.
4. *UVTOP Technical Data*, Sensor Electronic Technology, Inc. (Columbia, SC, USA), <http://www.s-et.com/datasheet/SET_UVTOP_Catalog.pdf> 2009, accessed on 28th August 2010.
5. Ren, K., Liang, Q., Mu, X., Luo, G., Wang, Y., *Lab Chip* 2009, *9*, 733-736.
6. *Ultraviolet (UV) and Deep UV LED Based Light Sources*, Sensor Electronic Technology, <http://www.s-et.com> accessed on 28th August 2010.
7. Taniyasu, Y., Kasu, M., Makimoto, T., *Nature* 2006, *441*, 325-328.
8. Adams, S. R., Tsien, R. Y., *Annu*. *Rev*. *Physiol*. 1993, *55*, 755-784.
9. Pelliccioli, A. P., Wirz, J., *Photochem*. *Photobio*. *Sci*. 2002, *1*, 441-458.
10. Sheehan, J. C., Wilson, R. M., *J*. *Am*. *Chem*. *Soc*. 1964, *86*, 5277-81.

11. Bantu, N. R., Kotch, T. G., Lees, A. J., *Tetrahedron Lett*. 1993, *34*, 2039-2042.

12. Sheehan, J. C., Wilson, R. M., Oxford, A. W., *J*. *Am*. *Chem*. *Soc*. 2002, *93*, 7222-7228.

13. *Caged Nucleotides,* Molecular Probes, <http://probes.invitrogen.com/media/pis/mp01037.pdf> accessed on 28th of August 2010.

14. Schworer, M., Wirz, J., *Helv*. *Chim*. *Acta* 2001, *84*, 1441-1458.

15. Il'ichev, Y. V., Schwoerer, M. A., Wirz, J., *J*. *Am*. *Chem*. *Soc*. 2004, *126*, 4581-4595.

16. Sheehan, J. C., Umezawa, K., *J*. *Org*. *Chem*. 1973, *38*, 3771-3774.

17. Zabadal, M., Pelliccioli, A. P., Klan, P., Wirz, J., *J*. *Phys*. *Chem*. *A* 2001, *105*, 10329-10333.

18. Klan, P., Pelliccioli, A. P., Pospisil, T., Wirz, J., *Photochem*. *Photobio*. *Sci*. 2002, *1*, 920-923.

19. Park, C.-H., Givens, R. S., *J*. *Am*. *Chem*. *Soc*. 1997, *119*, 2453-2463.

5 Alternative applications of photochemical eluent control

5.1 Introduction

As mentioned in Chapter 3, photochemical eluent control could be used for concentration gradients for any type of microscale liquid chromatography eluent provided that an appropriate photochemical system can be found. This chapter conceptually explores a few different types of photochemical systems and suggests how they might be used. Later in the chapter, a buffered photochemical eluent control system with programmable pH is identified as being a relatively simple modification of the system presented in Chapter 3. Such a system is then developed and demonstrated for microscale pH dependant reversed phase LC-MS of antipsychotic drugs.

5.1.1 Generation of acid and base for ion chromatography

The previous two chapters described photochemical eluent control systems that generate programmable concentrations of HCl and HBr. Pure acid eluents such as these are favoured for ion chromatography of simple cations, especially inorganic and ammonium species. One of the main reasons for this is that they can be used for suppressed conductivity detection [1] as was demonstrated in Chapter 3. For anion exchange chromatography with suppressed conductivity detection, it would be necessary to form alkaline eluents such as solutions of KOH. There are several photochemical systems that are known to release bases [2, 3], however they are generally not as appealing as photoacid systems such as those described in the previous chapter. Many suffer from disadvantages including the requirements of multiple components, larger and more complex molecules, or the generation of

gaseous products. Nevertheless, if an appropriate photobase system could be identified, it should be fairly straightforward to design a system that could work for anion exchange chromatography with suppressed conductivity detection.

5.1.2 Control over pH

Photochemical control over the pH of a chromatography eluent was demonstrated by Salamoun and Slais in 1990 [4]. However, their system (described in Chapter 3) had the disadvantages of requiring a mercury lamp and the presence of peroxide in the eluent. Running at 50 μL/min or higher, their system was not truly microscale and it is difficult to see how it could be miniaturised. Alternative approaches to designing a photochemical eluent pH control system should be explored.

Consider the acid generating compounds that were described in the previous chapter. These compounds generate both H_3O^+ and halide ions when irradiated, either of which could be useful for controlling elution in a cation exchange or anion exchange system. However, by considering the fact that H_3O^+ can also function as an acid, it is immediately apparent that the same flow photolysis system could be modified to give programmable control over eluent pH. The only modification that would be needed is the addition of buffer compounds which can be "titrated" by different amounts of generated HCl so that the eluent can be set (buffered) at different pH values. Therefore, it would seem that the same approach to photochemical eluent control can potentially be used for any form of pH dependant chromatography.

The concept of using a mobile phase pH gradient in chromatography first gained popularity during the 1950s when such gradients became important in the

separation of amino acids and peptides [5, 6]. Today, changes in eluent pH are common in high resolution ion exchange chromatography of proteins and peptides [7, 8]. The use of pH gradients in ion exchange chromatography of biomolecules results in an elution order that tends to depend on their relative acidity (or basicity) in terms of pI [9], which means the pH at which they have a neutral net charge. Originally, the pH gradients were generated within the column by the use of a multitude of different buffer compounds which interact with the ion exchange sites, allowing use of a single eluent solution on a properly equilibrated column. This technique, known as chromatofocusing, is now facing increasing competition from an alternative pH dependant technique. Termed "pH gradient ion exchange chromatography" or "gradient chromatofocusing", this new approach uses a smooth gradient of two eluents which each contain a relatively simple set of buffer compounds at different pH values. There is evidence that this relatively new approach gives significantly better performance than traditional chromatofocusing [7] and it is showing great promise for separating biotherapeutics such as monoclonal antibodies [10].

In addition to controlling coulombic interactions in ion exchange chromatography, a change in pH can also dramatically alter the more complicated affinity interactions between biomolecules. Mobile phase pH gradients (especially step-gradients) are therefore common in affinity chromatography procedures [11]. Given the interest in preparing miniaturised systems for medical diagnostics [12], the use of photochemical eluent control for this type of affinity chromatography is especially interesting,

Reversed phase chromatography of weakly acidic and basic analytes is strongly influenced by eluent pH because the hydrophobicity of such analytes can vary

hugely depending on their ionisation state. Whilst there have been reports of pH gradients in reversed phase chromatography since the early 1990s [4, 13], they are rarely used because reversed phase chromatographers are accustomed to controlling retention by gradients in the fraction of organic modifier. Consequentially, the concept of pH gradient reversed phase chromatography was not formally developed until an article by Kaliszan *et al*. in 2003 [14] who later proposed that the method be used for determination of pK_a values [15]. Recently, Kaliszan *et al*. have developed a theoretical framework for optimising pH gradient reversed phase chromatography [16]. The application of photochemical eluent control to pH gradient reversed phase chromatography is demonstrated in the results and discussion section of this chapter.

5.1.3 Photolabile protecting groups

More specialised photochemicals could be used for specific elution affinity chromatography. In this type of affinity chromatography, the target compounds are eluted by displacing them from the stationary phase by a high concentration of a molecule that has a competitive affinity for the stationary phase. One example of this is avidin-biotin affinity chromatography, which uses a stationary phase with an immobilised protein "avidin" to bind target biomolecules which have been pre-conjugated to a small molecule called biotin [17]. After washing, the target biomolecules are released by displacing them from the column with a buffer containing free biotin.

A photochemical eluent control method could be used for avidin-biotin affinity chromatography by preparing a biotin molecule with a photochemical protecting group. Given that biotin has a carboxylic acid group, a simple approach would be to conjugate biotin to one of the protecting groups described in Chapter 4. This

might, in principle, allow the use of a single eluent for binding and elution of the target biomolecules in avidin-biotin affinity chromatogrpahy. The protected biotin would be present (but inert) in the binding buffer during the binding and washing steps. For the desportion step, the biotin molecules would be released from their protecting groups by irradiation in a photochemical reactor upstream of the column so that they could effect elution. The avidin-biotin affinity scenario is only one form of specific elution affinity chromatography that might be achievable using photochemical eluent control. Compounds such as nucleosides and peptides with photochemical protecting groups attached are already available [18, 19] and these might also have relevance as eluting compounds for specific affinity chromatography.

5.1.4 Speculative possibilities

Having discussed the most promising potential photochemical eluent control schemes above, the remaining possibilities are of a more speculative nature. One of the most appealing ideas is that of a photochemical system that could reproduce the effects of a gradient in organic modifier fraction versus water fraction. Such a system would allow photochemical eluent control to be applied to reversed phase chromatography and hydrophilic interaction chromatography. The problem with this idea is that these types of gradient chromatography involve very dramatic changes in concentration. For example, it is difficult to imagine how a gradient of 20% organic solvent in water increasing up to 80% could be achieved through photochemical reactions. The photoinitiated reactive components of the system would need to have extremely high concentrations that would most likely be measured in terms of mole or weight fraction rather than molarity. In other words, the solvent itself would need to be affected by a photochemical reaction.

Therefore, whilst the author can imagine a system in which a solvated chemical such as desyl hydroxide releases H_2O upon photolysis, such a system is unlikely to give sufficiently large changes in fraction of water versus organic solvent. If anyone were to approach this problem, the author would suggest that they begin by asking "what microscale photochemical flow system could provide the largest possible concentration changes?". It might be possible to identify solvent molecules that can change structure by a photochemically controlled process.

There is a class of photochemical called photolabile calcium chelators [18, 19]. Photolabile calcium chelators have high binding affinity for calcium which is reduced by orders of magnitude after photo-rearrangement or photolysis. Such compounds could conceivable be used for ion chromatography by controlling the activity of calcium as a competitive eluting ion, or by binding divalent metal ions if they are the subject of analysis.

Another possibility is the use of photoinitiated polymerisation reactions. Photoinitiated polymerisation in a flowing reactor cell could potentially be used to create gradients in degree of polymerisation. This property is not normally associated with chromatography eluents. However, the author imagines a system in which charged polymers are created out of charged monomers by a photoiniated polymerisation. Due to their multiple charges, the polymers would have a very powerful eluting effect for ion chromatography and could therefore be used to elute very strongly retained analytes.

5.1.5 Summary

Table 5.1 summarises the various photochemical reaction systems that have been suggested along with the types of chromatography that they might be used for.

Photochemical process	*Chromatographic application*
Acid release (e.g. HCl) e.g. DeCl CDMEP **Base release**	Ion exchange chromatography pH-dependant reversed phase chromatography pH dependant affinity chromatography[#] pH dependant ion exchange[#]
Photosensitive chelator e.g. DM-Nitrophen™ (Merck)	Ion exchange chromatography Ion pair chromatography
Ligand release (e.g. 2-nitrobenzyl-R where R is a caged ligand)	Specific elution affinity chromatography where R binds to the stationary phase and displaces the target compounds.
H_2O release e.g. desyl hydroxide **Solvent modification**	Reversed phase chromatography Normal phase chromatography Hydrophilic interaction chromatography
Polymerisation by photoinitiators *Charged polymers*	Ion Chromatography (elution strength should dramatically increase with increased degree of polymerisation)

Table 5.1 – Photochemical Eluent Chromatography

[#] Broad control over pH gradients could be achieved simply by using acid-releasing photochemical reagents in buffered eluents. As the intensity of light can be increased or decreased during a separation it would be possible to generate both increasing and decreasing pH gradients.

Looking at the first row of Table 5.1, it is clear that a photochemical eluent pH control system would have many potential applications because of its applicability to three different modes of chromatography. However, these modes of chromatography are most associated with only two common forms of detection: UV absorbance and mass spectrometry. As discussed in Chapter 4, it may be difficult to use UV absorbance detection with photochemical eluent control methods. Therefore, the remainder of this chapter deals with the development of photochemical eluent pH control system for LC-MS.

5.2 Experimental

5.2.1 Materials and Equipment

Ammonium carbonate (mass spectrometry grade) was purchased from Fluka (Buchs, Germany), whilst ammonium bicarbonate >98%, imidazole 99%, HCl 37% and NaOH 98% were purchased from Sigma-Alrich, (St Louis, MI, USA). Piperazine dihydrochloride was purchased from Aldrich (St Louis, MO, USA). Unichrom HPLC grade acetonitilre was aquired from Ajax Fine Chemicals (Seven Hills, Australia).

Chlorpromazine hydrochloride (CHL), clozapine (CLO), haloperidol (HAL), thioridazine hydrochloride (THI), flupenthixol dihydrochloride (FPE), and fluphenazine dihydrochloride (FPH) were obtained from Sigma–Aldrich whilst amisulpride (AMI), aripiprazole (ARI) and risperidone (RIS) were obtained from Sequoia (Oxford, UK). Zuclopenthixol dihydrochloride (ZUC) was donated by Lundbeck (Copenhagen, Denmark). The photochemical reagent 2-chloro-1-(2,5-dimethylphenyl)ethanone 95% was purchased from ChemBridge (San Diego, CA, USA).

5.2.2 Assessment of pH system

Approximately 800 µL of eluent was collected from the photochemical eluent pH control system at various LED current settings and was measured with a glass electrode pH meter. Whilst calibration of the pH meter was conducted using fully aqueous buffers in the appropriate range for each measurement, it is important to note that the irradiated eluent was in fact a 50% acetonitrile-water solution. Therefore, the results of the pH measurements are denoted as pH^* to represent that they were determined in non-aqueous conditions.

5.2.3 Chromatography

The column was a Zorbax SB-C18 with 5 µm particles, measuring 150 x 0.5 mm (Agilent, Santa Clara, CA, USA). The pump was the same Agilent 1200 Series capillary pump that was used in the previous chapters, Separations were at ambient temperature at 4.4 µL with 20 seconds sample injections.

5.2.4 Mass spectrometry

The mass spectrometer was an Agilent 6320 Series Ion Trap with an electrospray ionisation source. The photochemical eluent pH control system apparatus was plumbed into the mass spectrometer by 100 cm of 25 µm ID fused silica capillary which connected the 6-port injector outlet to the electrospray source. A smoothing algorithm of one Gaussian cycle across 1.88 seconds was used for all extracted ion chromatograms unless otherwise stated. The optimised settings were as follows:

MODE: Standard – Enhanced (range 50 – 2200 Hz, speed 8,100 m/z /sec); Diverter Valve: to source; Include Profile Spectra: ON; POLARITY: positive.

TRAP OPTIONS: ICC: active; smart target: 3000; Max accu time: 50 ms; Scan: 300 to 450 m/z, Averages: 5.

TUNE OPTIONS: Nebulizer: 15 psi; Dry Gas 5 L/min; Source: Capillary -4500 V, end plate offset -500V.

EXPERT SETTINGS: Skimmer 15 V; Cap Exit: 158.3 V; Oct 1: DC 8.92 V; Oct 2: DC 1.96 V; Trap Drive: 43.3; Oct RF: 166.7 Vpp; Lens 1: -5.8 V; Lens 2: -100 V.

5.3 Results and Discussion

5.3.1 Design of photochemical eluent pH control systems

As described above, the acid-releasing flow photolysis system developed in Chapter 3 can be modified into a photochemical pH control system by the addition of buffer compounds. Whilst pH could theoretically be controlled without buffers, this is unlikely to be practical for applications that involve working anywhere near neutral, where the concentrations of H_3O^+ or OH^- are extremely low. For example, the difference between pH 4 and 10 in an unbuffered system is merely 0.2 mmol/L of strong acid or base.

The author developed a system with a slightly higher flow rate in order to work with commercially available capillary columns. CDMEP was used as the photochemical due to its greater acid generating performance and reduced tendency for reaction cell fouling compared to DeCl. The neutral character of CDMEP was expected to reduce ionization suppression or adduct formation in the ESI source. A 310 nm LED was used because it was previously shown to be the best LED for photolysis of CDMEP.

The acid concentration range of the flow photolysis system determines what concentration of buffer compounds should be added to the eluent in order to ensure that the full pH range is accessible. If the buffer concentration is too high, then the maximum acid generated will not be sufficient to reach low pH values. On the other hand, if the concentration of buffers is too low, the buffer capacity of the eluent will be lower and part of the range of the flow photolysis system would be "wasted". This was considered undesirable because it might make the system more sensitive to minor changes in light intensity and therefore less reproducible.

The results and experience obtained from the work described in Chapter 4 facilitated the estimation of appropriate reagent concentration, whilst appropriate buffer compounds were selected on the basis of their literature pKa values. Ammonium provides buffering capacity in the region of 9.24 [20], bicarbonate in the region of 6.32 [21], and acetic acid in the region of 4.76 [22]. Whilst these values are for fully aqueous solutions, it seems likely that these three species will still give a reasonable spread of pKa values in the 50% w/w acetonitrile-water mixture. On the basis of these considerations, the author used an eluent of 10.0 mmol/L CDMEP in 50% w/w acetonitrile-water mixture with 0.87 mmol/L each of ammonium acetate and ammonium bicarbonate, running at 4.4 μL/min.

5.3.2 Proof of principle of photochemical eluent pH control system with reversed phase LC-ESI-MS

The photochemical eluent pH control system was tested by connecting it to a C18 reversed phase chromatography capillary column. The outlet of this column was connected to an Agilent 6320 Ion Trap mass spectrometer with an electrospray ionisation source. The entire apparatus is symbolised in Figure 5.1.

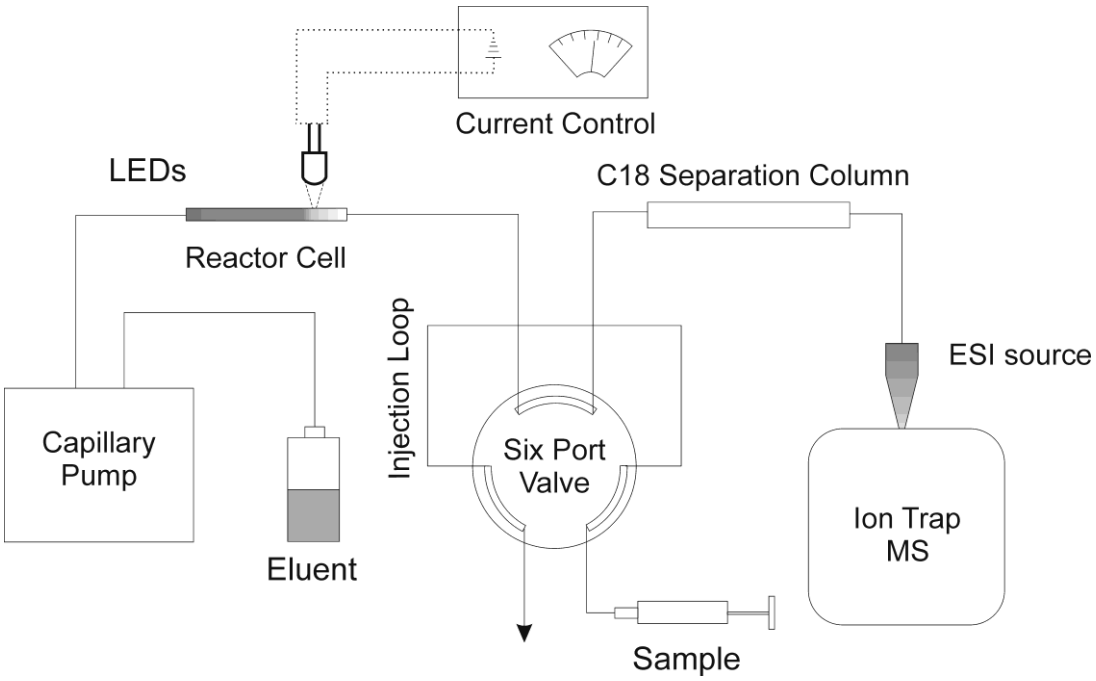

Figure 5.1 – Photochemical eluent pH control apparatus for pH dependant reversed phase LC-ESI-MS. The system is similar to the apparatus used in Chapter 3 except that it uses only one single LED, it uses of a reversed phase column (with no suppressor), and detection is achieved by ESI-MS rather than conductivity.

Seven compounds were used in this proof of principle demonstration. These compounds are antipsychotic drugs and their separation is of interest because they are important candidates for therapeutic drug monitoring [23]. They have highly varied structures, although they all have aromatic and aliphatic moieties and each has a tertiary amine group that can act as a base. Since the ionisation state of the compounds is an important factor in determining their hydrophobicity, one expects their retention on the C18 silica column to be heavily dependant on pH.

It was expected that the pH of the eluent would be determined by the current supplied to the LED, with higher currents predicted to give lower pH due to the increased concentration of HCl generated in the eluent. Therefore, the current was increased throughout the runs in order to give a decreasing pH.

Figure 5.2 shows three different gradient separations. Gradient A was an intermediate slope gradient which started at 6 mA and levelled off at 20 mA after 16 minutes, Gradient B was steeper and more complicated gradient that started at 8 mA and levelled off at 20 mA after 8 minutes, whilst Gradient C was a more shallow gradient which started at 6 mA and levelled off at 16 mA after 20 minutes. The gradient programs are detailed in the figure caption. The results show that the selectivity of the antipsychotic drugs on the column was indeed affected by the different gradient programs. Gradient C performed the best, separating all but two of the drugs.

Unfortunately, as the system was not calibrated it is difficult to accurately predict the pH values that would be generated by these gradient programs. The author had intended to calibrate the system, but the reaction cell was broken during the course of these experiments. Furthermore, the ion trap reported unstable masses, with masses shifting in the range of at least 0.5 m/z throughout these runs. This

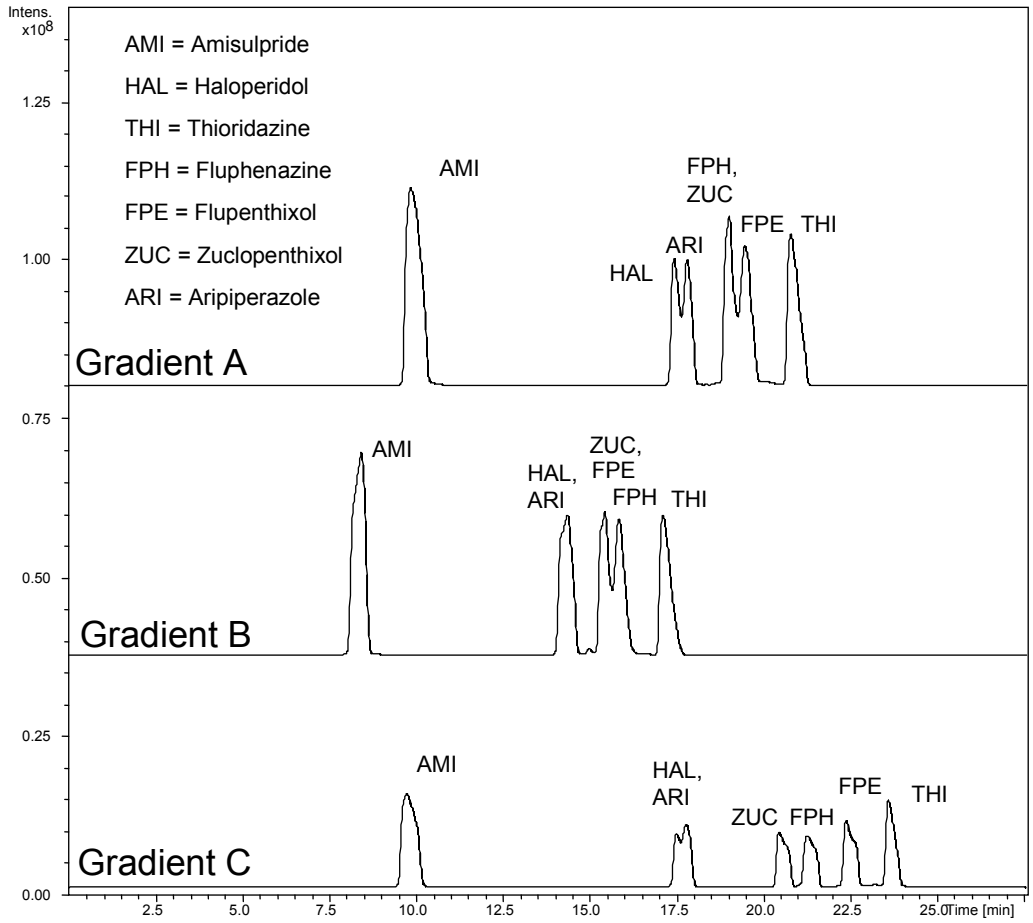

Figure 5.2 – Three extracted ion chromatograms for reversed phase separations of 7 antipsychotic drugs. The extracted ions are m/z = 370.17, 371.15, 376.14, 401.13, 435.16, 438.17, 448.14, all with range of ±0.5 m/z. Gradient A: Started at 6 mA, increased to 8 mA at 4 minutes and then proceed to increased current by 2 mA every 2 minutes after that until t = 16 minutes at which time the current was held at 20 mA for the rest of the run. Gradient B: Started at 8 mA, increased to 10 mA at t = 2 minutes, then up to 12 mA at t = 3 minutes, then increased by 1 mA every minute after that until t = 6 minutes at which time the current was increased to 16 mA and then increased by 2 mA every minute after that until t = 8 minutes at which time the current was held at 20 mA for the rest of the run. Gradient C: Started at 6 mA, increased by 0.5 mA every minute after that until t = 20 minutes at which time the current was held at 16 mA for the rest of the run.

may indicate an ion trap overloading effect. Calibration and optimisation of the system was required before more conclusions could be drawn.

5.3.3 Calibration and testing of photochemical eluent pH control system

A new reactor cell was prepared and the system was calibrated by collecting the eluent from the system at various current settings and measuring the effluent as described in the experimental section. The results are shown in figure 5.3. It was discovered that the eluent system gave a pH* range of 8.2 down to 2.7 with a reasonably smooth progression from high to low pH* as the LED current was increased.

The system was reattached to the ion trap MS, as before. However, the trap settings were changed by reducing the trap smart target to 3000 (this setting had been at 30000 in the previous experiments). This significantly reduced effects of the trap overloading, giving better peak shape and more stable m/z values.

Two isocratic reversed phase separations were run using the calibrated system, taking care to keep the apparatus in the same configuration and (including LED alignment) as it had been in for the pH^* measurements. A new set of six antipsychotic drugs were chosen for these experiments. Figure 5.4 shows an isocratic separation in which the pH^* is expected to be 5.5 (10 mA, top). It can be seen that the drugs elute in an early group (consisting of AMI, RIS, CLO and HAL) and a late group (CHL and THI) after 30 minutes. The separation can be shortened to just 10 minutes by increasing the current to 22 mA to give a pH^* of 2.7 (Figure 5.4. bottom). However, the selectivity between AMI, RIS and CLO is lost, possibly because they enter a doubly charged state at this low pH that

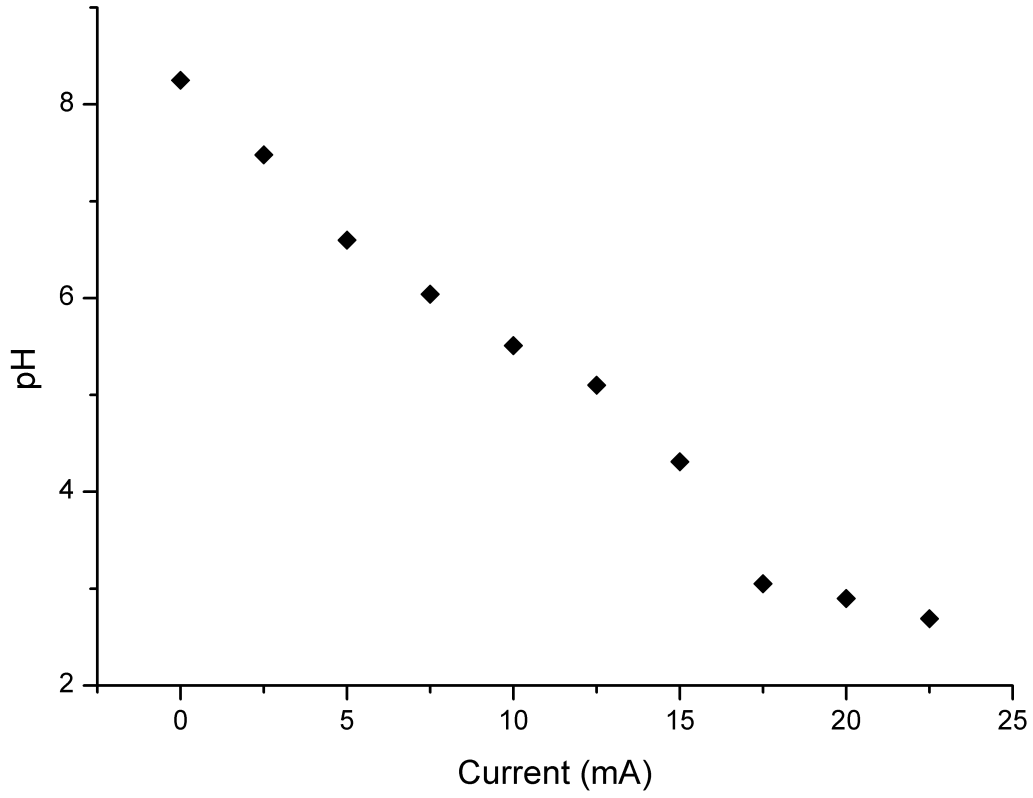

Figure 5.3 – Calibration of photochemical eluent pH control system for reversed phase chromatography. This system runs at 4.4 µL/min and uses 10.0 mmol/L CDMEP in 50% w/w MeCN-Water with 0.87 mmol/L each of ammonium acetate and ammonium bicarbonate.

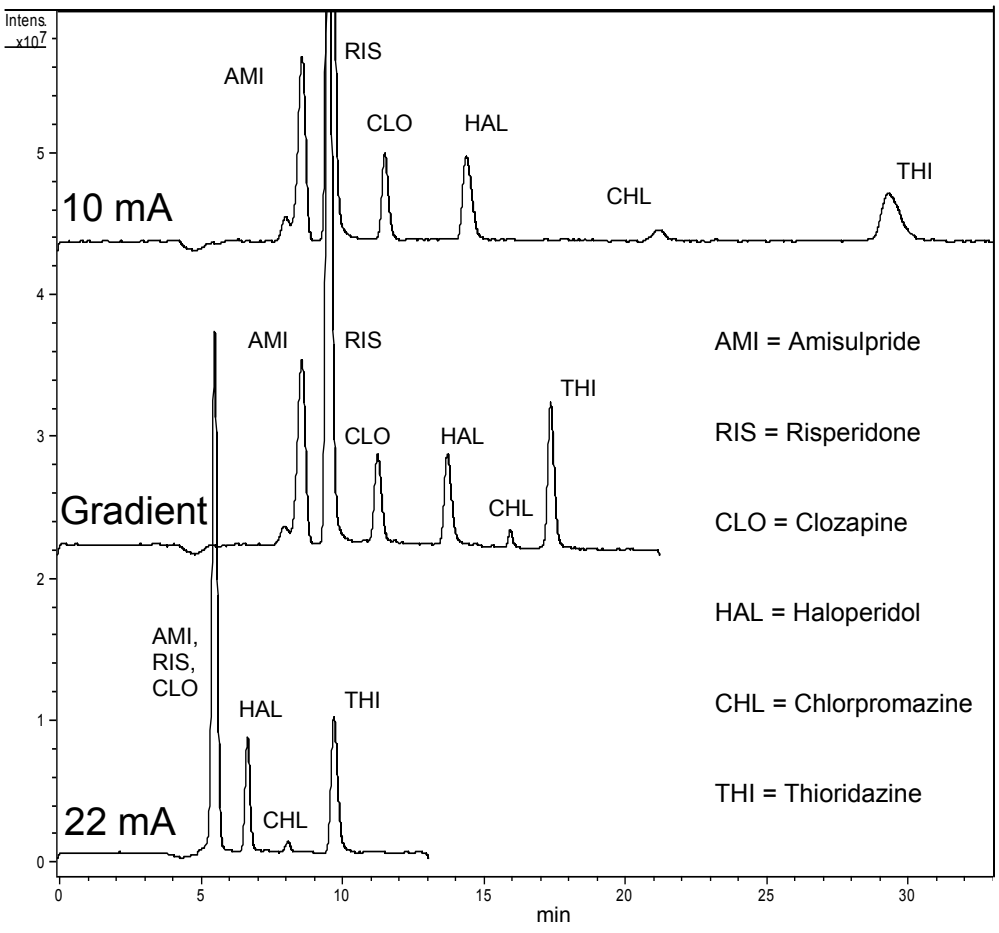

Figure 5.4 –Reversed phase LC-MS of antipsychotic drugs using the photochemical eluent pH control system. All chromatograms are combined extracted ion chromatograms including the monoisotopic masses for each drug (MH+) with a ± 0.2 m/z window with 3 cycles of Gaussian smoothing across 1.88 seconds. The system was operated at 4.4 uL per minute with one 310 nm LED. All samples were 20 second injections of 3 ppm clozapine 3 ppm, 7 ppm risperidone, and 10 ppm each of haloperidol, thioridazine hydrochloride, chlorpromazine and amisulpride dissolved in the eluent (without CDMEP). The pH gradient program was as follows: Begin with current at 10 mA at t = 0 minutes, then increased current to 12 mA at t = 12 and continued to increase by an increment of 2 mA every 2 minutes after than until t = 22 minutes.

reduces their hydrophobicity to very low levels. The potential for RIS and CLO to enter a doubly charged state is supported by Johns *et al*. [23] whilst AMI has an aniline group that might also be protonatable. Meanwhile, the selectivity of HAL, THI and CHL, which are not considered to be doubly chargeable by Johns *et al*. [23], is maintained, though their retention times are shortened.

The gradient capability of the photochemical eluent pH control system was again demonstrated by performing a gradient elution (Figure 5.4, middle) with ascending current (descending pH^*) as described in the figure caption. The program is described in the figure caption. It was expected to give a steady pH* of 5.5 for the first 6 minutes, followed by a steady decrease in pH* to 2.7 over a 5 minute period. This gradient allowed the selectivity of AMI, RIS and CLO to be maintained whilst the peak shape of THI was improved and the elution time was reduced to 17 minutes. The sensitivity achieved by the system was assessed by estimating the limit of detection for THI in this separation. Based on the size of the signal at 10 ppm, the limit of detection for THI at three times signal-to-noise would be 0.4 ppm.

Finally, the run-to-run reproducibility of the photochemical eluent pH control system was investigated. Figure 5.5 shows three isocratic runs with the current at 20 mA, giving a pH* of 2.9. The reproducibility appeared to be reasonable for this proof-of-principle experiment, with a retention time RSD of 0.7% for thioridazine and 2.1% for amisulpride. The sources of variance are likely to include human error (with the manually controlled injection). Another source of potential error is in the reproducibility of the capillary pump behaviour in response to the injection process, which caused a temporary change in the back pressure of the system. The Agilent 1200 series capillary pump was operating

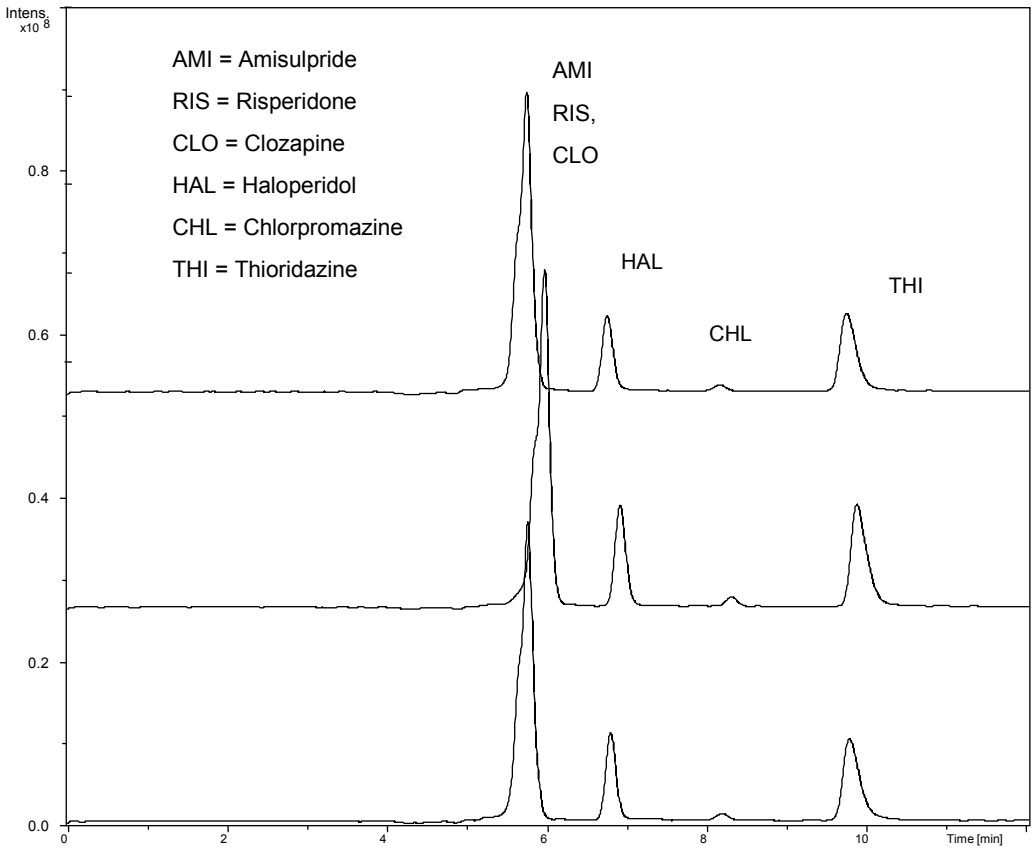

Figure 5.5 – Reversed phase LC-MS of antipsychotic drugs using the photochemical eluent pH control system. All three separations are run with the photochemical pH control system set to 20 mA to show run-to-run reproducibility. All chromatograms are combined extracted ion chromatograms including the monoisotopic masses for each drug (MH+) with a ± 0.2 m/z window.

outside its normal conditions in the sense that it was pumping at a relatively low speed and nevertheless had to pressurise a relatively large dead volume of liquid upstream of the column (in the reactor cell). The cell may even have had some potential compressibility near its outlet and inlet which were sealed by epoxy adhesive. Given that only a small fraction of the length of the reaction cell was needed for exposure to the LED light, this problem might be ameliorated by employing a more appropriate reaction cell with less unnecessary volume.

5.3.4 Design of alternative buffer system

The results presented above show a photochemical eluent pH control system which is compatible with pH dependant reversed phase chromatography. As mentioned in the introduction to this chapter, another potential application of this system would be pH dependent ion exchange chromatography. However, the requirements of this type of chromatography are somewhat different due to presence of functional groups on the stationary phase that can interact with the charged buffer compounds. If the charged buffer compounds are retained by the stationary phase, they will act to counter any attempt to change the pH within the column throughout the run [24]. This problem would be particularly significant in situations where a strong, high capacity ion exchange material is used with a relatively low concentration eluent mixture. One way of dealing with this problem is to use buffer compounds which are not retained by the column. Andersen *et al*. adopted this approach by using amine buffers for their pH gradient capillary anion exchange chromatography system [25]. They chose piperazine (pKa 4.94 and 9.09) and imidazole (pKa 6.95) as buffers, both of which exist in either neutral or positively charged states depending on the pH and therefore should not be retained on the anion exchange column.

A new eluent was tested for the photochemical eluent pH control system, consisting of 1.0 mmol/L each of imidazole and piperazine dihydrochloride in 50% w/w acetonitrile-water with 2.0 mmol/L NaOH and 10.0 mmol/L CDMEP. Due to the slightly higher concentration of buffers used in this system, it was anticipated that a higher concentration of HCl would need to be generated so that the system was capable of protonating all of the buffer compounds and accessing the lowest pH values. Therefore, a slightly lower flow rate (3.0 μL/min) was used so that a greater portion of the CDMEP could be converted into HCl. This new buffer system was calibrated by collecting the eluent after setting the current to different levels. The results are presented in Figure 5.6. The new eluent mixture performs similarly to the original one, although it is able to access higher pH values. The maximum pH achieved was 9, whilst the minimum was 2.7. Compared to the original eluent system, this amine buffer approach gave a similarly smooth response in pH versus LED current.

5.4 Conclusions

The most important conclusion from this chapter is that it is possible to modify the acid generating flow photolysis system presented in chapter 3 to make a pH controlled system by adding buffer compounds. The fact that the photolysis process would be compatible with the presence of a variety of buffer compounds and a wide pH range was not taken for granted and is therefore an auspicious finding. Whilst it may be that many photochemical reagents would demonstrate this sort of compatibility, this finding is another reason why CDMEP is a promising photochemical reagent.

With a maximum pH range of 2.7 up to either 8.2 or 9, the photochemical eluent pH control systems presented in this chapter both compare favourably with the

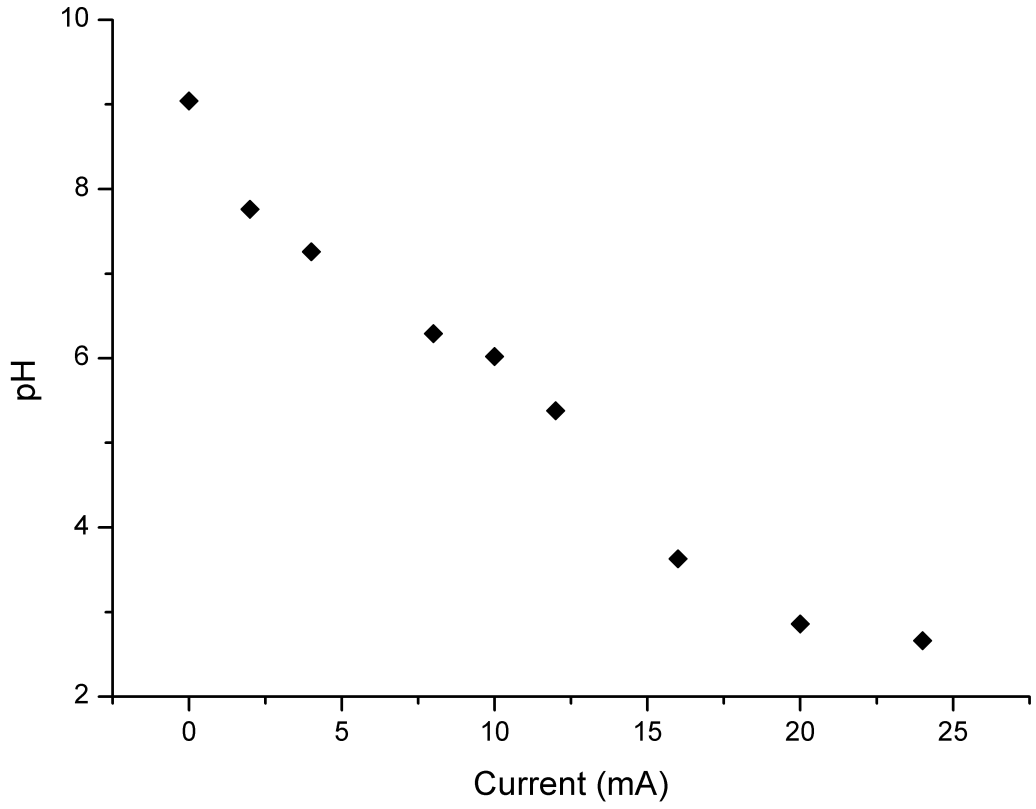

Figure 5.6 – Calibration of a photochemical eluent pH control system that would be suitable for pH gradient anion exchange chromatography with 10.0 mmol/L CDMEP in 50% w/w MeCN-Water with 1.0 mmol/L each of imidazole and piperazine dihydrochloride and 2.0 mmol/L NaOH, using a 310 nM LED at 3.0 μL/min.

system developed by Salamoun and Slais [4], which achieved a pH range of 3.3 up to 6.

A further finding in this chapter is that photochemical eluent control methods can be used for controlling the pH for reversed phase chromatography, in both isocratic and gradient pH modes. Meanwhile, the development of a system with positive/neutral buffer compounds adds weight to the suggestion that photochemical eluent control could be used for pH dependant ion exchange chromatography.

One additional conclusion from this chapter is that photochemical eluent control is compatible with electrospray ionisation-mass spectrometry. There had been some concern that the inclusion of 10.0 mmol/L CDMEP would interfere with the electrospray ionisation process and make it impossible to detect the analytes. Whilst clear signals were observed for all analytes that were tested, the detection and chromatography conditions would need to be optimised before a conclusion could be reached about the effects of the CDMEP on sensitivity. Further potential applications of photochemical eluent pH control for LC-MS are described in the conclusions and future work section.

5.5 References

1. Haddad, P. R., Jackson, P. E., Shaw, M. J., *J. Chromatogr. A* 2003, *1000*, 725-742.

2. Shirai, M., Tsunooka, M., *Prog. Polym. Sci.* 1996, *21*, 1-45.

3. Suyama, K., Shirai, M., *Prog. Polym. Sci.* 2009, *34*, 194-209.

4. Salamoun, J., Slais, K., *J. Chromatogr.* 1990, *522*, 205-11.

5. Moore, S., Stein, W. H., *J*. *Biol*. *Chem*. 1954, *211*, 893-906.

6. Piez, K. A., *Anal*. *Chem*. 1956, *28*, 1451-1454.

7. Shan, L., Anderson, D. J., *Anal*. *Chem*. 2002, *74*, 5641-5649.

8. Ivanov, A. V., Nesterenko, P. N., *Anal*. *Chem*. 1999, *54*, 494-510.

9. Ahamed, T., Nfor, B. K., Verhaert, P. D. E. M., van Dedem, G. W. K., van der Wielen, L. A. M., Eppink, M. H. M., van de Sandt, E. J. A. X., Ottens, M., *J*. *Chromatogr*. *A* 2007, *1164*, 181-188.

10. Farnan, D., Moreno, G. T., *Anal*. *Chem*. 2009, *81*, 8846-8857.

11. Mallik, R., Hage, D. S., *J*. *Sep*. *Sci*. 2006, *29*, 1686-1704.

12. Manz, A., Graber, M., Widmer, H. M., *Sens*. *Acuators, B* 1990, *B1*, 244-248.

13. Little, E. L., Jeansonne, M. S., Foley, J. P., *Anal*. *Chem*. 1991, *63*, 33-44.

14. Kaliszan, R., Wiczling, P., Markuszewski, M. J., *Anal*. *Chem*. 2003, *76*, 749-760.

15. Wiczling, P., Markuszewski, M. J., Kaliszan, R., *Anal*. *Chem*. 2004, *76*, 3069-3077.

16. Wiczling, P., Kaliszan, R., *Anal*. *Chem*. 2010, *82*, 3692-3698.

17. Laitinen, O. H., Nordlund, H. R., Hytönen, V. P., Uotila, S. T. H., Marttila, A. T., Savolainen, J., Airenne, K. J., Livnah, O., Bayer, E. A., Wilchek, M., Kulomaa, M. S., *J*. *Biol*. *Chem*. 2003 *278* 4010-4014

18. Adams, S. R., Tsien, R. Y., *Annu*. *Rev*. *Physiol*. 1993, *55*, 755-784.

19. Pelliccioli, A. P., Wirz, J., *Photochem*. *Photobio*. *Sci*. 2002, *1*, 441-458.

20. Bjerrum, J., *Stability Constants*. 1958, Chemical Society, London.

21. Hildebrand, J. H., *Principles of Chemistry*. 1940, New York: The Macmillan Company.

22. Dippy, J. F. J., Hughes, S. R. C., Rozanski, A. J., *Chem*. *Soc*. 1959, 2492.

23. Johns, K. F., Breadmore, M. C., Bruno, R., Haddad, P. R., *Electrophoresis* 2009, *30*, 839-847.

24. Dai, J., Wang, L.-S., Wu, Y.-B., Sheng, Q.-H., Wu, J.-R., Shieh, C.-H., Zeng, R., *J*. *Proteome Res*. 2009, *8*, 133-141.

25. Andersen, T., Pepaj, M., Trones, R., Lundanes, E., Greibrokk, T., *J*. *Chromatogr*. *A* 2004, *1025*, 217-226.

General Conclusions and Future Work

Polymer Monoliths for Miniaturised Affinity Chromatography

It is possible to produce porous polymer monoliths for BAC using a multistep synthesis starting with poly(BuMA-co-EDMA) monoliths, photografting with poly(GMA) and then reacting with HPBA. These monoliths have a respectable binding capacity and are suitable for miniaturised chromatography because they could be formed within fused silica capillaries. There is reason to believe that they could be formed within capillaries or channels with much smaller dimensions if this were required [1, 2]. The monoliths are able to withstand high pressures and have selectivity for nucleosides and glycopeptides, even showing some potential for extracting nucleosides from a complex sample matrix. Such favourable qualities mean that these monoliths show some potential for miniaturised BAC, whether it be for low flow rate applications hyphenated to MS detection or as part of a miniaturised analytical device.

Unfortunately, the monoliths developed in this project also exhibit non-specific interactions which may limit their potential application to real analytical problems. Furthermore, they exhibit an ionic strength dependant swelling effect which could cause a large change in pressure drop across the monolith during operation if mobile phases are not chosen with care. Whilst it might be possible to ameliorate these problems by testing the ideas outlined in the conclusion of Chapter 2, this is not necessarily the best way to proceed with the goal of developing polymer monolith stationary phases for miniaturised BAC.

At the commencement of the project, there had been no published demonstration of BAC using a porous polymer monolith stationary phase. Over the past two years there have been a few reports of different boronate affinity monoliths by other researchers who have used quite different synthesis methods. Therefore, the next step in designing an effective polymer monolith for miniaturised BAC would be to investigate these different approaches. This process must begin by looking at the strengths and weaknesses of the various types of boronate affinity monolith demonstrated to date. This process is somewhat confounded by the fact that the different monoliths have been characterised and demonstrated in a highly inconsistent manner.

As noted in Chapter 2, Ren *et al*. [3] prepared a monolith which was, broadly speaking, similar in terms of capacity and selectivity to the HPBA monolith described in this thesis. However, they subsequently improved on this design by using a more hydrophilic crosslinking reagent to produce a monolith with significantly less reversed phase type interaction [4], achieving a similar capacity. This poly(VPBA-co-N,N'methylenebisacrylamide) monolith requires only a relatively simple synthesis and showed very good selective retention of glycoproteins versus non-glycosilated proteins. On the basis of these strengths and despite the limited information available, this second approach by Ren *et al*. appears to be the most worthy of further investigation out of all of the synthesis methods presented thus far.

The epoxy based boronate affinity monolith that was also produced by Ren *et al*. [5] remains poorly characterised at this stage. Nevertheless, the fact that it showed moderate capacity for catechol at the relatively low pH of 7 is interesting because extending the functional pH range of boronate affinity chromatography

may enhance its utility for glycan and glycoprotein preconcentration. More investigation of this material, including a broader demonstration of its selectivity and tests for non-specific interactions, will be needed before any judgements can be made. The same can be said of the monolith produced by Gillespie *et al*. which is yet to be demonstrated for boronate affinity chromatography [6].

The poly(3-acrylamidophenylboronic acid-co-EDMA) monolith produced by Chen *et al*. [7] had a relatively low specific binding capacity and was demonstrated only in offline sample preparation mode in the form of a relatively wide diameter column. However, there is every reason to believe that this monolith could be downscaled and used for online extraction. It showed some potential for selective extraction of glycopeptides versus non-glycosilated peptides which is an application of great interest in the field of glycoproteomics. However, it is once again the case that more characterisation is needed with a wider range of samples before any conclusions can be drawn.

The author proposes that the best way forward would be to synthesise monoliths based on all these different recipes in the same format such as a 100 μm ID fused silica capillary. The monoliths could then be compared by measures of binding capacity (of one chosen diol compound) and pressure drop curves, as well as run-to-run and column-to-column reproducibility. Furthermore, the monoliths should be applied to high value separation problems such as selective enrichment of glycoproteins, glycopeptides and nucleosides with thorough analysis of the flow through and eluted fractions. In order to gain the best understanding of the selectivity and retention behaviour of the monoliths it would be preferable to test all of the monolithic columns online to a detection system rather than to collect fractions. After this comparison has been completed it should be possible to

identify which type of monolith holds the most promise for miniaturised BAC applications. Further developments can then focus on improving that monolith and applying it to some high value separation problems.

Photochemical Eluent Control

It is possible to create effective composition changes in microscale chromatography eluents using photochemicals and cheap, compact light sources. Light intensity can be set at a constant value to allow isocratic elution or it may be changed over time to create composition gradients. HCl can be generated from a variety of photochemical reagents and CDMEP was the most effective reagent out of the six that were tested. The generated acid can be used as a competing ion for ion chromatography or alternatively it can be used to control the pH in a buffered system for pH dependant reversed phase chromatography. The system can be used with suppressed conductivity detection or ESI-MS.

The next step in developing the concept would be to test whether the photochemical eluent pH control system can be used for pH gradient ion exchange chromatography and affinity chromatography. This might not require any further developments other than a change in the sample and the separation column and it could be performed online to ESI-MS. Given the growing interest in pH gradient ion exchange nano-LC [8], such a demonstration would point towards some high value applications. A similar approach could be used to investigate whether this invention can be used for affinity chromatography with elution by pH change. Finally, it would be interesting to attempt to build a photochemical eluent control system for the other types of chromatography suggested in Chapter 5.

A further step in demonstrating this technology would be to test how well it can be downscaled to ultra-low flow rates. Fortunately, there is every reason to believe that downscaling the photochemical eluent control system would be relatively simple, given that the only unusual component in the system is the light source. As the volume and flow rate of the liquid phase is reduced, the amount of light required to drive reactions in that liquid should also decrease, permitting the use of still cheaper and more compact light sources. One approach would be to fabricate a microfluidic chip from a material with appropriate deep UV transmittance such as Cyclic Olefin Copolymer. Long term goals could include systems with integrated excitation LEDs [9, 10], perhaps incorporating additional LEDs and photodiodes for fluorescence detection in order to achieve high detection sensitivity. It would also be important to switch to a simpler type of pump in order to demonstrate that the photochemical approach has capacity to be truly miniaturised and incorporated into a into a portable device.

The major stumbling block for photochemical eluent control is likely to be the multifaceted challenge of creating a system that produces the desired eluent composition change without unfavourably interfering with the sample, chromatography and detection processes. The incompatibility of the photochemical eluent control methods with UV absorbance detection was one of the most significant problems that were encountered in this project. This incompatibility was disappointing because UV absorbance is one of the most versatile detection methods with the additional benefits of low cost and compatibility with miniaturisation. As mentioned in Chapter 4, the simplest way around the UV absorbance detection problem would be to find reagents that absorb at lower wavelengths than the analytes, although this was not yet achieved.

Nevertheless, there may yet be some photochemical reagents that can operate at lower wavelengths, and there may soon be compact light sources that output at sufficiently short wavelengths to activate them.

It might also be possible to solve the UV absorbance problem by preventing the photochemical reagents from reaching the absorbance cell. One possible approach would be to capture the reagents on some kind of column upstream of the absorbance cell. For example, a C18 column could be used to capture the photochemical reagents and their organic photoproducts if they were sufficiently hydrophobic. Whilst this type of arrangement might be useful for a system which measures inorganic ions, it would obviously not work for the analysis of hydrophobic analytes because they would also be absorbed on the column before reaching the absorbance detector. An equivalent scenario would arise if charged photochemical reagents were used and captured on an ion exchange column before reaching the detector. Finally, it might be possible to find photochemicals that could be converted to non-absorbent products by the application of intense light in a secondary reaction chamber between the column and the absorbance detector. However, it might be very hard to find chemicals that could be destroyed by conditions that would leave the analytes in an intact and absorbent state. Furthermore, if any of the solutions listed were found to work, the extra layer of complexity that they would add to the photochemical eluent control system would detract from its proposed advantages of simplicity versus the mechanical and electrolytic alternatives described in Chapter 3.

Another disappointing feature of the photochemical eluent control method demonstrated in this thesis was that it required the use of eluents with relatively high amounts of organic solvent in order to solubilise the photochemical. It

would be worthwhile to conduct a search for (or design) photochemicals that have greater solubility in solutions with higher water content.

If solutions to the limitations above cannot be found, this would not necessarily mean that photochemical eluent control will have no application. Rather, it would simply mean that the implementation of photochemical eluent control, except for a special cases such as suppressed conductivity detection and ESI-MS, must be more complicated that merely plugging in a photochemical reactor 'module' into an existing chromatography system. In the worst cases, the entire chromatography system may need to be re-designed to cope with the requirements and limits of the photochemical approach. Whether or not the enhanced 'miniaturisability' afforded by the photochemical approach is worth this cost will depend on the requirements of the particular application and the development of alternative miniaturised chromatography methods.

Whilst the photochemical eluent control technique described in this thesis has been presented solely as a method for microscale chromatography, the concept might also have relevance for may be potential applications in other areas of separation science. For example, it may be possible to use light induced composition changes in the electrolyte of electrophoresis and electrochromatography systems. This idea is interesting because it is normally very difficult to control the composition of the electrolyte while the voltage is switched on, because the two ends of the capillary or channel usually terminate in reservoirs with a fixed composition. Photochemically induced composition changes might be used to create abrupt changes in pH at certain points within the capillary or channel, which could be used for sensitivity-enhancing preconcentration [11].

The development of photochemical eluent control as described in this thesis, and in particular the finding that compact LEDs are sufficiently powerful for making significant concentration changes, may also have some significance beyond the field of separation science. The largely ubiquitous approach to making temporal composition changes in microfluidic conduits is to somehow introduce a new liquid to that area. This typically requires that the system includes reservoirs of alternative liquids with various compositions as well as a mechanism for pumping or otherwise transporting those liquids to where they are needed in appropriately mixed ratios. The use of compact light sources and photochemicals to create composition changes *in situ* affords high design simplicity that could be highly advantageous. As such, this simple photochemical approach to controlling composition might find application in other types of microfluidic system with applications such as rapid compound screening [12] and cell biology research devices [13].

References

1. Nischang, I., Brueggemann, O., Svec, F., *Anal*. *Bioanal*. *Chem*. 2010, *397*, 953-960.

2. Nischang, I., Svec, F., FreÌ• chet, J. M. J., *Anal*. *Chem*. 2009, *81*, 7390-7396.

3. Ren, L., Liu, Z., Dong, M., Ye, M., Zou, H., *J*. *Chromatogr*. *A* 2009, *1216*, 4768-4774.

4. Ren, L., Liu, Y., Dong, M., Liu, Z., *J*. *Chromatogr*. *A* 2009, *1216*, 8421-8425.

5. Ren, L., Liu, Z., Liu, Y., Dou, P., Chen, H.-Y., *Angew*. *Chem*., *Int*. *Ed*. 2009, *48*, 6704-6707.

6. Gillespie, E., Connolly, D., Nesterenko, P. N., Paull, B., *Analyst* 2008, *133*, 874-876.

7. Chen, M., Lu, Y., Ma, Q., Guo, L., Feng, Y.-Q., *Analyst* 2009, *134*, 2158-2164.

8. Farnan, D., Moreno, G. T., *Anal*. *Chem*. 2009, *81*, 8846-8857.

9. Pais, A., Banerjee, A., Klotzkin, D., Papautsky, I., *Lab Chip* 2008, *8*, 794-800.

10. Ren, K., Liang, Q., Mu, X., Luo, G., Wang, Y., *Lab Chip* 2009, *9*, 733-736.

11. Breadmore, M. C., Thabano, J. R. E., Dawod, M., Kazarian, A. A., Quirino, J. P., Guijt, R. M., *Electrophoresis* 2009, *30*, 230-248.

12. Ohno, K.-I., Tachikawa, K., Manz, A., *Electrophoresis* 2008, *29*, 4443-4453.

13. Zhang, X. Y., Roper, M. G., *Anal*. *Chem*. 2009, *81*, 1162-1168.

Appendix

2NBC	**0.508 mM**					**2NBC**	**15.0 mM**				
	signal	eqn	B[HCl]E	INTPLT	ACID GEN (mM)		SIGNAL	eqn	B[HCl]E	INTPLT	ACID GEN (mM)
Baseline	0.0394	HSLV	0.01776			Baseline	0.03150	LSLV	0.00231		
250	0.0434	HSLV	0.01776	0.1117	0.09	250	0.0375	LSLV	0.00231	0.2844	0.28
270	0.0477	HSLV	0.01776	0.1717	0.15	270	0.0455	LSLV	0.00231	0.6015	0.60
290	0.0489	HSLV	0.01776	0.1858	0.17	290	0.0571	LSLV	0.00231	0.9850	0.98
310	0.0459	HSLV	0.01776	0.1487	0.13	310	0.0552	LSLV	0.00231	0.9269	0.92
335	0.0397	HSLV	0.01776	0.0293	0.01	335	0.0380	LSLV	0.00231	0.3059	0.30
355	0.0400	HSLV	0.01776	0.0392	0.02	355	0.0494	LSLV	0.00231	0.7387	0.74

2B4MA	**0.52 mM**					**2B4MA**	**15.1 mM**				
	SIGNAL	EQN	B[HBr]E	INTPLT	ACID GEN (mM)		SIGNAL	eqn	B[HBr]E	INTPLT	ACID GEN (mM)
Baseline	0.04020	HSLV	0.02093			Baseline	0.0318	LSLV	0.01414		
250	0.05270	HSLV	0.02093	0.2407	0.22	250	0.0405	LSLV	0.01414	0.3925	0.38
270	0.09400	HSLV	0.02093	0.6144	0.59	270	0.0535	LSLV	0.01414	0.7819	0.77
290	0.09600	HSLV	0.02093	0.6254	0.60	290	0.0884	LSHV	0.01414	1.5013	1.49
310	0.09250	HSLV	0.02093	0.6060	0.59	310	0.0835	LSHV	0.01414	1.3924	1.38
335	0.04440	HSLV	0.02093	0.0962	0.08	335	0.0486	LSLV	0.01414	0.6489	0.63
355	no abs	HSLV	0.02093		-0.02	355	0.0375	LSLV	0.01414	0.2797	0.27

This table gives the raw data for acid generation measurements in chapter 4. The Top left of each box is the chemical name abbreviation. To the right of that is found the concentration of the photochemical for a particular set of measurements. The left column indicates the wavelength of the LED that was used for the test (all LEDs were operated at 23 mA for these tests). The baseline row gives the results in the absence of any LEDs (that background or "baseline" signal). The SIGNAL column gives the signal measured by the conductivity detector. The EQN column explains which calibration was curved for the interpolation. The B[HCl]E or B[HBr]E standards for "baseline [HCl] (or [HBr]) equivalent, as appropriate. This is the "conductive contaminant score that is eplxained in chapter 4. The INTPLT column is the interpolation of the conductivity (preliminary acid generation score). The final column "ACID-GEN" was calculated by subtracting B[HCl]E or B[HBr]E from INTPLT to give the final acid generation score. The data continues on the next two pages.

CDHAP	**0.501 mM**					**CDHAP**	**15.0 mM**				
	SIGNAL	eqn	B[HCl]E	INTPLT	ACID GEN (mM)		SIGNAL	eqn	B[HCl]E	INTPLT	ACID GEN (mM)
Baseline	0.03920	HSLV	0.00847			Baseline	0.0315	LSLV	0.00231		
250	0.05050	HSLV	0.00847	0.2036	0.20	250	0.0422	LSLV	0.00231	0.4772	0.47
270	0.05967	HSLV	0.00847	0.2897	0.28	270	0.0689	LSLV	0.00231	1.3149	1.31
290	0.0940	HSLV	0.00847	0.5222	0.51	290	0.1280	LSHV	0.00231	2.7360	2.73
310	0.0950	HSLV	0.00847	0.5280	0.52	310	0.1015	LSHV	0.00231	2.0845	2.08
335	0.0563	HSLV	0.00847	0.2604	0.25	335	0.0640	LSLV	0.00231	1.1838	1.18
355	0.0406	HSLV	0.00847	0.0560	0.05	355	0.0528	LSLV	0.00231	0.8511	0.85

CDMEP	**0.628 mM**					**CDMEP**	**15.0 mM**				
	SIGNAL	EQN	B[HCl]E	INTPLT	ACID GEN (mM)		SIGNAL	eqn	B[HCl]E	INTPLT	ACID GEN (mM)
Baseline	0.04170	HSLV	0.08086			Baseline	0.0317	LSLV	0.01253		
250	0.07400	HSLV	0.08086	0.3970	0.32	250	0.0600	LSLV	0.01253	1.0708	1.06
270	0.06740	HSLV	0.08086	0.3502	0.27	270	0.1250	LSHV	0.01253	2.6601	2.65
290	0.09920	HSLV	0.08086	0.5522	0.47	290	0.2550	LSHV	0.01253	6.6280	6.62
310	0.10560	HSLV	0.08086	0.5880	0.51	310	0.2970	LSHV	0.01253	8.3718	8.36
335	0.04206	HSLV	0.08086	0.0880	0.01	335	0.0663	LSLV	0.01253	1.2463	1.23
355	0.04160	HSLV	0.08086	0.0788	0.00	355	0.0387	LSLV	0.01253	0.3356	0.32

Raw data for acid generation measurements, continued.

DeCL	**0.499 mM**					**DeCl**	**15 mM**				
	signal	eqn	B[HCl]E	INTPLT	ACID GEN (mM)		signal	eqn	B[HCl]E	INTPLT	ACID GEN (mM)
Baseline	0.0391	HSLV	0.00302			Baseline	0.0391	HSLV	0.00302		
250	0.0845	HSLV	0.00302	0.4651	0.46	250	0.225	HSHV	0.00302	1.1926	1.19
270	0.0870	HSLV	0.00302	0.4805	0.48	270	0.470	HSHV	0.00302	2.5563	2.55
290	0.0789	HSLV	0.00302	0.4296	0.43	290	0.709	HSHV	0.00302	4.3981	4.40
310	0.0625	HSLV	0.00302	0.3127	0.31	310	0.660	HSHV	0.00302	3.9450	3.94
335	0.0434	HSLV	0.00302	0.1117	0.11	335	0.320	HSHV	0.00302	1.6842	1.68
355		HSLV									

DMNBB	**0.50 mM**					**DMNBB**	**15.0 mM**				
	SIGNAL	eqn	B[HBr]E	INTPLT	ACID GEN (mM)		SIGNAL	eqn	B[HBr]E	INTPLT	ACID GEN (mM)
Baseline	0.0320	LSLV	0.02524			Baseline	0.04740	LSLV	0.61425		
250	0.0381	LSLV	0.02524	0.3049	0.28	250	0.06789	LSLV	0.61425	1.1152	0.50
270	0.0378	LSLV	0.02524	0.2923	0.27	270	0.07960	LSHV	0.61425	1.3063	0.69
290	0.0403	LSLV	0.02524	0.3850	0.36	290	0.07290	LSHV	0.61425	1.1595	0.55
310	0.0421	LSLV	0.02524	0.4469	0.42	310	0.09938	LSHV	0.61425	1.7486	1.13
335	0.0381	LSLV	0.02524	0.3037	0.28	335	0.07294	LSHV	0.61425	1.1604	0.55
355	0.0441	LSLV	0.02524	0.5135	0.49	355	0.13100	LSHV	0.61425	2.4863	1.87

Raw data for acid generation measurements, continued.

Below are the calibration curves for the acid generation calculations, as explained in Chapter 4. The graphs and curve equations are presented, followed by the data pairs themselves, which give the conductivity signal and the concentration of HCl or HBr in the standard, as appropriate.

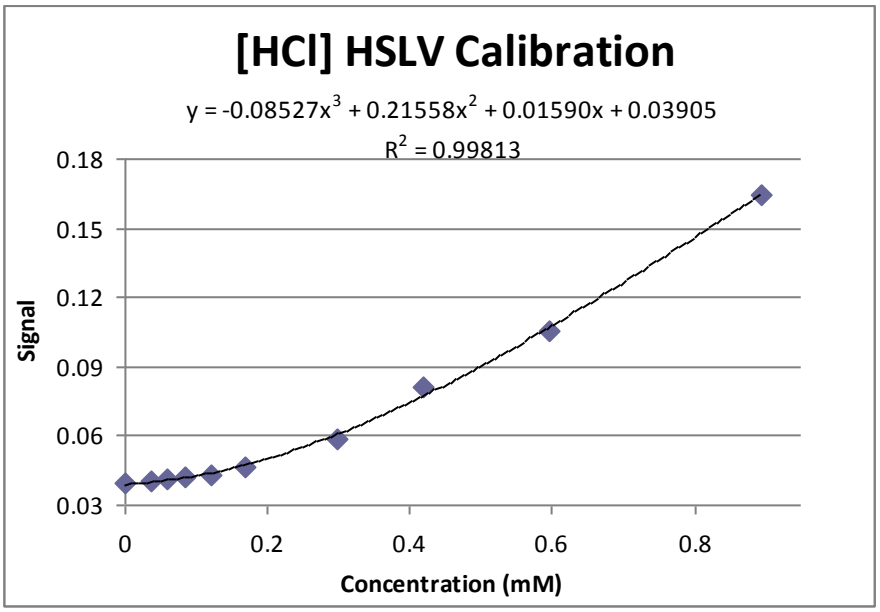

Conc. (mM)	0.000	0.0360	0.0600	0.0839	0.120	0.168	0.299	0.419	0.597	0.893
Signal	0.0393	0.0402	0.041	0.042	0.0433	0.0465	0.059	0.0815	0.105	0.1648

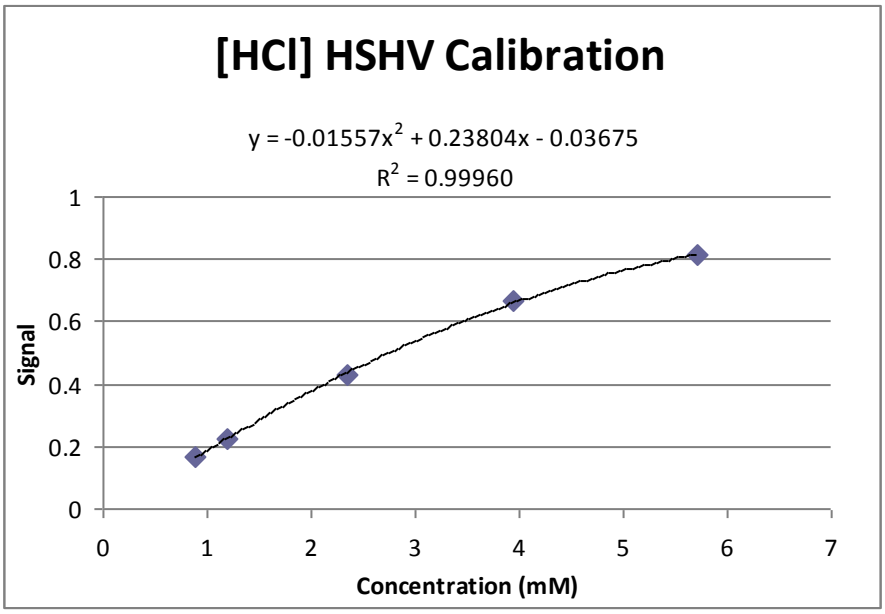

Conc. (mM)	0.893	1.19	2.35	3.95	5.71
Signal	0.1648	0.226	0.429	0.667	0.813

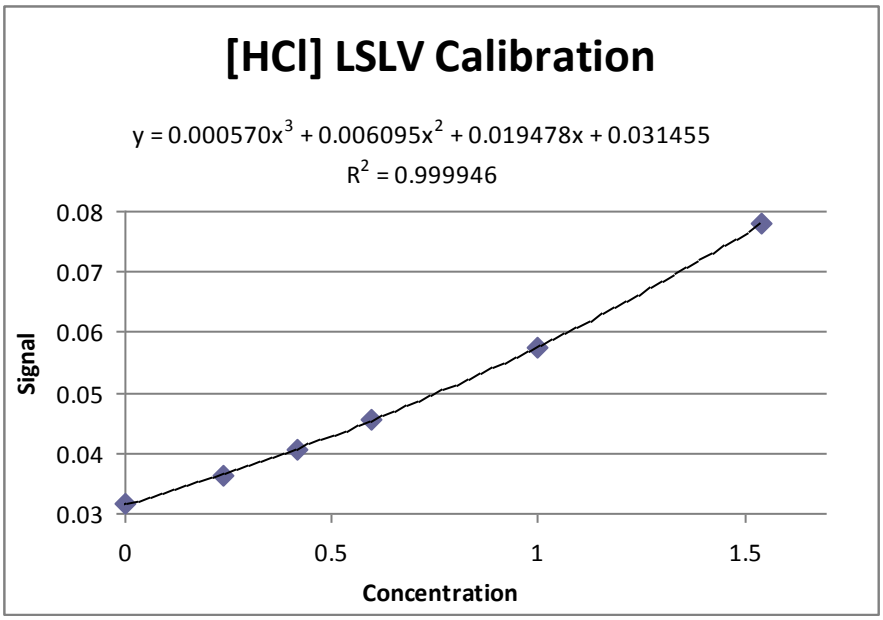

Conc. (mM)	17.4	15.7	13.8	11.9	9.91	7.85	5.71	3.50	2.35	1.54
Signal	0.425	0.407	0.386	0.361	0.328	0.284	0.231	0.156	0.113	0.078

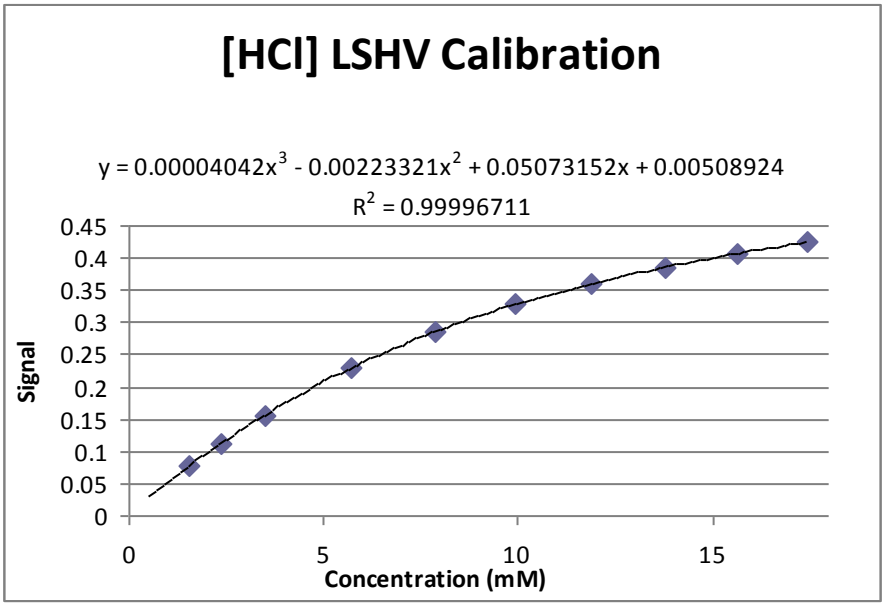

Conc. (mM)	0.893	1.19	2.35	3.95	5.71
Signal	0.1648	0.226	0.429	0.667	0.813

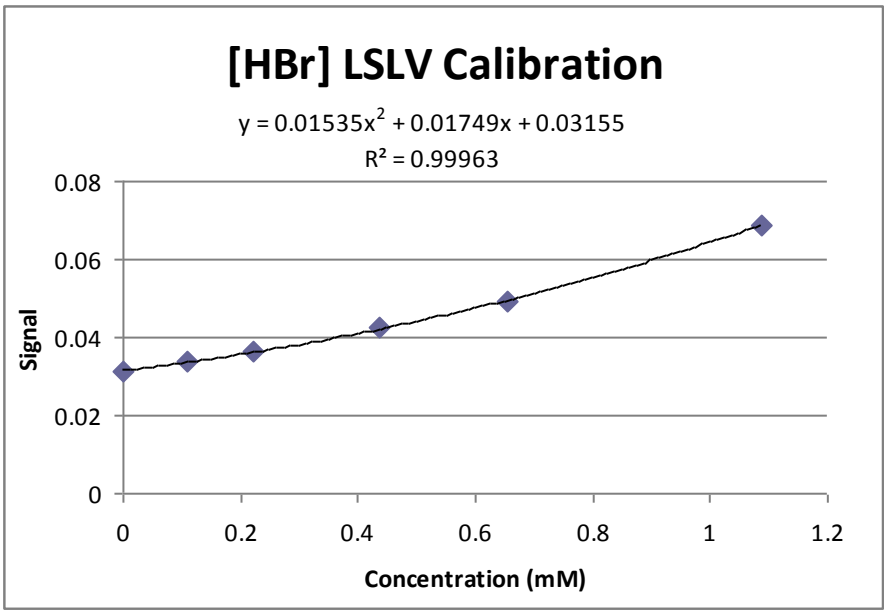

Conc. (mM)	0.000	0.110	0.220	0.438	0.656	1.089
Signal	0.0314	0.0336	0.0363	0.0425	0.0492	0.0689

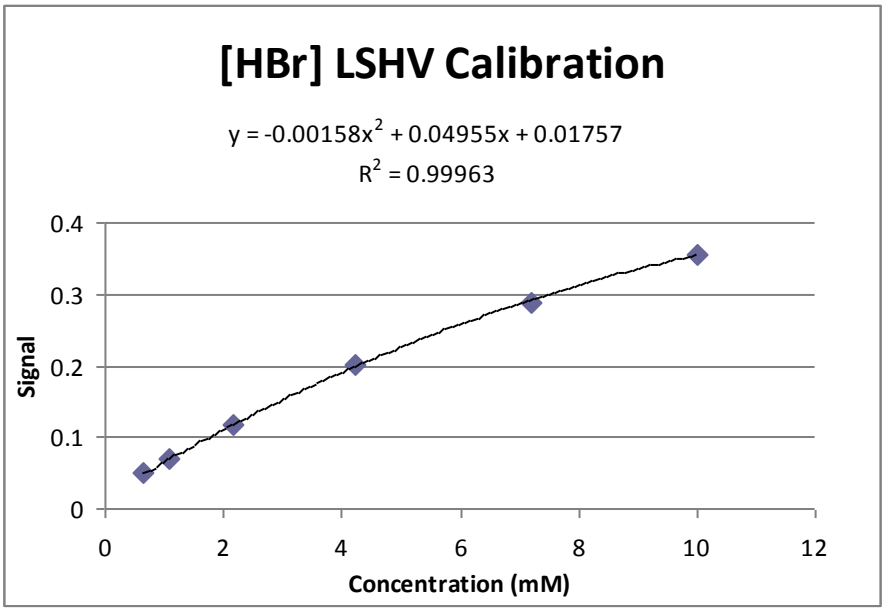

Conc. (mM)	0.656	1.09	2.16	4.23	7.20	10.00
Signal	0.0492	0.0689	0.1169	0.2024	0.2886	0.3561

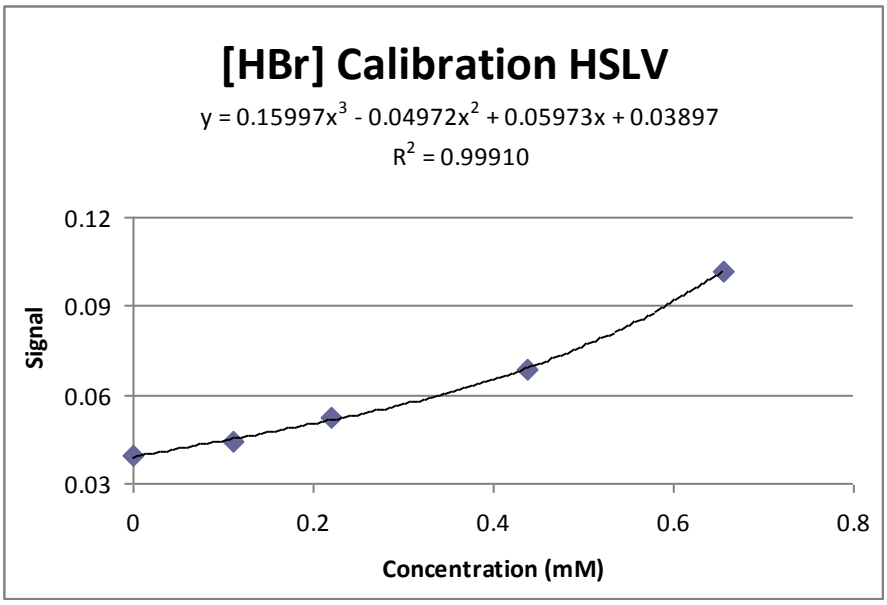

Conc. (mM)	0.000	0.110	0.220	0.438	0.656
Signal	0.0393	0.0441	0.0524	0.0687	0.102